Functional characterization of an LCK cysteine mutant

Thesis

for the degree of

doctor rerum naturalium (Dr. rer. nat.)

approved by the Faculty of Natural Sciences of Otto von Guericke University Magdeburg

by M.Sc. Andreas Kritikos

born on 27 December 1987 **in** Cholargos, Attiki, Greece

Examiner: Professor Dr. Luca Simeoni

Professor Dr. Ria Baumgrass

Submitted on: 19 July 2021

Defended on: 31 May 2022

B. TABLE OF CONTENTS

TABLE OF CONTENTS

C. LIST OF FIGURES AND TABLES

LIST OF FIGURES AND TABLES

D. ABBREVIATIONS

A	-Alanine
A.U.	-Arbitrary Units
Ab CTRL	-Antibody control
ABL	-Abelson murine leukemia
ACK	-Activated CDC42 kinase
ADAP	-Adhesion and degranulation promoting adapter protein
ADP	-Adenosine diphosphate
ALL	-Acute lymphocytic leukemia
AML	-Acute myeloid leukemia
AP-1	-Activator protein 1
APCs	-Antigen-presenting cells
APS	-Ammonium persulfate
ATP	-Adenosine triphosphate
BCL10	-B-cell chronic lymphocytic leukemia/lymphoma 10
BCR	-B-cell receptor
BLK	-B lymphocyte kinase
BSA	-Bovine serum albumin
BTK	-Bruton's tyrosine kinase
C	-Cysteine
Ca	-Calcium
CARD11	-Caspase recruitment domain family, member 11
CAT	-Catalase
CBL	-Casitas B-lineage lymphoma proto-oncogene
CBM	-CARD11–BCL10–MALT1 complex
CC	-Cysteine Clustered
CD	-cluster of differentiation (also known as cluster of designation)
CD3ζ	-CD3 zeta
CD3ε	-CD3 epsilon
CDC37	-Cell division cycle 37
CDC42	-Cell division control protein 42 homolog
CLL	-Chronic lymphocytic leukemia
CRAC	-Calcium release-activated channels
CSK	-C-terminal Src kinase
cSMAC	-Central supramolecular activation cluster
CVID	-Common variable immune deficiency
D	-Aspartic acid
DAG	-Diacylglycerol
DAPI	-4′,6-diamidino-2-phenylindole
DCP-Bio1	-3-(2,4-dioxocyclohexyl)propyl Bio 1
DDR	-Discoidin domain receptor
DMSO	-Dimethyl Sulfoxide Solvent
DN	-Double negative
DRMs	-detergent-resistant membranes
dSMAC	-Distal SMAC
DTT	-Dithiothreitol
DUOX1	-Dual oxidase 1

ABBREVIATIONS

E	-Glutamine
ECL	-Electrochemiluminescence
EDTA	-Ethylene diamine tetraacetic acid
EF1A	-Elongation Factor 1-Alpha
EGF	-Epidermal growth factor
EGFR	-Epidermal growth factor receptor
EMS	-Ethylmethanesulphonate
EPH	-Erythropoietin-producing human hepatocellular receptors
ER	-Endoplasmatic reticulum
ERK	-Extracellular signal-regulated kinase
ERO	-Endoplasmic reticulum oxidoreductin
F-actin	-Filamentous actin
FACS	-Fluorescence-activated cell sorting
FAK	-Focal adhesion kinase
FDA	-U.S. Food and Drug Administration
FES	-Feline sarcoma oncogene
FGFR	-Fibroblast growth factor receptor
FGR	-Gardner-Rasheed feline sarcoma viral (v-fgr) oncogene homolog
FLIM	-Fluorescence lifetime imaging microscopy
FRET	-Förster resonance energy transfer analysis
FRK	-Fyn-related kinase
FSC	-Forward scatter
FYN	-FYN oncogene related to SRC, FGR, YES
G	-Glycine
GA	-Glutaraldehyde
GADS	-GRB2-related adaptor protein
GFP	-Green Fluorescent Protein
GPX	-Glutathione peroxidase
GRB2	-Growth factor receptor-bound protein 2
GRX	-Glutaredoxins
GSH	-Glutathione
GSSG	-Glutathione disulfide
GTP	-Guanosine triphosphate
HCK	-Hematopoietic cell kinase
HGFR	-Hepatocyte growth factor receptor
HIV	-Human Immunodeficiency Virus
HSP90	-Heat-shock protein of 90 kDa
I	-Isoleucine
ICAM	-Intercellular Adhesion Molecule
ICL	-Idiopathic CD4 lymphocytopenia
IFN2	-Inverted formin-2
Ig	-Immunoglobulin
IL	-Interleukin
INSR	-Insulin Receptor
IP3	-1,4,5-triphosphate
IRF	-Instrument response function
IRK	-Insulin Receptor Kinase
IS	-Immunological synapse
ITAM	-Immune-receptor-Tyrosine-based-Activation-Motif

ABBREVIATIONS

ITK	-Interleukin-2-inducible T-cell kinase
J.CaM	-Jurkat Calcium Mutant T-cell variant
J.E6	-Jurkat T cells
J.LCK	-LCK-deficient Jurkat T-cell variant
JAK	-Janus kinase
K	-Lysine
KD	-Kinase domain
kDa	-Kilodaltons (molecular weight)
L	-Leucine
LAT	-Linker for activation of T cells
LB CTRL	-Lysis buffer control
LCK	-Lymphocyte-specific protein tyrosine kinase
LFA-1	-Lymphocyte function-associated antigen-1
LSTRA	-Lone Star Therapeutic Recreation Association
LYN	-Lck/Yes novel tyrosine kinase
M	-Methionine-
MAL	-Myelin and lymphocyte protein
MALT1	-Mucosa-associated lymphoid tissue lymphoma translocation gene 1
MAPK	-Mitogen-activated protein kinase
MCL	-Mantle cell lymphoma
MEK	-Mitogen-activated protein kinase kinase
MFI	-Mean florescence intensity
Mg	-Magnesium
MHC	-Major histocompatibility complex
MUSK	-Muscle-Specific Kinase
N	-Asparagine
NAC	-N-Acetyl Cysteine
NADPH	-Nicotinamide adenine dinucleotide phosphate
NCK1	-Non-catalytic region of tyrosine kinase adaptor protein 1
NF-κB	-Nuclear factor kappa-light-chain-enhancer of activated B cells
NFAT	-Nuclear factor of activated T-cells
NK	-Natural killer
NMT	-N-myristoyl transferase
Non-RTKs	-Non-receptor tyrosine kinases
NOS	-Nitric oxide synthases
NOX	-NADPH oxidase
NPR	-NADPH-P450 reductase
NSCLC	-Non-small-cell lung carcinoma
P	-Proline
PAMPs	-pathogen-associated molecular patterns
PBS	-Phosphate-buffered saline
PDGF	-Platelet-derived growth factor
PDGFR	-Platelet-derived growth factor receptor
PDI	-Protein disulfide isomerase
PDK1	-3-phosphoinositide-dependent protein kinase 1
PEP	-PEST domain-enriched tyrosine phosphatase
PFA	-Paraformaldehyde
PIP2	-Phosphatidylinositol 4,5-bisphosphate or PtdIns(4,5)P2

ABBREVIATIONS

PKC	-Protein kinase C
PKCθ	-Protein kinase C-theta
PLCγ-1	-Phospholipase Cγ-1
pMHC	-Peptide-MHC
PMSF	-Phenylmethylsulfonyl fluoride
pSMAC	-Peripheral SMAC
PTB	-Phosphotyrosine-binding
PTKs	-Protein Tyrosine Kinases
PTPs	-Protein tyrosine phosphatases
pY	-Phosphorylated Tyrosine
Q	-Glutamine
R	-Arginine
RAB11	-Ras-related protein
RAC	-Ras-related C3 botulinum toxin substrate
RAC1	-Ras-related C3 botulinum toxin substrate 1
RAF	-Rapidly Accelerated Fibrosarcoma
RAS	-Rat sarcoma
RASGRP	-RAS guanyl nucleotide-releasing protein
RK	-Receptor kinase motif
RNS	-Reactive nitrogen species
ROS	-Reactive oxygen species
RPMI	-Roswell Park Memorial Institute (culture medium)
RTKs	-Receptor tyrosine kinases
S59	-Serine 59
sAbs	-Soluble Antibodies
SAM	-Sterile alpha motif
SCF	-Stem cell factor
SCID	-Severe Combined Immunodeficiency
SCLC	-Small-cell lung carcinoma
SDS	-Sodium dodecyl sulfate
SDS-PAGE	-Sodium dodecyl sulfate- polyacrylamide gel electrophoresis
SEM	-Standard error of the mean
SFKs	-SRC family kinases
SH	-Src-homology
-SH	-Thiol group
SHP1	-Src homology region 2 domain-containing phosphatase-1
SLP-76	-SH2 domain-containing leukocyte protein of 76kDa
SMAC	-Supramolecular activation cluster
SNO	-S-nitrosylation
SO2H	-Sulphinic acid
SO3H	-Sulphonic acid
SOD	-Superoxide dismutases
SOH	-Sulfenic acid
SOP	-Standard operating procedure
SOS	-Son of sevenless protein
SSC	-Side scatter
SSG	-S-glutathionylation
SSH	-Sulfhydration
TBS	-Tert-butyldimethylsilyl

ABBREVIATIONS

TCR	-T-cell receptor
TEC	-Transient Erythroblastopenia Of Childhood and Agammaglobulinemia
TEMED	-Tetramethylethylenediamine
Tris	-Tris(hydroxymethyl)aminomethane
TRK	-Tropomyosin receptor kinase
TRX	-Thioredoxins
TRXR	-TRX reductases
TSCSP	-Time- and Space Correlated Single Photon
UD	-Unique domain
UNC119	-Uncoordinated-119
UR	-Unique region
v-SRC	-Viral SRC (sarcoma)
VAV1	-Vav Guanine Nucleotide Exchange Factor 1
VEGFR	-Vascular endothelial growth factor receptor
VEGFR	-Vascular Endothelial Growth Factor Receptor
W	-Tryptophan
WT	-Wild type
Y	-Tyrosine
YES	-Yamaguchi sarcoma viral oncogene homolog
YFP	-Yellow Fluorescent Protein
ZAP-70	-Zeta-chain-associated protein kinase 70
Zn	-Zinc

E. ABSTRACT

Last Name, First Name: M.Sc KRITIKOS ANDREAS

Title of the dissertation: Functional Characterization of an LCK cysteine mutant

Antigen-induced T-cell receptor phosphorylation is the first signaling event in T cells to activate adaptive immunity against invading pathogens and cancer cells. PTKs are key mediators in the generation of intracellular signals that culminate in the activation of T cells. LCK belongs to the SFKs and it is crucial during T-cell activation and T-cell development. Regulation of the enzymatic activity of LCK occurs via phosphorylation of two conserved tyrosine residues: phosphorylation of Y394 and the conformational opening of LCK are believed to activate the kinase, whereas Y505 phosphorylation is thought to generate a closed, inactive form of LCK. Recently, also conserved cysteine residues have gained the attention of many researchers because they are involved in the regulation of the activity of PTKs and therefore they can be targeted for the development of new specific PTK inhibitors.

In the context of my PhD thesis, I analyzed the functional relevance of the cysteine residue 476 of LCK, which is highly conserved among PTKs. To study the function of C476 in LCK, I have generated LCK constructs carrying a cysteine to alanine mutation. An LCK C476A mutant was expressed in the LCK-deficient Jurkat T-cell variant (J.LCK) and the stability, activity and function of the mutant were evaluated. First, I have shown that C476 regulates the protein stability and subcellular localization of LCK. Additionally, J.LCK T cells reconstituted with LCK C476A showed a strongly reduced phosphorylation of the regulatory residues, Y394 and Y505. Furthermore, analysis of the kinase activity of LCK C476A showed that it is enzymatically inactive. On the basis of these data, as well as analysis of its conformational status, it appears that LCK C476A adopts a conformation that resembles the so called “primed” LCK conformation. In line with these data, it is clear that the ability of LCK C476A to reconstitute TCR-mediated signaling is drastically attenuated. Moreover, I have

shown that overexpression of the co-chaperone CDC37 rescues the stability and partially the activity of the LCK C476A mutant.

Taking advantage of well-established techniques in my group, I investigated whether C476 is a target of reversible oxidation (Sulfenylation). It appears that C476 is not a direct target of Sulfenylation.

The results of my PhD thesis additionally show that the C476A substitution converts LCK into a temperature sensitive mutant. Analysis of LCK C476A at lower temperatures revealed that it has an enhanced activity and function.

Collectively, it appears that C476 is a crucial residue involved in the regulation of LCK activity and function. In the future, more information regarding the involvement of phosphatases in the regulation of LCK C476A phosphorylation as well as the investigations of other types of C476 post-translational modifications affecting this residue will contribute to the elucidation of the mechanistic aitiology of the regulatory role of the C476 residue.

F. ZUSSAMENFASSUNG

Nachname, Vorname: M.Sc. KRITIKOS ANDREAS

Titel der Dissertation: Funktionelle Charakterisierung einer LCK-Cystein-Mutante

Zur Bekämpfung eindringender Krankheitserreger und Tumorzellen wird die adaptive Immunantwort ausgelöst. Die Antigen-induzierte T-Zell-Rezeptor-Phosphorylierung ist das erste Signalisierungsereignis in T-Zellen zur Aktivierung dieser Immunantwort. Schlüsselmediatoren für die Aktivierung von T-Zellen sind Protein-Tyrosin-Kinasen, da sie intrazellulärer Signalkaskaden generieren. Die Protein-Tyrosine-Kinase LCK, aus der SRC-Kinase-Familie, ist essentiell für die T-Zell-Aktivierung und T-Zell-Entwicklung. Die Regulierung der enzymatischen Aktivität von LCK erfolgt hauptsächlich über die Phosphorylierung der zwei hochkonservierten Tyrosinresten, Y394 und Y505. Es wird angenommen, dass die Phosphorylierung von Y394 und die „Öffnung“ der LCK-Konformation die Kinase aktivieren, während die Phosphorylierung von Y505 zu einer geschlossenen, inaktiven Form von LCK führt. Weiterhin sind Cysteine an der Regulation der Protein-Tyrosin-Kinaseaktivität beteiligt. Diese konservierten Cysteinereste können Anwendung in der Entwicklung neuer spezifischer Protein-Tyrosin-Kinase-Inhibitoren finden und sind daher in jüngster Zeit in den Fokus der Forschung geraten.

Im Rahmen meiner Doktorarbeit habe ich die funktionelle Relevanz des Cysteinrestes 476 (C476) von LCK, der unter Protein-Tyrosine-Kinasen hochkonserviert ist, analysiert. Um die Funktion dieses Restes zu untersuchen, habe ich LCK-Konstrukte generiert, die eine Cystein-zu-Alanin-Mutation (C476A) tragen. Um die Stablität, Aktivität und Funktion der LCK-C476A-Mutante zu analysieren, wurde die Mutante in LCK-defizienten Jurkat-T-Zellen (J.LCK) exprimiert. Zunächst habe ich gezeigt, dass C476 die Proteinstabilität und die subzelluläre Lokalisation von LCK reguliert. Außerdem zeigten die mit LCK C476A rekonstituierten J.LCK-T-Zellen eine stark reduzierte Phosphorylierung der regulatorischen Reste Y394 und Y505. Des Weiteren zeigte die Analyse der Kinaseaktivität, dass LCK C476A enzymatisch inaktiv ist. Aufgrund dieser Daten, sowie Konformationsstudien, scheint LCK C476A

eine Konformation anzunehmen, die der sogenannten “primed LCK“-Konformation ähnelt.

Diese Daten stimmen mit der drastisch abgeschwächten Fähigkeit der LCK-C476A-Mutante überein, die T-Zell-Rezeptor-vermittelte Signalübertragung in LCK-defizienten Jurkat-T-Zellen (J.LCK) wiederherzustellen. Darüber hinaus habe ich gezeigt, dass die Überexpression des Ko-Chaperons CDC37 der Instabilität und Inaktivität der LCK-C476A-Mutante positiv entgegenwirkt.

Mithilfe etablierter Techniken in meiner Gruppe untersuchte ich, ob C476 ein Ziel der reversiblen Oxidation (Sulfenylierung) ist, was nicht bestätigt werde konnte.

Außerdem zeigten die Ergebnisse meiner Doktorarbeit, dass die Cystein-Alanin-Substitution an der Stelle 476, LCK in eine temperaturempfindliche Mutante umwandelt. Die Analyse von LCK C476A bei niedrigeren Temperaturen ergab eine verbesserte Aktivität und Funktion.
Zusammengefasst scheint C476 ein Proteinrest zu sein, der entscheidend an der Regulation der LCK-Aktivität und -Funktion beteiligt ist. Zur Aufklärung des regulatorischen Wirkmechanismus hinter der C476 sind weitere Informationen und Daten notwendig. Zum Einen, den Einfluss von Phosphatasen auf den Phosphorylierungstatus der LCK C476A Mutante, aber auch der Einfluss anderer posttranslationaler Modifikationen an gleicher Stelle.

1. INTRODUCTION

1.1 Adaptive immunity and signaling

In order to repel disease-causing pathogens, all organisms have developed different defense strategies. In particular, advanced vertebrates (including humans) possess sophisticated mechanisms of defense responses to fight against pathogenic microorganisms. This protective system, which has evolved from simpler defense mechanisms, is called **the immune system**.

The immune system is formally divided into two branches, the innate and the adaptive immunity. The **innate immunity** consists of non-specific defense mechanisms set in motion within minutes after an infection, which are activated by particular chemical properties common to many pathogens (e.g. pathogen-associated molecular patterns/PAMPs on the pathogen's surface). Conversely, the **adaptive immunity** is a more complex form of immune response specifically directed against a pathogen.

The adaptive immunity is driven by T and B lymphocytes. To recognize pathogen-specific antigens, these cells express specialized receptors: the T-cell receptor (TCR) on T cells and the B-cell receptor (BCR) on B cells. The recognition of the antigen by the TCR and the BCR activates a variety of signaling molecules leading to the activation of intracellular signaling pathways and cell activation. In addition, intracellular signaling induced by the engagement of costimulatory molecules and by cytokines is integrated with the signal from the antigen receptor to ultimately regulate proliferation, differentiation, and effector functions.

The primary response to an antigen results in clonal expansion of T or B cells that react against this specific antigen and produces a large number of effector lymphocytes that are able to eliminate the pathogen. After the elimination of the pathogen, the immune response undergoes a contraction phase characterized by the loss of effector lymphocytes and the appearance of memory cells that are capable of initiating rapid secondary responses to reinfection with the original pathogen (Cantrell, 2015).

1.2. Tyrosine phosphorylation and Protein Tyrosine Kinases (PTKs)

In multicellular organisms, communication between cells and their environment is fundamental for their survival. Cells communicate with their environment through a plethora of receptors expressed on the cell surface that recognize and bind molecules present in the extracellular environment. Binding of antigens to immune cells' receptors generates intracellular signals that alter the cells' behavior and finally culminate in the activation of immune cells. **Tyrosine phosphorylation** of particular amino acids plays a central role, as a covalent post-translational modification, in intracellular signal transduction. Tyrosine phosphorylation was discovered in 1980 during studies of polyomavirus middle T and v-SRC associated kinase activities as a new type of post-translational modification (Hunter and Sefton, 1980). The enzymes that accomplish this modification are named **Protein Tyrosine kinases (PTKs)**. Among the 518 kinases in the human genome, only about 1/6 (90 kinases) are PTKs, a proportion that is markedly less than those encoding for serine/threonine protein kinases.

PTKs create a phosphate ester by catalyzing the transfer of the *γ* phosphate of ATP to the hydroxyl group of tyrosine residues of protein substrates. Phosphorylation by protein kinases influences the function, activity and also subcellular localization of proteins (Krauss, 2014). PTKs play a fundamental role in all cellular processes such as embryogenesis, metabolism and immune cell function. However, several PTKs have been revealed to act also as oncogenes when their activity is altered (Hunter, 1997). Therefore, cells have developed sophisticated mechanisms to tightly regulate the activation of PTKs.

1.2.1 Structure of PTKs

Structurally, PTKs share a common folded core comprising a small and a large lobe within the kinase domain, which form a pocket representing the active site of the kinase. As shown in **Fig. 1.1**, the smaller lobe is named N-terminal lobe and contains five β-sheets and one α-helix, which is called C-helix. The salt bridge that is formed between C-helix and a Lysine residue

allows optimal positioning of the ATP phosphate. The P-loop (glycine rich loop) in the N-terminal lobe (**Fig. 1.1, yellow**), anchors the non-transferable ATP phosphates, thus controlling the affinity and specificity of the nucleotide.

The larger lobe is named C-terminal and comprises a four-helix bundle, along with more α-helixes and two short β-sheets. It provides catalytic residues and surface where protein or peptide substrates can dock on. An important regulatory element in the catalytic procedure is the “opening” and “closing” of the active site cleft. Most kinases are activated by phosphorylation of specific residues in the activation loop. As shown in **Fig. 1.1 (green),** the activation loop is flexible and is located close to the catalytic loop. The positive charge of the arginine (R) in the catalytic loop provides a link between the catalytic loop, the phosphorylation site and the magnesium-binding loop (**Fig. 1.1, orange**). Moreover, two conserved residues within the catalytic loop, aspartic acid (D) and asparagine (N), are responsible for the phosphate transfer and the stabilization of the Mg^{2+} that is associated to the ATP (**Fig. 1.1,** R, N, D).

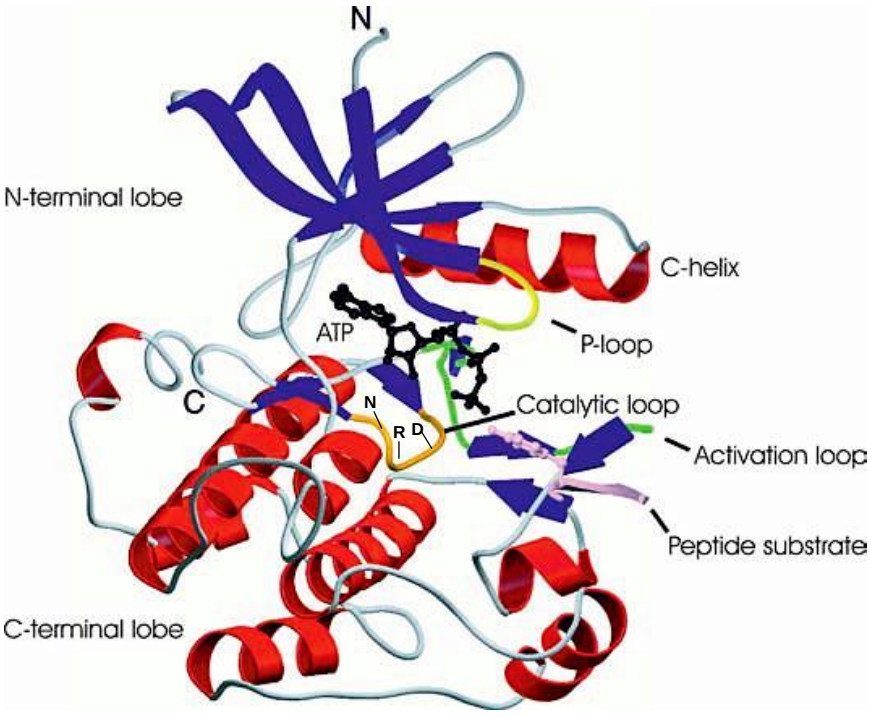

Figure 1.1: Structure of PTK domain
The main structural components of PTK kinase domain are highlighted in this scheme. The amino-terminal and carboxy-terminal domains are shown with the N- and the C-lobe, respectively. The α-helices are depicted with red color whereas the β-strands are shown in blue. The P-loop is colored in yellow, the activation loop in green, and the catalytic loop in orange. The three functional amino acids arginine (R), asparagine (N) and aspartic acid (D) are represented within the catalytic loop. Here, the insulin receptor is bound to ATP and a peptide substrate (modified from Krauss, 2014).

1.2.2 Classification of PTKs

In cells, there exist two classes of PTKs: the transmembrane PTKs referred to as **receptor tyrosine kinases (RTKs),** and the **non-receptor tyrosine kinases (Non-RTKs),** which are localized in the cytoplasm or anchored at the plasma membrane via post-translational modifications (Hubbard and Till, 2000).

1.3 Receptor Tyrosine kinases (RTKs)

RTKs are transmembrane proteins that possess a ligand-binding domain on the extracellular part and a cytoplasmic part that harbors a domain with tyrosine kinase activity. Depending on the domain organization of the extracellular part (e.g. cysteine rich domains, immunoglobulin (Ig)-like domains or EGF-like domains), mammalian RTKs can be classified into subfamilies (**Fig. 1.2)**. In most of the cases, the transmembrane domain consists of an α-helical structure. The cytoplasmic domain consists of a juxtamembrane region, the tyrosine kinase domain, a carboxy-terminal region (C-terminal), and possesses also regulatory tyrosine residues within or out of the kinase domain (Krauss, 2014).

RTKs exist in the “inactive-autoinhibited” state as monomers, or in some rare cases as dimers (e.g. PDGF receptor). Upon ligand binding, the RTK dimerizes or oligomerizes. Oligomerization of monomeric receptors induces *trans*-phosphorylation of regulatory tyrosine residues in the activation loop which leads to the stimulation of the kinase activity. The phosphorylation of additional tyrosine residues results in the formation of docking sites for downstream effector proteins that bind to the phosphorylated tyrosines via SH2 (Src-homology 2) or PTB (phosphotyrosine-binding) domains. Additional tyrosine phosphorylation of the effector proteins transmit signals further downstream (Hubbard and Till, 2000).

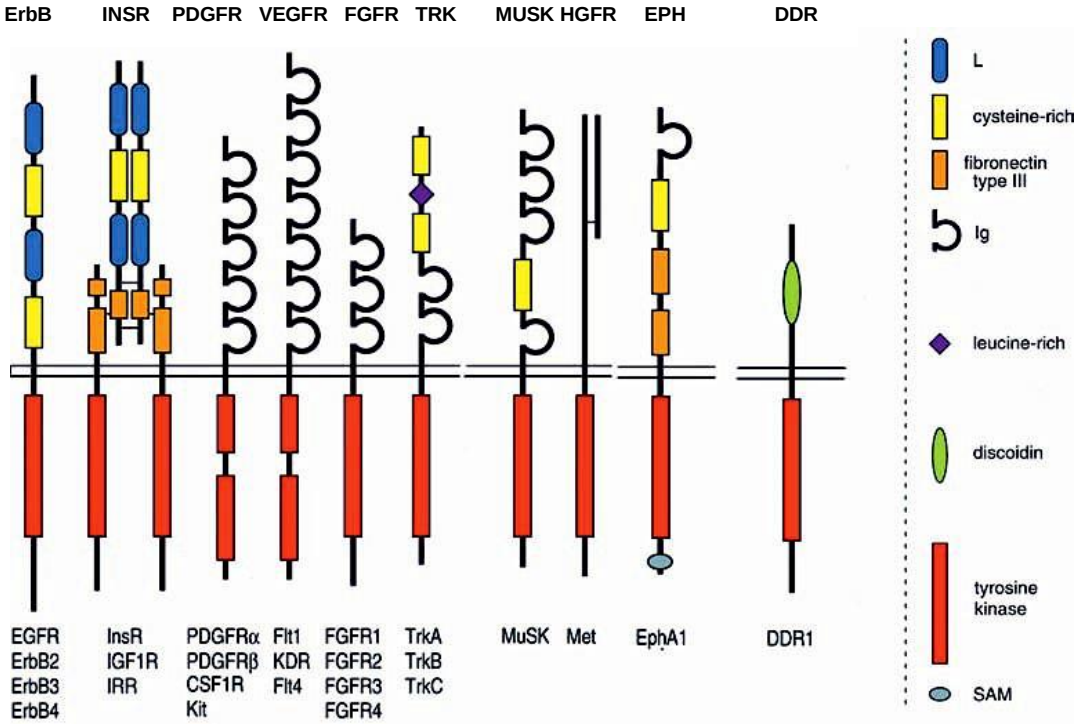

Figure 1.2: Structural examples of RTK subfamilies
The intracellular tyrosine kinase domains are relatively conserved between RTK subfamilies whereas the ligand-binding ectodomains differ substantially due to the different specificity of the interactions between ligands and receptors. On the right side of the scheme, the characteristic domain motifs are presented. On the lower part of the scheme members of the 10 (of the approximately 20 identified so far) RTK subfamilies are presented such as EGF receptor family, Insulin receptor family, PDGF receptor family**,** FGF receptor family**,** EPH receptor family**,** Discoidin domain receptor (DDR) family. The name of each family is shown on the upper part of the scheme (modified from Krauss, 2014).

1.4 Non-Receptor Tyrosine kinases (Non-RTKs)

As mentioned above, cells contain also PTKs that lack an extracellular ligand-binding domain and the transmembrane domain. These tyrosine kinases are named **non-receptor protein tyrosine kinases** or **non-RTKs.** In the human genome 32 genes are encoding for non-RTKs. Despite the absence of receptor and transmembrane domains, non-RTKs mostly localize in the cytoplasm but there are also some non-RTKs (SRC kinase) anchored to the plasma membrane. Based on their domain organization, mammalian non-RTKs can be clustered into 10 subfamilies referred to as ABL, ACK, CSK, FAK, FES, FRK, JAK, SRC, and TEC.

The non-RTKs play a fundamental role in signal transduction via cytokine receptors and antigen receptors, as well as in other signaling pathways. Non-RTKs represent one of the most studied groups of enzymes, as

they are able to regulate several cellular processes, such as cell division, proliferation and survival, gene expression, and immune responses. Deregulation of the activity of Non-RTKs due to genetic alterations or alterations of their activation can culminate in the development of hematological malignancies and tumorigenesis (Paul and Mukhopadhyay, 2004).

1.4.1 SRC family kinases (SFKs)

The largest subfamily of non-RTKs is the SFKs. The discovery of *v-Src* in 1979 by J.Michael Bishop and Harold E. Vamus, who won the Nobel Prize for physiology and medicine in 1989, completely changed the view of the scientific community about carcinogenesis. SFKs comprise 9 kinases (SRC, FGR, LCK, FYN, YES, BLK, HCK, LYN, FRK). SFKs are present in all metazoan cells and they participate in many signaling pathways (Parsons and Parsons, 2004). Furthermore, they are involved in many diseases and specifically cancer (Thomas and Brugge, 1997). Comparisons of the amino acid sequence of the kinase domain have resulted in the classification of SFKs into three subgroups: the Src A group (including FGR, FYN, SRC, and YES), the Src B group (including BLK, HCK, LCK, and LYN), and FRK in its own subfamily (**Fig. 1.3A)** (Huang et al., 2016).

As shown in **Fig. 1.3B**, all SFKs share a conserved domain structure. At their N-terminus, SFKs contain a membrane localization motif (SH4, Src-homology 4). This domain is followed by a unique region (UR, also known as Unique domain, UD), whose amino acid sequence is less conserved among SFKs members. Next, SFKs possess an SH3 and a SH2 domain, a regulatory linker, the kinase domain (KD), and a C-terminal regulatory tail. In the activation loop of the kinase domain, SFKs share a conserved autophosphorylation tyrosine residue, which in SRC is at position 416. Additionally, a general characteristic of SFKs is an inhibitory tyrosine phosphorylation site in the C-terminal regulatory tail (in c-SRC at position 527) (Boggon and Eck, 2004, Bradshaw, 2010). These structural similarities of SFKs imply that they share a common mechanisms of regulation including the phosphorylation of the conserved tyrosine residues (Y416 and Y527, activatory and inhibitory,

respectively) and the intramolecular interaction between the SH3 and a proline rich domain located between the SH2 domain and the KD (Okada, 2012).

The protein tyrosine kinase p56 LCK (Lymphocyte specific-protein tyrosine kinase) is a non-RTK and a well-characterized member of the SFKs. The description of the domain organization and the mechanisms governing the regulation of LCK activation in the next chapter will offer a deeper insight on the structure and regulation of the SFKs.

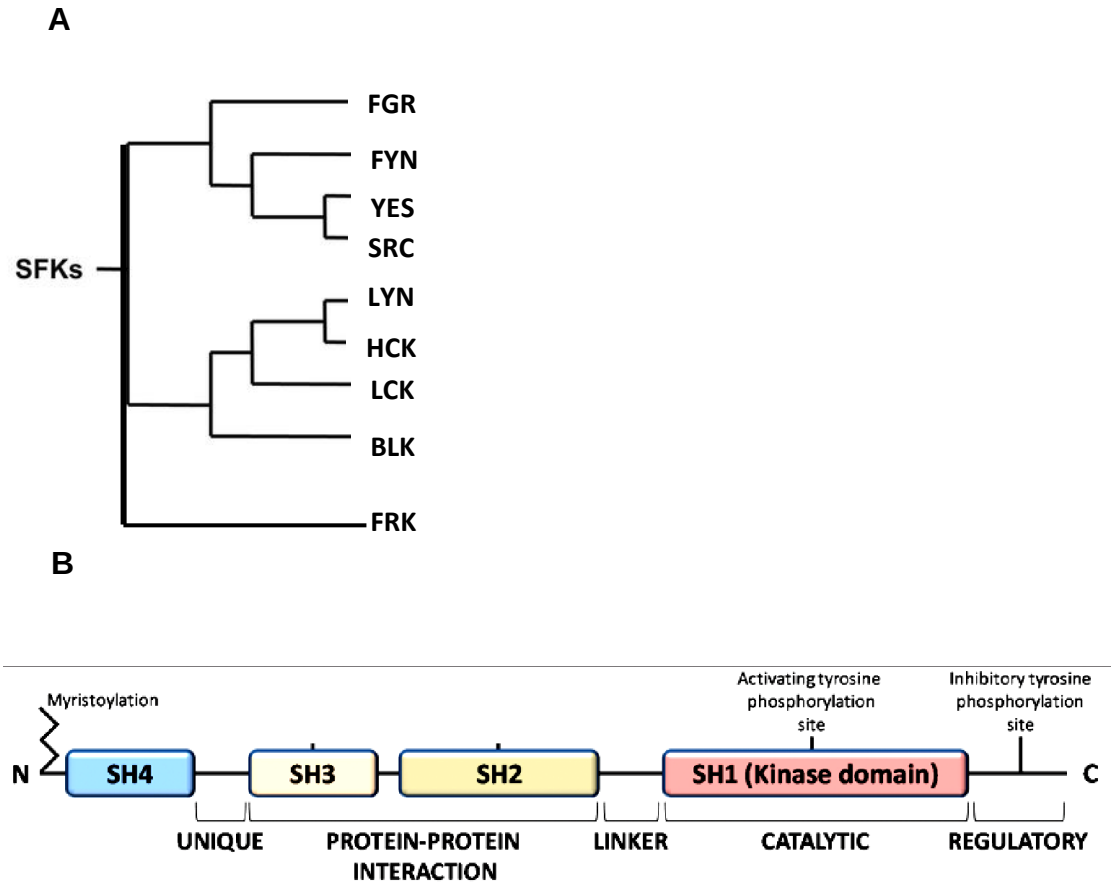

Figure 1.3: Molecular organization and activation of SRC family kinases
(A) SFKs can be subgrouped into three families, the SRC A family (FGR, FYN, SRC, and YES) and the SRC B family (BLK, HCK, LCK, and LYN) and FRK subfamily (B) SFKs share a conserved domain structure. From the N-terminus, they contain a SH4 membrane localization motif harboring a myristoylation and palmitoylation site, a Unique Region, an SH3 and SH2 domain, a regulatory linker, the kinase domain (SH1), with a conserved autophosphorylation tyrosine residue (Y416 in SRC), and a C-terminal regulatory tail with an autoinhibitory phosphorylation site (in c-SRC is Y527) (modified from Okada, 2012, Huang et al., 2016).

1.5 LCK ($p56^{LCK}$)

LCK (lymphocyte-specific protein tyrosine kinase) has a molecular weight of 56 kDa and it is expressed mainly in T cells and also in NK cells, CD5+ B-1 B cells, germinal center and mantle zone B cells, and in aryl hydrocarbon receptor-activated primary human B cells (Bommhardt et al., 2019). LCK was first identified in the early 80s as a 56 kDa protein tyrosine kinase that is overexpressed in the murine T-cell lymphoma LSTRA (Marth et al., 1985). LCK plays a pivotal role in T-cell responses and T-cell activation, because LCK initiates proximal signaling triggered upon engagement of the TCR.

The establishment of the Jurkat T-cell line in the early 1980s was fundamental for the discovery of the role of LCK in TCR signaling (Gillis and Watson, 1980)(Weiss et al., 1984). Jurkat T cells were first identified as a transformed leukemic human T-cell line that spontaneously or inducibly released large quantities of interleukin-2 (IL-2). By the mid-1990s, to study the function of effector molecules in TCR signaling, Jurkat T cells were genetically altered using mutagenesis (e.g. ionizing radiation, the point mutagen ethylmethanesulphonate or the frameshift mutagen ICR-191 in order to generate Jurkat T-cell variants lacking the expression of selected signaling molecules (Conzelmann et al., 1980, Abraham and Weiss, 2004). The observation that a T-cell line (Jurkat Calcium Mutant, J.CaM1.6), in which LCK was knocked out by chemical mutagenesis, displayed no calcium flux and impaired inducible tyrosine phosphorylation upon TCR stimulation demonstrated that LCK has an essential role in TCR-mediated signaling (Straus and Weiss, 1992).

LCK is crucial also in T-cell development (Palacios and Weiss, 2004). Indeed, it has been reported that LCK-deficient mice show a strong block in T-cell development at the DN3 (double-negative 3) stage and are mostly devoided of peripheral T cells (Molina et al., 1992). The role of LCK appears to be pivotal for the pre-TCR signaling and progression from the DN3 to the DN4 stage of T-cell development.

1.5.1 Domain organization and localization of LCK

LCK shares the same domain organization as all SFKs. As represented in **Fig. 1.4**, LCK comprises seven functional domains: the SH4 domain, the unique region, the SH3 and SH2 domains, the linker region between the SH2- and kinase domain, the kinase domain and the C-terminal regulatory tail.

The **SH4 domain** plays a crucial role in the intracellular localization of LCK. LCK localizes at the cytosolic side of the plasma membrane of T cells where it has the ability to associate with the co-receptors CD4 and CD8. In addition, LCK is also found in the pericentrosomal endosomes (Ley et al., 1994). More specifically, it has been previously reported that the 40-60% of the total amount of LCK in the cell is detected in lipid microdomains in the plasma membrane named lipid rafts (or membrane rafts or detergent-resistant membranes/DRMs) (Alonso and Milan, 2001). These domains contain glycosphingolipids, cholesterol, and protein receptors and they facilitate compartmentalization of signaling processes.

LCK is not able to fulfill its role in T-cell signaling effectively when not targeted to the plasma membrane and lipid rafts. In order to phosphorylate the TCR, the kinase (LCK) and its substrate (TCR/CD3/ζ-chains) must be in close proximity in order to interact, initiate and sustain T-cell signaling. In T cells, LCK is targeted to the plasma membrane via the exocytic pathway (Bijlmakers et al., 1999). This process relies on a specialized transport machinery. It has been previously shown that LCK travels from the Golgi apparatus via transport vesicles (endosomes) to the plasma membrane. In these vesicles, LCK interacts with the small GTPases RAB11 and UNC119 that together coordinate the correct targeting of LCK at the plasma membrane (Gorska et al., 2009). In addition, interaction of MAL with the IFN2 protein promotes movement of the transporting vesicles along the microtubular array. Rho-family GTPases, CDC42 and RAC1, regulate and empower the movement of the transporting vesicles via the formation of short actin filaments (Andrés-Delgado et al., 2010). MAL is also responsible for the correct positioning of the raft-associated LCK into the SMAC (supramolecular activation cluster) during the formation of the Immunological synapse (IS) (Antón et al., 2008).

Myristoylation is an essential irreversible modification that is critical for membrane association of SFKs. It occurs co-translationally and is catalyzed by the enzyme N-myristoyl transferase (NMT). Myristoylation and palmitoylation, which comprises of the attachment of the palmitate (16-carbon saturated fatty acid) to cysteine residues at the N terminus, together form a “dual signal” motif that contribute to the membrane localization and the delivery of individual SFKs to particular membrane microdomains (Patwardhan and Resh, 2010). However, SRC itself and BLK are not palmitoylated (Koegl et al., 1994). Conversely, the **SH4 domain** of LCK contains acylation sites required to anchor it at the cytoplasmic side of the plasma membrane. Specifically, LCK is myristoylated on a glycine at position 2 and palmitoylated on two cysteine residues at positions 3 and 5 (Kwong and Lublin, 1995) (**Fig. 1.4**).

The SH4 domain is followed by the **Unique Region** (UR). This domain is less conserved among SFK members and in LCK it is involved in the association with the CD4 and CD8 co-receptors. The interaction between LCK and co-receptors is coordinated by a zinc ion (Zn^{2+}) that is formed between a cysteine-X-X-cysteine motif, within the UR of LCK, and a cysteine-X-cysteine-proline motif located in the cytosolic tail of the co-receptors (Kim et al., 2003). LCK exists not only associated with the CD4 and CD8 coreceptors but also free (Roh et al., 2015). It has been shown that the association of LCK with the co-receptors CD4 or CD8 is not essential for the initiation of signaling, as free LCK is able to phosphorylate the TCR/CD3 complex and thus initiating TCR-mediated signaling (Casas et al., 2014). A recent study suggested that ionic interaction between acidic residues in the UR of LCK and basic residues of the CD3ε chains mediate the association of LCK with the TCR/CD3 complex (Li et al., 2017). The UR of LCK harbors also a serine (S59) residue. S59 is phosphorylated by ERK 1/2 and dephosphorylated by Calcineurin (Watts et al., 1993, Dutta et al., 2017). It is not yet clear whether S59 contributes positively or negatively to the regulation of LCK activity/function. Accumulating evidence suggests that S59 participates in a positive feedback loop that involves phosphorylation of LCK on this residue by ERK 1/2 (Stefanová et al., 2003) (for more details on this regulatory mechanism, please see chapter 1.5.3).

The **SH3 domain** is a small protein domain of about 60 amino acid residues. It has been shown that the SH3 domain is important for the regulation of LCK conformation and activity. The SH3 domain interacts with a proline-rich sequence (P-Q-K-P motif) in the linker region between the SH2 domain and the kinase domain (**Fig. 1.4)**. This interaction contributes to the maintenance of the inactive/closed conformation of LCK (Xu et al., 1997).

Next, the **SH2 domain** mediates protein interactions as it is able to bind phosphotyrosine residues and it is present in a variety of signal-transducing proteins. The SH2 domain of the SFKs contributes to the control of kinase activity through an intramolecular interaction with a carboxy-terminal phosphotyrosine residue (Straus et al., 1996). In LCK, the SH2 domain can bind the phosphorylated carboxy-terminal regulatory tyrosine 505 (Peri et al., 1993). This interaction negatively modulates LCK activity as it imposes a closed, inactive conformation (Xu et al., 1997). It has been suggested that phosphorylation of Y192, a conserved residue among human SFKs which is located within the SH2 domain of LCK (**Fig. 1.4**), plays an important role in the regulation of the affinity of the SH2 domain. (Courtney et al., 2017) (for more details on this regulatory mechanism, please see chapter 1.5.3).

The **kinase domain** of LCK (~300 residues) consists of two lobes: the smaller N-terminal lobe and the larger C-terminal lobe. ATP binds in the interface between the two lobes. In the heart of the catalytic cleft, there are two important contiguous loops for catalysis and regulation: the catalytic loop and the activation loop, respectively. Apart from a number of residues important for ATP binding, a highly conserved phospho-transfer motif is located around Lysine residue 273 in the catalytic segment. Mutation of this residue leads to a catalytically inactive form of LCK (Laham et al., 2000). In the activation loop of the kinase domain (or SH1 domain), LCK harbors an activation-regulating Y394 residue (**Fig. 1.4**). Our group has recently shown that TCR signaling is highly dependent on *de novo* phosphorylation of Y394 (Philipsen et al., 2017). Autophosphorylation or transphosphorylation of Y394 induces a fully enzymatically active and conformationally open form of LCK.

At the C-terminal regulatory region, LCK contains a negative regulatory residue Y505 (**Fig. 1.4**). When phosphorylated by the cytoplasmic tyrosine

kinase CSK (C-terminal SRC kinase), Y505 interacts intramolecularly with the SH2 domain and promotes the formation of a closed and inactive conformation of LCK.

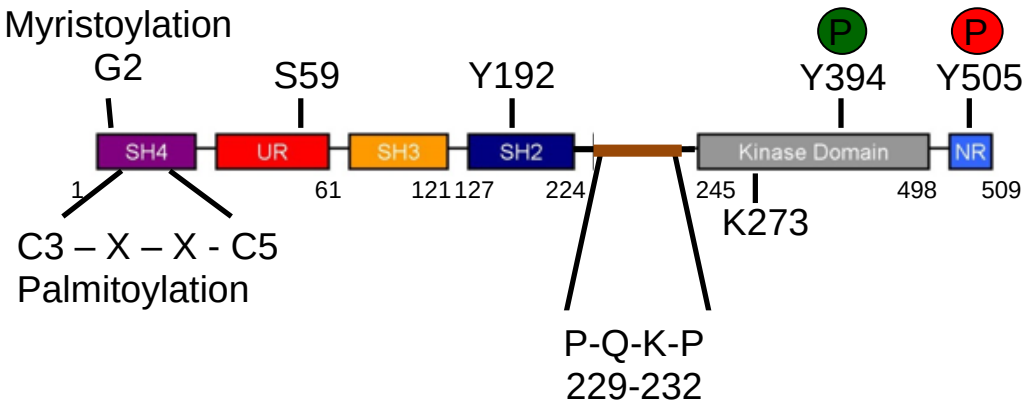

Figure 1.4: Domain organization of LCK
From N-terminus (left) to the C-terminus (right): SH4 domain with the myristoylation site (G2) and the palmitoylation residues cysteines 3 and 5. Unique region (UR) with the regulatory S59. SH3 domain, and SH2 domain with the negative regulatory Y192, for inter- and intra- molecular interactions. SH2-kinase domain linker region, with the characteristic polyproline motif P-Q-K-P. Kinase domain with the phospho-transfer activity residue K273 and the activatory Y394 residue. The C-terminal tail with the negative regulatory site Y505.

1.5.2 Regulation of LCK activation

Because of its importance in physiological processes, the regulation of LCK activation is in the center of scientific investigations since more than two decades. However, there are still many open questions that need to be answered in order to fully understand the mechanisms governing the regulation of LCK activation.

As already described above, LCK possesses two important regulatory tyrosine residues, the first in the kinase domain **Y394** and the other in the carboxy-terminal regulatory tail **Y505**. The activation of LCK is tightly regulated by the phosphorylation of those two tyrosine residues and also by spatiotemporal changes in the conformational state of the kinase (Salmond et al., 2009). In the autoinhibited or "***inactive/closed***" conformation, LCK is packed via intramolecular interactions in a state where the catalytic activity is restricted. As shown in **Fig. 1.5,** the ubiquitously expressed cytosolic tyrosine kinase CSK (C-terminal SRC kinase) phosphorylates LCK on the inhibitory

Y505. Once phosphorylated by CSK, pY505 interacts with the SH2 domain of LCK. This inactive/closed conformation is further stabilized by another intramolecular interaction occurring between the SH3 domain and the proline-rich motif of the linker region between the SH2 and the kinase domain (**Fig. 1.5, right**).

The protein tyrosine phosphatase CD45 dephosphorylates LCK on Y505, and thus, by counteracting CSK-mediated phosphorylation, unlocks LCK from the "*inactive/closed"* conformation (Mustelin et al., 1989, Mustelin and Altman, 1990). At this point, LCK is not phosphorylated at both regulatory tyrosine residues and adopts an "*open*" conformation. In this state LCK is named "***primed****"* (Nika et al., 2010) (**Fig. 1.5, middle**). Our group has recently shown that "*primed*" LCK displays a very low kinase activity despite it adopts an "*open*" conformation (Philipsen et al., 2017). For the full activation of LCK, phosphorylation of the activatory Y394 is mandatory (**Fig. 1.5, left**). Indeed, it has been recently shown by our group and others that LCK is not fully enzymatically active without phosphorylation of Y394 (Philipsen et al., 2017, Liaunardy-Jopeace et al., 2017). Moreover, an additional form of open/active LCK exists in which both regulatory tyrosine residues are phosphorylated. This **double-phosphorylated** form accounts for ~20% of all LCK in T lymphocyte (**Fig. 1.5**) (Nika et al., 2010, Hui and Vale, 2014).

Currently, it is believed that CD45 acts predominately positively on LCK activity by dephosphorylating Y505 (D'Oro and Ashwell, 1999, Wong et al., 2008). Two additional phosphatases SHP1 (Src homology region 2 domain-containing phosphatase-1) and PEP (PEST domain-enriched tyrosine phosphatase) have also been shown to dephosphorylate LCK on Y394 (Gjörloff-Wingren et al., 1999, Kosugi et al., 2001). Dephospsphorylation of Y394 suppresses the kinase activity of LCK and drives the kinase back to the "primed/inactive" conformation (**Fig. 1.5, middle**).

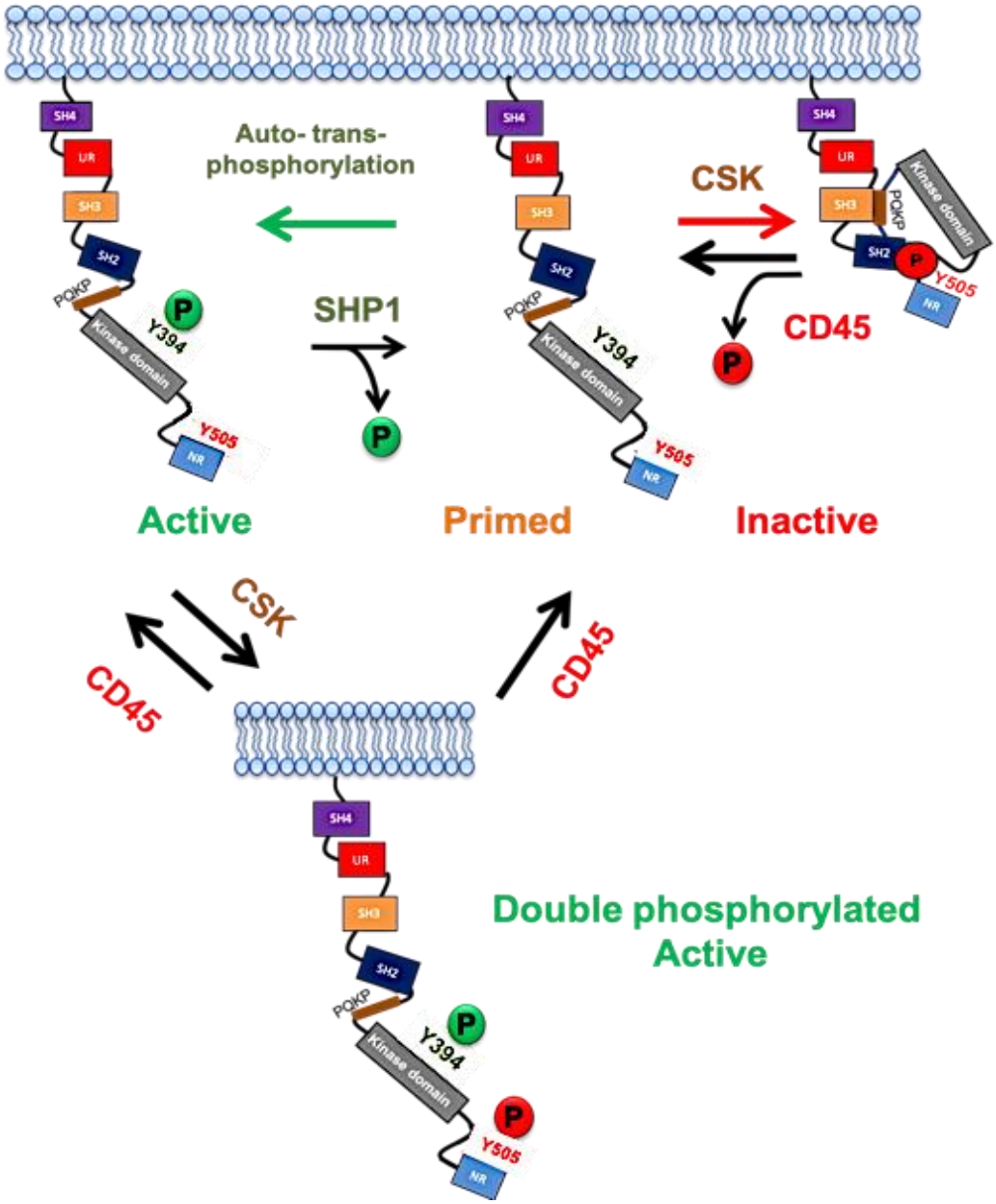

Figure 1.5: Regulation of LCK activation
Upon phosphorylation of Y505 by CSK, LCK adopts the "***closed/inactive***" conformation (please read the carton from right to left). CD45 dephosphorylates Y505 and shifts LCK to an open but not active conformation, the so called "***primed***" conformation. *De novo* auto- trans-phosphorylation of Y394 fully activates LCK, which adapts the "***open/active***" conformation. LCK can return to the "***primed***" conformation after de-phosphorylation of Y394 by phosphatases (mostly SHP1). LCK can also exist in a form in which the protein is **double-phosphorylated** on both regulatory tyrosine residues and is catalytically active (depicted below). PQKP: proline rich motif Pro-Gln-Lys-Pro in the linker region of SH2-kinase domain.

1.5.3 Role of LCK in T-cell activation

T-cell activation is initiated upon triggering of the TCR. In humans, 95% of T lymphocytes express a TCR consisting of an αβ heterodimer. On the other hand, in 5% of T cells the TCR is composed of a γδ chain (Holtmeier and Kabelitz, 2005). Every T cell possesses a unique TCR recognizing with high specificity antigenic peptide ligands presented in complex with MHC (major histocompatibility complex) molecules on the surface of antigen-presenting cells (APCs). The αβ TCR is associated with one ζζ-chains homodimer and CD3 chains: two heterodimers εδ and εγ, respectively.

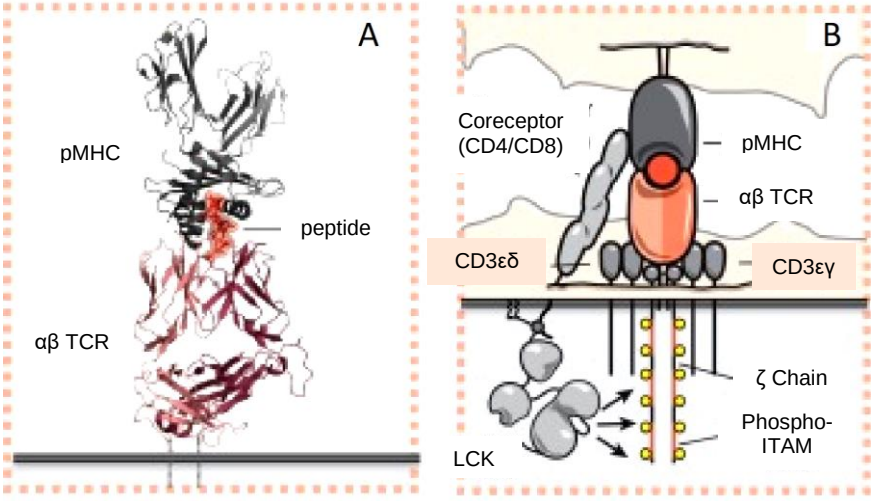

Figure 1.6: Schematic representation of the T-cell antigen receptor (TCR)
A) The TCR is crucial for the recognition of antigens. In humans, the TCR consists predominantly of an αβ heterodimer. Each T cell possesses a TCR with unique properties for peptide-MHC (pMHC) complex binding B) The αβ TCR is associated with one ζζ-chain homodimer and with two CD3 heterodimers εδ and εγ, respectively. The ζ and CD3 subunits contain tyrosine residues within a conserved sequence YxxL/I-X6-8-YxxL/I (where x is any amino-acid, Y is a tyrosine residue, I is isoleucine and L is leucine) called ITAM (Immune-receptor-Tyrosine-based-Activation-Motif). Upon phosphorylation of the ITAMs by LCK, signaling can be further propagated (modified from (Courtney et al., 2018).

The TCR requires the ζ-chains and CD3 chains in order to carry out signal transduction. The CD3 subunits contain tyrosine residues within a conserved sequence YxxL/I-X6-8-YxxL/I (where x is any amino-acid, Y is a tyrosine residue, I is isoleucine and L is leucine) called ITAM (Immune-receptor-Tyrosine-based-Activation-Motif) (Love and Hayes, 2010) (**Fig. 1.6**).The recognition of peptides-MHC (pMHCs) by a T cell leads to the formation of the **immunological synapse** (IS) (or immune synapse). The IS is the interface between an APC and a T cell. The IS is the site where the TCR is triggered by

its antigen ligand. The IS, also known as supramolecular activation cluster (SMAC), is composed of three concentric rings comprising membrane receptors and their underlying cytoskeletal and signaling proteins (Alarcón et al., 2011). The inner circle, or central supramolecular activation cluster (cSMAC), concentrates most of the TCR and the costimulatory molecule CD28. The cSMAC is surrounded by the peripheral SMAC (pSMAC) containing the lymphocyte function-associated antigen-1 (LFA-1), which mediates the initial interaction of a T cell with a target cell via binding to adhesion molecules (such as ICAM-1 or ICAM-2). The most external ring or distal SMAC (dSMAC) is where proteins with large ectodomains and phosphatases (e.g. CD43 and CD45) are located in order to be excluded from the cSMAC (Davis and Dustin, 2004).

The subsequent initiation of downstream intracellular signaling and the mechanism that drives it remain enigmatic, despite years of intensive studies. Several models on the initiation of TCR signaling have been proposed (reviewed in Courtney et al., 2018). A recently proposed model suggests that the TCR exists in an equilibrium between a resting (inactive) and active state, prior to ligand binding (Swamy et al., 2016). Binding to pMHC stabilizes the active conformation of the TCR, thus allowing signaling. There is evidence that CD3 chains associate with acidic phospholipids of the plasma membrane (Aivazian and Stern, 2000). This interaction appears to stabilize a folded (inactive) structure of the TCR/CD3 complex and buries the tyrosine residues of the ITAMs in the plasma membrane of resting T cells, thus precluding their phosphorylation by LCK and unwanted signaling.

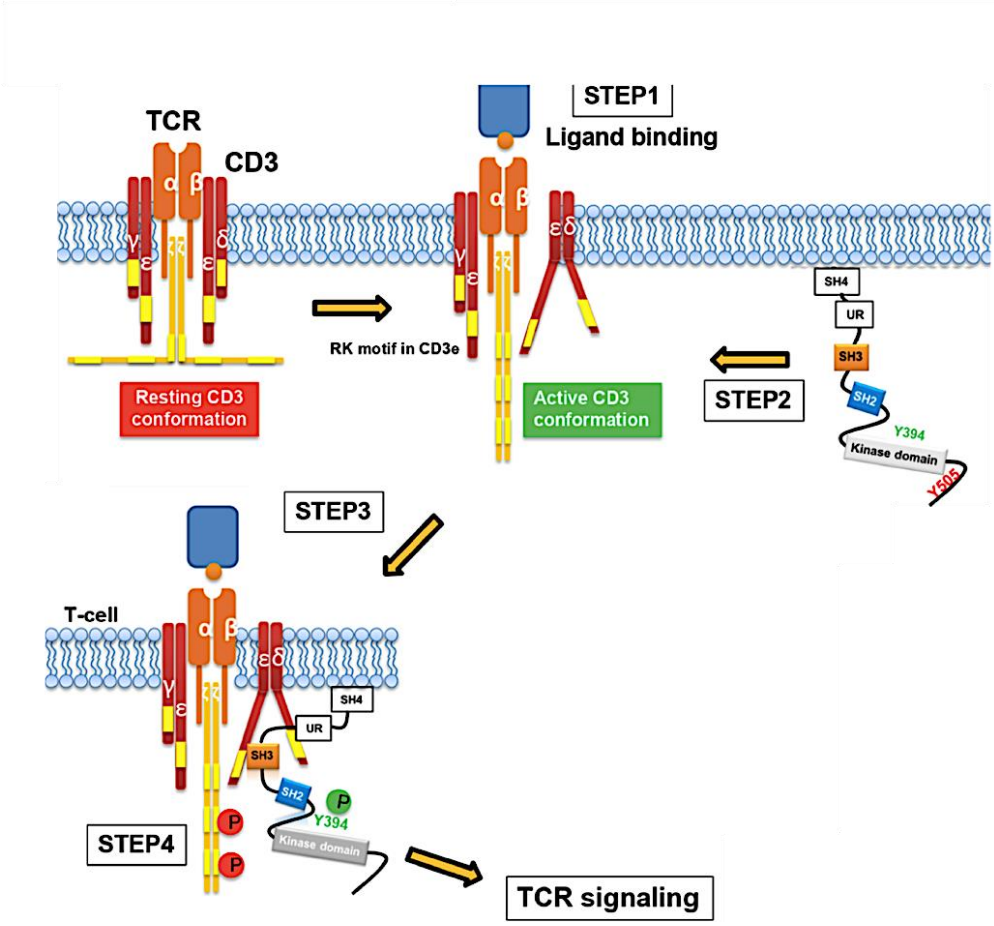

Figure 1.7: Proposed model for the initiation of TCR signaling
the TCR/CD3 complex exists in an equilibrium between a resting (inactive) and primed (active) state, Cholesterol binding stabilizes the inactive conformation of the TCR/CD3 complex under steady-state conditions, whereas pMHC binding stabilizes the active conformation of the TCR/CD3 complex, which becomes available for phosphorylation by LCK (**STEP 1**). LCK is recruited to the TCR/CD3 complex upon ionic interactions between acidic residues in the unique region of LCK and the basic residue-rich sequences of CD3ε (receptor kinase motif (RK) motif) (**STEP 2**). The LCK-CD3ε interaction stabilizes both LCK and the TCR/CD3 complex in the open conformation. Opening of LCK facilitates its *de novo* activation (**STEP 3**), thereby allowing phosphorylation of the ITAMs and subsequent signal transduction.

LCK is critical for the initiation of TCR signaling. Phosphorylation of the tyrosine residues in the ITAMs of the TCR/CD3 complex by LCK converts an extracellular recognition event (TCR-pMHC binding) into an intracellular biochemical signal. However, the events that link the adoption of the “active” conformation of TCR/CD3 complex and the phosphorylation of the ITAMs by LCK remains still to be investigated. It was believed that co-receptors CD4/CD8 are able to bind weakly to non-polymorphic regions of MHC I and II molecules, thus bringing LCK in close proximity with the TCR/ζ-chains complex. However, it has been recently proposed that LCK is recruited to the TCR/CD3 complex via ionic interactions between acidic residues in the UR domain of LCK and the

basic residue-rich sequences of TCR/CD3ε chains (**Fig. 1.7)** (Li et al., 2017, Hartl et al., 2020).

Another issue that still remains in the center of ongoing scientific discussion is how LCK is activated (Simeoni, 2017). According to the so called "standby" model, 40% of total LCK is constitutively activated in resting naïve T cells and the levels of LCK activation (Y394 phosphorylation) do not change upon TCR ligation (Nika et al., 2010). According to this model, there is no need of "*de novo*" LCK activation, because the available pool of active LCK is recruited to the TCR/CD3 complex, where it can phosphorylate the ITAMs. However, our group has recently demonstrated that a significant fraction of LCK (about 20%) is *de novo* activated at the engaged TCR upon antigen recognition ("*de novo* activation" model) (Stirnweiss et al., 2013, Philipsen et al., 2017).

Once phosphorylated, the ITAMs create binding sites for the tandem SH2 domains of the cytosolic tyrosine kinase ZAP-70. The binding to the phosphorylated ITAMs results in (i) the recruitment of ZAP-70 to activated receptor and (ii) the disruption of the autoinhibited conformation of ZAP-70 (Yan et al., 2013). Full activation of ZAP-70 requires phosphorylation by LCK. LCK contributes to the activation of ZAP-70 by phosphorylating Y319 and Y315 in the interdomain B of ZAP-70 (**Fig. 1.8**). Auto- trans- phosphorylation of tyrosine residue Y493 in the activation loop of the kinase domain of ZAP-70 is necessary in order to fully activate ZAP-70 (LoGrasso et al., 1996). Activated ZAP-70 phosphorylates the transmembrane adaptor protein LAT (linker for activation of T cells), thus promoting the formation of the LAT signalosome (Courtney et al., 2018). It was recently proposed that LCK also facilitates ZAP-70-mediated LAT phosphorylation (Lo et al., 2018). It was found that LCK associates via its SH3 domain with a proline-rich motif in LAT and via its SH2 domain to phosphorylated ZAP-70. Therefore, this model proposes that LCK acts as a molecular bridge that facilitates the interaction between ZAP-70 and LAT.

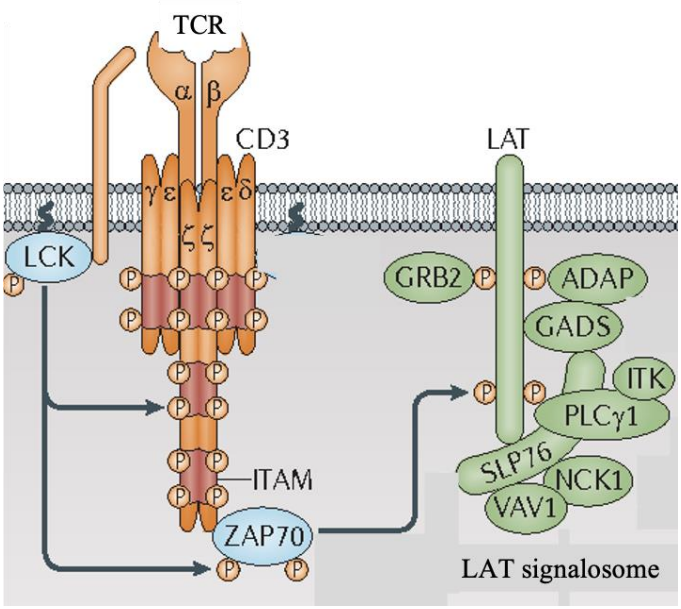

Figure 1.8: Initiation of TCR signaling and assembly of the LAT signalosome
Phosphorylation of the ITAMs of the TCR/CD3 complex by LCK creates binding sites for ZAP-70. ZAP-70 binds to the activated ITAMs and its autoinhibited conformation is released. Full activation of ZAP-70 requires phosphorylation by LCK and auto- trans- phosphorylation. Activated ZAP-70 phosphorylates the transmembrane adaptor protein LAT, thus promoting the formation of the LAT signalosome. Important molecules that constitute the LAT signalosome complex include PLCγ, GRB2, GADS, SLP-76, SOS, ADAP, ITK, NCK1 and VAV1 (modified from Brownlie and Zamoyska, 2013).

The LAT signalosome consists of a macromolecular complex that is crucial for the connection of the TCR (at the plasma membrane) to distal signaling cascades (Werlen and Palmer, 2002). Important molecules that constitute the LAT signalosome complex include phospholipase Cγ-1 (PLCγ-1), growth factor receptor-bound protein 2 (GRB2), GRB2-related adaptor protein GADS, SH2 domain-containing leukocyte protein of 76kDa (SLP-76), son of sevenless protein (SOS), adhesion and degranulation promoting adapter protein (ADAP), interleukin-2-inducible T-cell kinase (ITK), NCK1 and VAV1 (**Fig. 1.8**) (Brownlie and Zamoyska, 2013).

The formation of the LAT signalosome is crucial for the activation of PLCγ-1, via ITK-mediated phosphorylation at Y783 (Perez-Villar and Kanner, 1999). Subsequently, PLCγ-1 hydrolyzes PIP_2, thus generating the second messengers inositol 1,4,5-triphosphate (IP_3) and diacylglycerol (DAG). IP_3 diffuses in the cytoplasm and binds to its receptor (IP3R) on the endoplasmatic reticulum (ER). This event causes the release of the intracellular Ca^{2+} stores from the ER. In turn, the calcium depletion from the ER leads to extracellular calcium influx from the calcium release-activated channels (CRAC) located at

the plasma membrane (**Fig. 1.9**)(Feske et al., 2006). Elevated levels of cytosolic Ca^{2+} activate signaling events which lead to the activation of the transcription factor NFAT. On the other hand, DAG activates protein kinase C (PKC) and RASGRP1. RASGRP1 and SOS action lead to the rapid activation of the RAS pathway (RAS-RAF-MEK-ERK cascade) which culminates in the activation of the transcription factor AP1 (Warnecke et al., 2012, Jun et al., 2013, Poltorak et al., 2014). In parallel, activated PKC orchestrates the assembly of the CBM complex (caspase recruitment domain family, member 11 [(CARD11)-B-cell chronic lymphocytic leukemia/lymphoma 10 (BCL10)-mucosa-associated lymphoid tissue lymphoma translocation gene 1 (MALT1)] leading to the activation of the transcription factor NF-κB (Thome et al., 2010). Activation of these transcriptional regulators drives gene transcription that culminates into T-cell activation and differentiation. (**Fig. 1.9**) (Acuto et al., 2008, Smith-Garvin et al., 2009, Thome et al., 2010).

Next to its important role in TCR-mediated signaling, LCK displays key function in co-stimulatory CD28 signaling. T-cell activation is characterized by the fact that solely TCR-mediated signaling result in T-cell anergy, a non-responsive state of T cells. Among other cell surface receptors, CD28 co-stimulation provides the most robust signaling for the avoidance of T-cell anergy. Although CD28 doesn't have intrinsic enzymatic activity, its cytoplasmic tail contains highly conserved tyrosine-based signaling motifs that are phosphorylated upon TCR or CD28 stimulation. Therefore, proteins with SH2 domains are able to bind in a phosphotyrosine-dependent manner to CD28. Moreover, CD28 cytoplasmic tail possesses proline rich sequences that offers binding sites for SH3-domain containing proteins. In particular, the YMNM (tyrosine-methionine-asparagine-methionine) and PYAP (proline-tyrosine-alanine-proline) motifs have been shown to associate with several kinases and adaptor proteins (Esensten et al., 2016). Upon association of CD28 ligands CD80 or CD86, it has been suggested that signaling events downstream of the PYAP motif include the phosphorylation and activation of the kinases PDK1 (3-phosphoinositide-dependent protein kinase 1) and PKCθ (protein kinase C-theta), leading to the activation of the NF-κB, AP-1, and NF-AT transcription factors. It is generally accepted that LCK mediates the phosphorylation of

tyrosine residues in both CD28 cytoplasmic motifs. It is proposed that LCK binds, via its SH3 domain, to the C-terminal PYAP motif and activates the NF-κB activation pathway (Holdorf et al., 1999). CD28-bound LCK is believed to phosphorylate PDK1 on Y9 (Park et al., 2001). Subsequently, PDK1 phosphorylates and activates PKCθ, an important downstream effector of CD28. Alternatively, LCK may bind to the PYAP motif of CD28 also via its SH2 domain in a phosphotyrosine-dependent manner (King et al., 1997). In this case, interaction of the V3 domain of PKCθ with the SH3 domain of CD28-bound LCK may bring in proximity PDK1 and PKCθ (Kong et al., 2011).

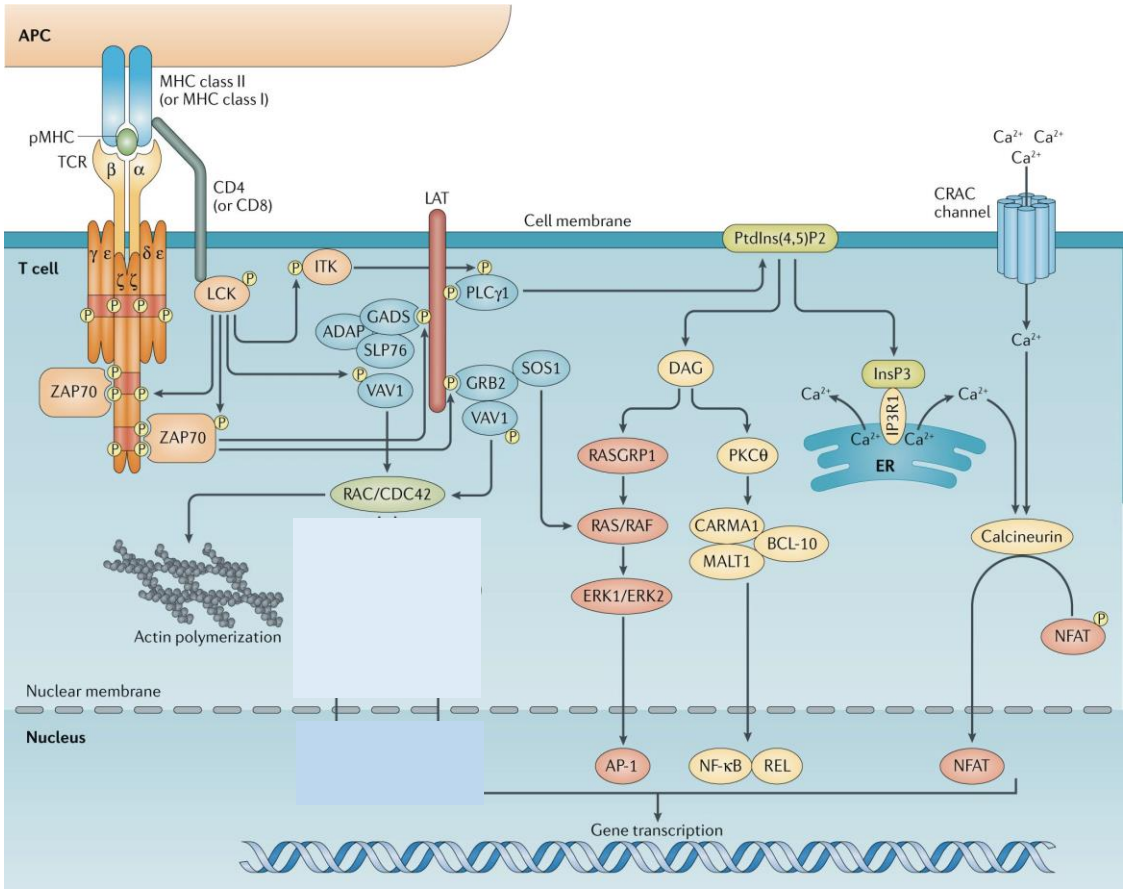

Figure 1.9: T-cell activation
Activated ZAP-70 phosphorylates LAT and promotes the formation of the LAT signalosome. PLCγ-1 is activated via ITK-mediated phosphorylation at Y783. PLCγ-1 cleaves PIP2 in order to generate the secondary messengers IP3 and DAG. IP3 diffuses in the cytoplasm and binds to its receptor (IP3R) on the ER. This event causes the release of the intracellular Ca^{2+} stores from the ER. In turn, the calcium depletion from the ER leads to extracellular calcium influx from the CRAC channels. Elevated cytosolic Ca^{2+} activates signaling events which lead to the dephosphorylation and activation of the transcription factor NFAT (nuclear factor of activated T cells). DAG activates PKCθ and RASGRP1. RASGRP1 and SOS action lead to the rapid activation of the RAS pathway (RAS-RAF-MEK-ERK cascade) which culminates in the activation of the transcription factor AP1. In parallel, activated PKCθ orchestrates the assembly of the CBM complex (CARD11- BCL10- MALT1) leading to the activation of the transcription factor NF-κB. Activation of these transcriptional regulators drives gene transcription that culminate into T-cell activation and differentiation. RAC and CDC42 RAS-related GTP-binding proteins control the assembly and disassembly of the actin cytoskeleton in response to extracellular signals (modified from Gaud et al., 2018).

1.5.4 Feedback regulation of LCK by post-translational modifications

Despite the crucial role of the regulatory Y394 and Y505, LCK activity and function is additionally regulated by post-translational modifications on other amino acid residues. Y192, which is located within the SH2 domain of LCK (**Fig. 1.4**), has been suggested to play an important role in the regulation of LCK activity. Early studies have reported that upon TCR stimulation a significant proportion of LCK is phosphorylated on Y192 (Couture et al., 1996, Granum et al., 2014, Kästle et al., 2020). Moreover, these studies have proposed that phosphorylation of Y192 can alter the specificity of the SH2 domain of LCK for the phosphorylated Y505 residue. Although the exact details of Y192 phosphorylation remain unclear, several kinases have been suggested to phosphorylate Y192. A recent study suggested that ZAP-70 is responsible for the inhibition of LCK by phosphorylating Y192 (Goodfellow et al., 2015).

Two additional recent studies showed that a phosphomimetic Y192E LCK mutant is uncapable of inducing TCR signaling and thymocyte maturation (Courtney et al., 2017, Kästle et al., 2020). The authors also suggested that phosphorylation on Y192 attenuates the association between LCK and phosphatase CD45 (Courtney et al., 2017). In this way, CD45 cannot longer dephosphorylate LCK, which in turn becomes hyperphosphorylated on Y505 and hence inactivated (**Fig. 1.10A**).

Phosphorylation of Serine 59 (S59), located within the unique region of LCK, has also been suggested to play a crucial role in the regulation of LCK activity and function. In the early 1990s, it was demonstrated that LCK is phosphorylated on S59 by ERK1/2, a MAP kinase downstream of LCK in the TCR signaling cascade (Watts et al., 1993). Moreover, it was reported that phosphorylation of S59 was capable of reducing the activity of LCK in vitro. A more recent study reported that T cells stably expressing the S59E LCK mutant, which mimics phosphorylation on S59 (serine to glutamic acid substitution) showed a reduction in TCR-mediated signaling. Conversely, T cells stably expressing a S59A LCK mutant, which mimics the non-phosphorylated form S59 (serine to alanine substitution) showed an induction in TCR-mediated signaling (Dutta et al., 2017). In the same study, it was also demonstrated that S59 of LCK is a substrate for the serine–threonine phosphatase Calcineurin

(Dutta et al., 2017). However, a report from Stefanova and coworkers proposed a positive role for S59 phosphorylation on LCK activity and TCR-mediated signaling (Stefanová et al., 2003). In this study, T cells transfected with a S59A LCK mutant showed a reduced TCR signaling, whereas the opposite was observed with T cells expressing the S59E mutant. Moreover, it was shown that S59 phosphorylation interferes with the interaction between LCK and the phosphatase SHP1, as S59E LCK has a diminished binding to SHP1. In line with these findings, our research group has shown that inhibition of ERK-mediated LCK phosphorylation on S59 resulted in a reduction of its activity and rapid termination of TCR-mediated signaling (Poltorak et al., 2013) (**Fig. 1.10B**).

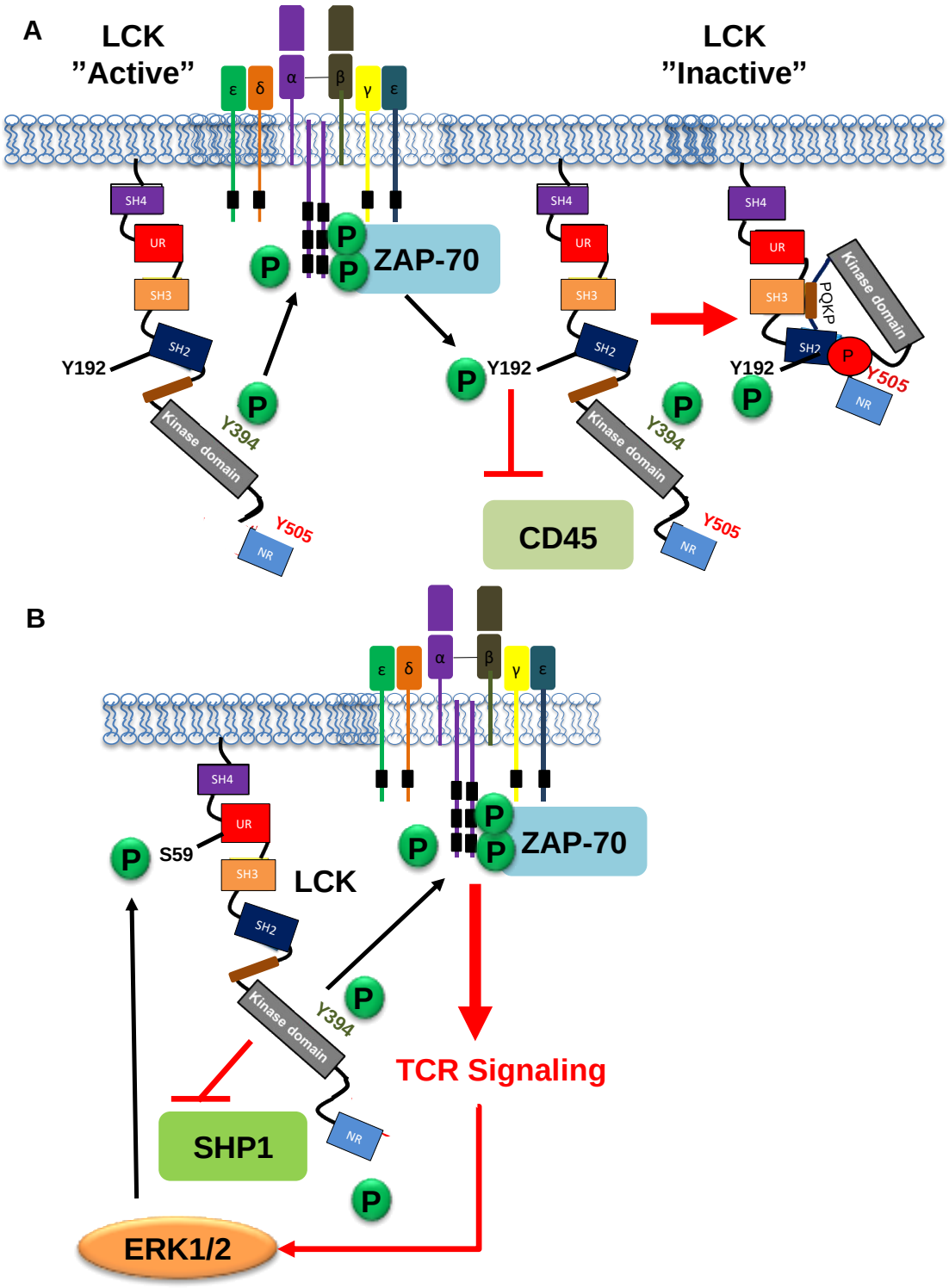

Figure 1.10: Positive and negative feedback regulation of LCK by post-translational modifications
A) Phosphorylation of LCK Y192 by ZAP-70 is proposed to disrupt the interaction of LCK with the phosphatase CD45 and therefore the activation of the kinase via dephosphorylation of Y505. B) A positive feedback loop that involves ERK-mediated phosphorylation of LCK on S59 abrogates the interaction between LCK with SHP1, thus keeping LCK active and functional in order to initiate downstream signal transduction and T-cell activation.

1.5.5 Regulation of LCK expression by the chaperone HSP90 and Cbl-mediated ubiquitination

Newly synthesized proteins are at great risk of abnormal folding and aggregation, which can potentially lead to generation of toxic products. To avoid such a danger, cells have developed a complex network of proteins named molecular chaperones, which use sophisticated mechanisms to prevent aggregation and promote efficient protein folding (Hartl et al., 2011). The stabilization, folding, and functional regulation of a selected group of proteins, which are involved in signal transduction, are regulated by the cytosolic chaperone Heat-shock protein of 90 kDa (HSP90) (Young et al., 2001). Several SFKs including LCK have been reported to interact with HSP90 (Hartson and Matts, 1994). Using geldanamycin and radicidol, two specific inhibitors of HSP90 that bind with high affinity to the ATP-binding site of the chaperone, it was shown that HSP90 is indispensable for the synthesis, membrane targeting and maintenance of LCK (Bijlmakers and Marsh, 2000).

The recruitment of protein kinase clients to HSP90 needs the assistance of the cochaperone CDC37. CDC37 binds between the two kinase lobes of an early folded immature client of HSP90. Subsequently, CDC37 interacts with the N terminal domain of an open HSP90. CDC37 binding facilitates client-protein folding, conferring specificity and arresting the ATPase cycle of HSP90 during client protein loading (Roe et al., 2004, Verba and Agard, 2017). LCK interacts with the cochaperone CDC37 via its N-terminal lobe, requiring also the a-C-helix and β4- and β5-strands of this lobe (Prince and Matts, 2004). Conversely to these studies, published data from our group show that CDC37 is dispensable for the regulation of LCK activity/stability (Kowallik et al., 2020).

Regarding the activation and conformational state of LCK, initially it was shown that only the constitutively active form of LCK required stabilization from HSP90 (Hartson et al., 1996). In agreement with this observation, a different study showed that the ***primed/inactive*** and ***closed/inactive*** forms of LCK do not require binding to HSP90 in order to prevent degradation (Nika et al., 2010). However, Giannini and Bijlmakers showed that HSP90 is also important for the stability of activated LCK upon TCR-mediated stimulation (Giannini and Bijlmakers, 2004a).

After its activation, LCK is subjected to the negative regulation of CBL-family ubiquitin ligases, which function by facilitating LCK ubiquitination and subsequent targeting to lysosomes. There are three classes of enzymes mediating ubiquitination: E1 that activates ubiquitin and transports it to E2-conjugating enzyme, which attach ubiquitin on the substrate, and E3 ligase which interacts selectively with the substrate (Liu et al., 2014). It has been demonstrated that LCK associates with the E3 ligase Casitas B-lineage lymphoma proto-oncogene (CBL), upon TCR- and CD4-mediated activation. CBL-dependent ubiquitination targets LCK for proteasomal degradation (Rao et al., 2002). Therefore, CBL is a negative regulator of LCK and T-cell activation.

1.6 Role of LCK in diseases

To date, several kinases have been established as key mediators in multiple pathological conditions. Given the major role of LCK in T-cell activation, signaling, and development, alterations in its expression and kinase activity are known to be critical factors for several inflammatory mediated pathological conditions (Page et al., 2009). Patients with LCK deficiency frequently have forms of immune deficiency and autoimmunity (see below) (Kumar Singh et al., 2018). On the contrary, over-expression of LCK can lead to other diseases like cancer, asthma, diabetes 1, rheumatoid arthritis and organ graft rejection (Bommhardt et al., 2019). The role of LCK in human diseases is summarized in **Table 1.1** and **Table 1.2** and recently reviewed in Bommhardt et al., 2019.

Disease	Effect on LCK	Mutation	Reference
Idiopathic CD4+ T lymphocytopenia (ICL)	50% reduction of kinase activity	-	Hubert et al., 2000
Common variable immunodeficiency (CVID)	Reduction of LCK expression	LCK transcript, lacking the entire exon 7	Sawabe et al., 2001
Severe combined immune deficiency (SCID)	Reduction of LCK expression	LCK transcript, lacking the entire exon 7	Goldman et al., 1998
Immunodeficiency	Weak expression and no kinase activity of LCK	L341P mutation	Hauck et al., 2012
Asthma	Overexression of LCK	-	Pernis and Rothman, 2002
Atherosclerosis	Increased LCK kinase activity	-	Liu et al., 2020
Autoimmune mediated Type I diabetes	Increased LCK kinase activity	-	Nervi et al., 2000
Organ graft rejection	Increased LCK kinase activity	-	Wen et al., 1995

Table 1.1: LCK role in immunodeficiency, autoimmunity and organ graft rejection
The table summarizes the effects of LCK expression, kinase activity, as well as LCK mutations in diseases.

Disease	Effect on LCK	Role in the disease	Reference
Thymoma	Overexpression or dysregulated LCK	Abnormal proliferation of immature thymocytes	Thomas et al., 1999
Thymoma	Mis-localization of LCK	Thymic tumorigenesis	Salmond et al., 2011
Breast cancer	LCK expression in non-lymphoid tumor cells	Breast cancer progression	Köster et al., 1991
Colorectal cancer	LCK expression in non-lymphoid tumor cells	Potential diagnostic biomarker	Veillette et al., 1987
Lung carcinoma	LCK expression in non-lymphoid tumor cells	Stem cell factor (SCF)-mediated proliferation and apoptosis	Veillette et al., 1987
Cholangiocarcinoma	LCK overexpression	Associated with poor prognosis	Sugihara et al., 2018
Endometrioid cancer	LCK overexpression	Resistance to cisplatin	Saygin et al., 2017
Glioma cancer	LCK overexpression	Resistance to cisplatin	Kim et al., 2010
Small and non-small cell lung cancer (SCLC and NSCLC)	LCK overexpression	Diagnostic biomarker	D'Andrilli et al., 2012
Chronic lymphocytic leukemia (CLL)	LCK expression in B cells or ectopic expression of LCK	Negative correlation with responsiveness to pharmacological treatment Better survival and proliferation of B cells	Theofani et al., 2018
Acute lymphoplastic leukemia (ALL)	LCK overexpression and hyperactivation	B cell proliferation and survival	Accordi et al., 2010
Acute myeloid leukemia (AML)	LCK expression	Enhanced Proliferation and survival Pharmacological target	Rouer et al., 1994

Table 1.2: LCK functions in Cancer diseases
The table summarizes forms of cancer in which LCK was reported to be involved.

1.7 Redox regulation in adaptive immunity and T-cell functions

Growing evidence indicates that reactive oxygen species (ROS) and reactive nitrogen species (RNS) have a physiological role in many cell types of the immune system due to their role in signaling processes. ROS have various effects on T-cell function and proliferation (Belikov et al., 2015).

Although the exact effect of ROS on T cells function remains unclear, the balance between ROS accumulation (e.g. endogenously by chronically stimulated T cells or ROS-generated by activated granulocytes and macrophages during inflammation) and the oxidative stress caused by redox milieu in their microenvironment is an important factor that determines T-cell function, activation, and inactivation. While their accumulation can become cytotoxic and lead to apoptosis/necrosis, lower concentrations of ROS in T cells are a prerequisite for cell survival (Simeoni and Bogeski, 2015, Simeoni et al., 2016). Therefore, they function in a concentration-dependent manner.

Along with proinflammatory cytokines, ROS can also enhance and prolong the antigen-specific proliferative response in T cells (Sena et al., 2013). Furthermore, the redox state could modulate T-cell differentiation (generation of different T-cell subsets). Moreover, the differential ROS susceptibility of the various T-cell subsets has been proposed to alter the outcome of an immune response (Kesarwani et al., 2013).

ROS and RNS affect multiple cellular components, such as DNA, proteins, and lipids. The cellular redox level of a T cell can affect and modulate various signaling cascade including TCR signaling. An important role of ROS and RNS in signal transduction is the modulation of the activity of protein tyrosine or serine kinases and phosphatases via oxidative post-translational modifications (Nathan and Cunningham-Bussel, 2013).

1.7.1 ROS and RNS sources

ROS and RNS can be divided in two groups: free radicals and non-radicals. Free radicals include singlet oxygen ($^1O_2$), superoxide ($O_2^{\bullet-}$), hydroxyl ($HO^{\bullet}$), hydroperoxyl ($HO_2^{\bullet}$), carbonate ($CO_3^{\bullet-}$), peroxyl ($RO_2^{\bullet}$), alkoxyl ($RO^{\bullet}$), and carbon dioxide radical ($CO_2^{\bullet-}$). The non-radicals include hydrogen peroxide (H_2O_2), hypobromous acid (HOBr), hypochlorous acid (HOCl), ozone (O_3),

organic peroxides (ROOH), peroxynitrite ($ONOO^-$), peroxynitrate ($O2NOO^-$), peroxynitrous acid (ONOOH), peroxomonocarbonate ($HOOCO_2^-$), nitric oxide (NO), and hypochlorite (OCl^-) (Di Meo et al., 2016). Incomplete electron reduction of O_2 leads to superoxide production and ultimately conversion into H_2O_2 by superoxide dismutases (SOD). Among ROS, H_2O_2 has a longer biological lifespan and higher stability and it is believed to be an important signaling molecule. The cellular levels of ROS/RNS are strongly regulated by various detoxifying enzymes, such as SOD, glutathione peroxidase (GPX), and catalase (CAT), or by different antioxidants, including flavonoids, ascorbic acids, vitamin E, and glutathione (GSH) (Ray et al., 2012).

The main intrinsic source of ROS is mitochondria, where ROS are produced via the mitochondrial electron-transport system (Zorov et al., 2014). Within the mitochondria, superoxide is the type of ROS that is primarily produced. Most of the superoxide is converted to hydrogen peroxide by the action of superoxide dismutase. Several enzymes of the electron transport chain including Complexes I and III and glycerol-3-phosphate dehydrogenase have been shown to host the production of superoxide in mitochondria (Lambert and Brand, 2009). The main non-mitochondrial source of ROS is NOX (NADPH oxidase) that facilitate superoxide formation via oxygen reduction mediated by the electron donor NADPH. There exist seven mammalian NOX isoforms which are NOX1-5, Dual oxidase 1 (DUOX1), and (DUOX2) (Lambeth, 2004). In T cells, $O_2^{\bullet-}$ and H_2O_2, are rapidly generated upon TCR stimulation in a sustained manner for up to 60 min after stimulation, via most likely NOX2 and DUOX1 enzymes (predominant in T cells (Belikov et al., 2014, reviewed in Simeoni and Bogeski, 2015). Generation of ROS takes also place in the smooth ER that presents a chain of electron transport, constituted by two systems devoted to xenobiotic metabolism and introduction of double bonds in fatty acids. Accumulating evidence suggests that ROS production in the ER, during ER-stress conditions, is related with redox signaling mediators such as protein disulfide isomerase (PDI)-endoplasmic reticulum oxidoreductin (ERO)-1, glutathione (GSH)/glutathione disulphide (GSSG), NADPH oxidase 4 (NOX4), NADPH-P450 reductase (NPR), and calcium (Zeeshan et al., 2016). Several other cellular enzymes are involved in process of ROS generation, such as

xanthine oxidoreductase, nitric oxide (NO) synthase, cytochrome P_{450} monoxygenase, lipoxygenase, and cyclooxygenase (Abdal Dayem et al., 2017). Nitric oxide synthases (NOS) (three major isoenzymes are known: neuronal nNOS, inducible iNOS, and endothelial eNOS) synthesize NO by conversion of L-arginine to L-citrulline (Knowles and Moncada, 1994, Alderton et al., 2001). iNOS and endothelial (e)NOS influence both T-cell activation and the differentiation programs of T cells (García-Ortiz and Serrador, 2018).

1.7.2 Oxidative post-translational modifications

The specific effects of ROS/RNS are mediated partially through the covalent modification of specific cysteine (Cys) residues found within several proteins. The cysteine side chain possesses unique properties that permit a variety of different oxidative post-translational modifications (Wani et al., 2014). The side chain of a cysteine residue contains a thiol (-SH) functional group. The sulfur atom of the thiol is electron rich and facilitates multiple oxidation states. The specific reactivity of each cysteine thiol is strongly correlated with their p*Ka,* which represents the ability to form the anionic form of the sulfur, called thiolate (R-S–) (much more reactive than the thiol). Furthermore, the microenvironment of the protein, in terms of the local polarity and interactions with neighboring residues and also the type of oxidants, influence the redox potential of each cysteine thiol (Chung et al., 2013).

As illustrated in **Fig. 1.11**, the availability of different oxidation states permits the formation of a diverse range of oxidative post-translational modifications. Most of the cysteine oxidative modifications are reversible and they can be reduced back to a free thiol (SH) by the antioxidant defense system or converted to other oxidative modifications, depending on the cell's redox-state (Kaludercic et al., 2014). The first oxidation step of cysteinyl thiols (Cys-SH) by H_2O_2 leads to cysteine sulfenic acid (Cys-SOH) formation (named S-sulfenylation). Under more oxidative conditions, sulfenic acid can be further oxidized to more stable products, such as sulfinic (Cys-SO_2H) or sulfonic (Cys-SO_3H) acid. These higher oxidation states have been generally regarded as irreversible. To avoid this dangerous pathway, the electrophilic sulfur atom (-SOH) can react with an intramolecular neighboring protein thiol nucleophile to

form a stable disulfide bond (RS-SR) (Beedle et al., 2016). Reactive nitrogen species (RNS) like nitrogen oxide (NO) can react with cysteine residues causing *S*-nitrosylation (SNO). Cysteine residues can also undergo other types of post-translational modifications such as sulfhydration (SSH) and S-glutathionylation (SSG) (Alcock et al., 2018).

Antioxidants and antioxidant enzymes are thiol based. Among them, glutathione (GSH, γ-L-Glutamyl-L-cysteinylglycine) acts as a redox buffer and a cofactor of other enzymes including glutathione peroxidases (GPX) that scavenge peroxides generating oxidized glutathione (GSSG) (Forman et al., 2009). In humans, the key peroxide scavengers are peroxiredoxins. Two of them thioredoxins (TRX) and glutaredoxins (GRX) reduce oxidized protein thiols. Oxidized TRX and GRX can be reduced by TRX reductases (TRXR) and GSH, respectively (Fra et al., 2017).

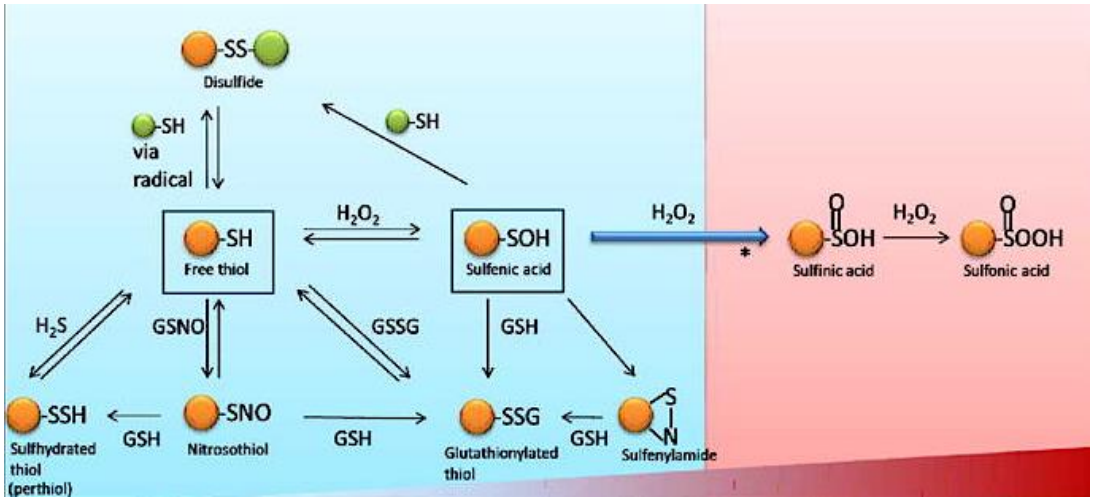

Figure 1.11: Oxidative post-translational modifications of cysteine
(**Left**) In the blue color area, reversible modifications are represented. These modifications include: disulfide bond formation (top), sulfhydration, *S*-nitrosylation, *S*-glutahionylation, (bottom) and sulfenylation (middle). (**Right**) Once formed, the sulfenic acid (SOH) can be reduced to thiol or further oxidized to generate sulfinic and sulfonic acid. In the red area are represented irreversible modifications that are detrimental to cell functions (modified from Chung et al., 2013).

1.8 Regulation of protein tyrosine phosphatases (PTPs) by reversible oxidation

PTPs are enzymes that remove phosphate groups from phosphorylated tyrosine residues on proteins (dual-specificity PTPs can also remove serine/threonine residues). Oxidation of PTPs leads to their reversible inactivation. Therefore, oxidized and inactivated PTP are unable to fulfill their physiological role and intracellular signal transduction is strongly impacted (Ostman et al., 2011). PTPs have at least one catalytic domain with a conserved signature motif (I/V)H**C**SAGXXR(S/T)G that contains the catalytic cysteine. This residue is essential for catalyzing the removal of the phosphate group from phosphorylated tyrosine residues. It was shown that H_2O_2 can inhibit PTPs via oxidation of this cysteine residue in their catalytic center (Huyer et al., 1997). PTPs are reversibly oxidized, in an intermediate state, to sulfenic acid (SOH). This state rapidly rearranges to form a sulfenylamide with a nitrogen or a disulfide bond with a nearby cysteine. These states contribute to protect the catalytic cysteine from further irreversible hyperoxidation to sulphinic acid (SO_2H) or sulphonic acid (SO_3H) states (Wu et al., 2017).

In T and B cells many functionally important PTPs have been reported to be oxidized, and thus inactivated by ROS. Both CD45 and SHP1, which as previously described have a pivotal role in TCR proximal signaling, were shown to be inactivated upon hydrogen peroxide treatment in T cells (Secrist et al., 1993 and Cunnick et al., 1998, respectively). Additionally, it was shown that, upon antigen ligation, both SHP1 and SHP2, the two members of the SH2-containing PTPs family, undergo sulfenylation in $CD8^+$ T cells (Michalek et al., 2007). These PTPs were also shown to be sulfenylated and inactivated in B cells, thus promoting activation and signal transduction (Capasso et al., 2010). Therefore, it is likely that through oxidation and inactivation of PTPs, the activation of PTKs is enhanced and hence signal initiation and propagation is promoted (Simeoni and Bogeski, 2015).

1.9 Redox regulation of protein kinases

PTPs and PTKs are the two different sites of the phospho-tyrosine signaling dynamic, with PTPs playing the eraser role and PTKs the writer role of phosphate groups, according to the model proposed by Lim and Pawson (Lim and Pawson, 2010). There is growing evidence that PTKs function can be also directly regulated via oxidative post-translational modifications (Corcoran and Cotter, 2013) and that ROS may directly influence the activity of PTKs (Belikov et al., 2014, Simeoni and Bogeski, 2015, Simeoni et al., 2016). Numerous examples of both RTKs and non-RTKs have been reported to be targets of redox-dependent regulation.

As regarding receptor tyrosine kinases, it has been shown that Platelet-Derived Growth Factor Receptor (PDGFR) stimulation induces covalent receptor dimerization through the formation of disulfide bonds within the extracellular domain (Li and Schlessinger, 1991). In a separate study, mass spectrometry analysis revealed that cysteine residues, C822 and C940 located in the kinase domain, play a crucial role in the enzymatic activity of PDGFR-beta and could be possible targets for redox regulation (Lee et al., 2004). The kinase activity of the Epidermal Growth Factor Receptor (EGFR) was also shown to be regulated via oxidative modification and specifically sulfenylation. Mass spectrometry revealed C797 as the site of EGFR modifyed by oxidation (Paulsen et al., 2011, Modjtahedi et al., 2014). Furthermore, the kinase activity of Vascular Endothelial Growth Factor Receptor (VEGFR) was reported to be negatively regulated through the formation of an intramolecular disulfide bond between C1209 and C1199 (Kang et al., 2011). Exposure of another member of RTKs, the Insulin Receptor Kinase (IRK), to hydrogen peroxide induces oxidation of two residues C1245 and C1308 and contributes to kinase activation via reversing inhibition caused by ADP binding within the catalytic active site (Schmitt et al., 2005).

Regarding non-receptor tyrosine kinases, our group has recently shown that cysteine at position 575 in the tyrosine kinase ZAP-70 regulates the stability and the function of the protein and it is a target for oxidation (Thurm et al., 2017a). This cysteine is highly conserved among tyrosine kinases and previous

studies showed that this residue is oxidized and that it is crucial for the kinase activity of c-SRC (C498), c-RET (C376), and PDGFR-beta (C940) (Kato et al., 2000, Rahman et al., 2010).

1.9.1 Role of cysteine residues in the redox-mediated regulation of SFKs

SRC family kinases have been shown to be regulated via oxidative modifications either from ROS or RNS. As shown in **Table 1.3**, several studies have illustrated the role of cysteine modifications in the regulation of the activation and the enzymatic activity of SRC (Giannoni et al., 2010). For c-SRC, the group of Chiarugi P. proposed that oxidation of C245 and C487 in the SH2 domain and kinase domain leads to a strong activation of the kinase via the formation of an intramolecular disulfide bridge (Giannoni et al., 2005). A different study has shown that SRC activity can also be inhibited upon oxidation of C277, which results in a homodimerization of SRC with a disulfide-bond formation (Kemble and Sun, 2009). A recent study revealed a novel redox-dependent SRC activation mechanism, in which H_2O_2-mediated sulfenylation of SRC residue C185 destabilizes the interaction between phosphorylated Y527 and the SH2 domain, whereas sulfenylation of SRC C277 promotes Y416 autophosphorylation (Heppner et al., 2018)

Many different studies have addressed the role of the Cysteine Clustered (CC) motif, which compromises C483, C487, C496, and C498 in the regulation of SRC activity. Oo et al. reported that cysteines residues of the CC motif could be involved in the regulation of SRC activity via *S*-nitrosylation (Oo et al., 2003). In line with this observation, C498 of c-SRC was found to be a target of *S*-nitrosylation, which stimulates the kinase activity. In the same study also C506 of c-YES, another SFKs member, was found to be nitrosylated (Rahman et al., 2010). Additionally, in a cerebral ischemia and reperfusion model, FYN has also been reported to be a target of *S*-nitrosylation both *in vitro* and in *vivo.* Inhibition of this post-translational modifications could have neuroprotective effect, as it attenuated Ischemia/Reperfusion-induced neuronal degeneration and cell death caused by S-nitrosylation of FYN kinase (Hao et al., 2016). Furthermore, H_2O_2 derived from a wound is responsible for the oxidation of LYN on C466 and subsequent activation of the kinase, which

recruits neutrophil to the wound (Yoo et al., 2011). Collectively, cysteine residues are crucial in the redox-dependent regulation of SFKs activity and function.

SFK Kinase	Oxidation type	Cysteine residue	Impact on the kinase activity	Reference
c-SRC	Disulfide bridge	C245	Activation	Giannoni E. et al., 2005
c-SRC	Disulfide bridge	C487	Activation	Giannoni E. et al., 2005
c-SRC	Disulfide bridge	C277	Inactivation	Kemble D.J. and Sun G., 2009
c-SRC	Sulfenylation	C185	Activation	Heppner D. E. et al., 2018
c-SRC	Sulfenylation	C277	Activation	Heppner D. E. et al., 2018
c-SRC	S-nitrosylation	C498	Activation	Rahman M. A. et al., 2010
c-YES	S-nitrosylation	C506	Activation	Rahman M. A. et al., 2010
FYN	S-nitrosylation	-	Activation	Hao L. et al., 2016
LYN	Sulfenylation	C466	Activation	Yoo S. C. et al., 2012

Table 1. 3: SFKs oxidation
The table summarizes oxidative modifications and the corresponding cysteine residues of SFKs. The impact of the oxidative modification on the kinase activity is also reported**.**

1.9.2 LCK oxidation

LCK has also been suggested to be a target of oxidative post-translational modifications. However, there is no clear evidence about which cysteines are involved in the oxidative post-translational modifications. Furthermore, there exists contradicting experimental evidence about the impact of oxidation on the activity of LCK. In an initial study, T lymphocytes were treated with oxidative reagents such as hydrogen peroxide (H_2O_2) and diamide (Nakamura et al., 1993). Diamide is a thiol-oxidizing agent that easily penetrates cell membranes and rapidly reacts with thiols (such as GSH) and promotes intracellular protein disulfide cross-linking. Treatment with diamide increased tyrosine phosphorylation (of both regulatory residues Y394 and Y505) and the kinase activity of LCK, thus suggesting that LCK mediates redox-sensitive signaling mechanism in T cells. A follow-up study from the same group discovered altered interactions of LCK with proteins of the T-cell signaling machinery upon oxidative stress (Nakamura et al., 1996). This observation suggest that T cells may use a redox-dependent mechanism for the activation of LCK.

Conversely, another study using isolated T cells from HIV patients suggested that oxidation of LCK inhibits its kinase activity by changing its conformational state (Stefanová et al., 1996). In line with this study, the group of Trevillyan J.M. suggested that the kinase activity of LCK can be inhibited via thiol (-SH) oxidation of cysteine residues 378, 465 and 476 in the carboxy-terminal catalytic domain of the kinase (Trevillyan et al., 1999). They proposed a mechanism where the isothiazolone ring of a methyl 3-(N-isothiazolone)-2-thiophenecarboxylate (A-125800) LCK inhibitor reacts with the cysteine residues, thus leading to an inhibitory covalent modification. Furthermore, cysteines 465 and and 476 have been previously suggested to play a crucial role in the catalytic activity of LCK (Veillette et al., 1993).

LCK is also possible to undergo other types of post-translational modifications. In line with this hypothesis, theoretical studies of electrostatic, steric and hydrophobic properties of SFKs proposed that deeply buried cysteine residues (e.g. C465,C476), have the possibility to undergoes *S*-nitrosylation (Andre et al., 2016). Moreover, LCK may also be a target of *S*-glutathionylation,

the reversible formation of a mixed disulfide between an oxidized cysteine residue and glutathione. This modification is considered to protect proteins from further oxidation. Cysteines that are S-glutathionylated are likely to be crucial to the stability or activity of the kinase (Anselmo and Cobb, 2004).

Oxidation of LCK may be crucial for its function and activity. Post-translational modifications of LCK's cysteine residues can lead to activation or deactivation of kinase's enzymatic activity. Moreover, oxidative modifications can culminate into structural or conformational alterations of LCK. Protein-protein interactions or substrate specificity of LCK, may also be influenced from cysteine modifications. In the light of the foregoing oxidation of LCK can be crucial for the function of LCK in TCR-mediated signaling, the activation of T cells and collectively for the function of adaptive immune response.

1.10 AIM OF THE STUDY

As previously discussed, the functional role of cysteine residues on LCK and the regulation of this SFK via post-translational modifications is poorly understood. LCK possess five highly conserved cysteine residues: C217 and C224 within the SH2 domain and C378, C465, and C476 within the kinase domain. Previously, my working group performed a preliminary screening of the function of cysteine to alanine LCK mutants which revealed that LCK mutant carrying the C476A mutation was unable to reconstitute TCR-mediated signaling. This cysteine residue is highly conserved and it appears to be crucial for the kinase activity or/and protein stability of many other kinases (Kato et al., 2000, Lee et al., 2004, Rahman et al., 2010, Thurm et al., 2017). Therefore, the aim of this thesis was to investigate the role of LCK C476 in the regulation of LCK activity and function in more details.

To study the function of C476, I generated a C476A (cysteine to alanine) LCK mutant. I expressed the LCK WT and C476A proteins in an LCK-deficient Jurkat T-cell variant J.LCK displaying impaired TCR-mediated signaling (Courtney et al., 2017). Subsequently, I analyzed the expression/stability of LCK C476A, its cellular localization, its kinase activity, conformation, as well as its ability to reconstitute TCR-mediated signaling. Furthermore, I studied whether C476 is a target of oxidative post-translational modifications and specifically protein *S*-sulfenylation.

2. MATERIALS AND METHODS

2.1 Chemicals and reagents

Table 2.1: Chemicals, reagents and their suppliers

Plasmid	Supplier
ADP-Glo	Promega
ATP Mix	Promega
Cycloheximide	Carl Roth
DCP-Bio1	MerckMillipore
DMSO	Sigma Aldrich
Glutaraldehyde (GA)	Sigma Aldrich
High Capacity Streptavidin Agarose	Pierce
HRP-conjugated Streptavidin	ThermoFischer Scientific
Kinase Detection Reagent	Promega
Methanol	VWR
PBS	MerckMillipore
Penicillin/streptomycin	Biochrom AG
PFA (Paraformaldehyde)	Sigma Aldrich
Protein G PLUS-Agarose	SantaCruz Biotechnology
Substrate (PolyE4Y1)	Promega
Triton-X	Sigma Aldrich

2.2 Antibodies

2.2.1 Antibodies for Western Blot, immunoprecipitation, and immunofluorescence

Table 2.2: Antibodies for western blot, immunoprecipitation, and immunofluorescence
Western blot (WB), Immunoprecipitation (IP), Immunofluorescence (IF).

Antigen	Host	Supplier	Application
4G10	mouse	Hybridoma	WB
β-actin	mouse	Sigma Aldrich	WB
Alexa Fluor 488-labeled anti-mouse IgG	Goat	Cell Signaling	IF
Alexa Fluor 488-labeled anti-rabbit IgG	Goat	Cell Signaling	IF
Alexa Fluor 555-labeled anti-rabbit IgG	Goat	Cell Signaling	IF
Atto 550-labeled anti-mouse IgG2b	Goat	Antibodies-Online	IF
CDC37	mouse	SantaCruz Biotechnology	WB
IRDye® 800CW/680LT anti-mouse	goat	LiCor	WB
IRDye® 800CW/680LT anti-rabbit	goat	LiCor	WB
LCK	Rabbit	MerckMillipore	WB/IP
LCK (3A5)	mouse	SantaCruz Biotechnology	WB/IP
Phospho-LCK (Y505) Antibody	Rabbit	Cell Signaling	WB/IF
Phospho-p44/42 MAPK (ERK1/2)	Rabbit	Cell Signaling	WB

(Thr202/Tyr204) Antibody			
Phospho-SRC Family (Y416) Antibody	Rabbit	Cell Signaling	WB/IF
Phospho-TCR/ζ-chains (Y142)	mouse	-	WB
SHP1	Rabbit	Cell Signaling	WB
TCR/CD3/ζ-chains	mouse	SantaCruz Biotechnology	WB

2.2.2 Antibodies for TCR-stimulation

Table 2. 3: Antibodies for TCR stimulation

Antigen	Host	Clone	Supplier
Human CD3 antibody-biotin	mouse	UCHT1	Biolegend
Jurkat T-cell receptor	mouse	C305	hybridoma

2.3 Buffers and solutions

Table 2. 4: Buffers, solutions, and their suppliers

Lysis buffer 1	• 50mM Tris (pH 7.4, Carl Roth GmbH) • 1% NP-40 (Sigma Aldrich) • 165mM NaCl (Carl Roth GmbH) • 1% Lauryl maltoside (Calbiochem) • 10mM EDTA (pH 7.5, Carl Roth GmbH) • 10mM NaF (Sigma Aldrich) • 1mM Na_3VO_4 (Sigma Aldrich) • 1mM PMSF (Sigma Aldrich)

5x Sample buffer	• 100mM Tris (pH 6.8, Carl Roth GmbH) • 50% Glycerol (Sigma Aldrich) • 0.25% Bromophenol Blue (Carl Roth GmbH) • 5% SDS (Calbiochem) **<u>Reducing conditions</u>** • 10% β-mercaptoethanol (Sigma Aldrich)
SDS-PAGE resolving gel (10%)	• 400mM Tris (pH 8.8, Carl Roth GmbH) • 10% acrylamide (BioRad) • 0.1% SDS (Calbiochem) • 0.1% APS (Carl Roth GmbH) • 1% TEMED (Carl Roth GmbH)
SDS-PAGE stacking gel (5%)	• 120mM Tris (pH 6.8, Carl Roth GmbH) • 5% acrylamide (BioRad) • 0.1% SDS (Calbiochem) • 0.1% APS (Carl Roth GmbH) • 1% TEMED (Carl Roth GmbH)
Transfer buffer	• 50mM Tris (pH 6.8, Carl Roth GmbH) • 40mM Glycine (Carl Roth GmbH) • 0.000375% SDS (Calbiochem) • 20% Methanol (Carl Roth GmbH)

TBS buffer	• 25mM Tris (pH 8, Carl Roth GmbH) • 135mM NaCl (Carl Roth GmbH) • 2.5mM KCL (Sigma Aldrich)
TBS-Tween buffer **(membrane washing buffer)**	• TBS • 0.1% Tween 20
Blocking and antibody buffer	• TBS • 5% BSA/milk powder
IP Wash buffer **(Wash buffer 1)**	• 50mM Tris (pH 7.4, Carl Roth GmbH) • 0.1% NP-40 (Sigma Aldrich) • 0.1% Lauryl maltoside (Calbiochem) • 165mM NaCl (Carl Roth GmbH) • 10mM NaF (Sigma Aldrich) • 1mM PMSF (Sigma Aldrich)
Lysis buffer 2 **(*in vitro* kinase assay)**	• 1% Brij-58 (Sigma Aldrich) • 150mM NaCl (Carl Roth GmbH) • 10mM NaF (Sigma Aldrich) • 150mM Tris (pH 7.5, Carl Roth GmbH) • 1mM PMSF (Sigma Aldrich) • 1mM Na_3VO_4 (Sigma Aldrich)
Wash buffer 2 **(*in vitro* kinase assay)**	• 1% Brij-58 (Sigma) • 50mM Tris (pH 7.5, Carl Roth GmbH) • 165mM NaCl (Carl Roth GmbH)

Tyrosine kinase buffer	• 40mM Tris (pH 7.5, Carl Roth GmbH) • 20mM MgCl x 6 H_2O (Sigma Aldrich) • 1mM $MnCl_2$ (Sigma Aldrich) • 1mM DTT (Sigma Aldrich) • 150mM BSA (Sigma Aldrich)

2.4 Plasmids and constructs

Table 2. 5: Plasmids with their suppliers and constructs

Plasmid	Supplier
pEYFP-LCK WT	
pEYFP-LCK C476A	Site directed mutagenesis
pEGFP-N1 LCK WT	Vector Builder, customized
pEGFP-N1 LCK C476A	Site directed mutagenesis
pEGFP-N1 LCK Y394F	Site directed mutagenesis
pEGFP-N1 LCK Y505F	Site directed mutagenesis
LCK Biosensor TqLck-V5	Eurofins Genomics
LCK Biosensor TqLck-V5 C476A	Site directed mutagenesis
LCK Biosensor TqLck-V5 Y505F	Site directed mutagenesis

2.5 Site directed mutagenesis

The human plasmid pEYFP-N1 LCK was used as a template for the mutagenesis reaction. The C476A mutation was introduced by site-directed mutagenesis using the Quick-Change II XL Site-Directed Mutagenesis kit (Agilent) according to the manufacturer's protocol.

Forward primer: 5'-CTC ATG AGG CTG GCC TGG AAG GAG CGC CC-3'

Reverse primer: 5'-GGG CGC TCC TTC CAG GCC AGC CTC ATG AG -3'

The resulting cDNA was verified by sequencing.

2.6 Cell Culture

All cell culture work was performed in a laminar flow hood under appropriate aseptic conditions. Jurkat T-cell lines, JE6 and J.LCK cells were used in all experiments. Jurkat T cells are an immortalized line of human T lymphocyte that was established in the late 1970s from the peripheral blood of a 14-year-old boy with T cell leukemia (Schneider U. *et al*., 1977). Jurkat cells are mostly used to study T-cell signaling and T-cell activation. J.LCK T-cell line is an LCK-deficient Jurkat T-cell variant generated by CRISPR/Cas (Courtney et al., 2017). J.LCK T-cell line was kindly provided by the group of Dr Arthur Weiss as laboratory stock (University of California, San Francisco). J.LCK cells were maintained at 1-4x10^5 cells/ml, at 37ºC and 5% CO_2 in RPMI 1640 medium (Lonza) supplemented with 10% (v/v) FBS (PAN Biotech), 100U/mL penicillin (Biochrom AG), and 100 μg/mL streptomycin.

2.6.1 Freezing of Jurkat T cells

Prior to long-term usage, Jurkat T cells were kept at low temperature (<150°C) in liquid nitrogen. Prior to storage in liquid nitrogen, cells were counted and cell suspensions were formed with 10 million cells in 1ml of 10% (v/v) dimethyl sulfoxide (DMSO) in FBS. DMSO was used as a cryoprotective agent to protect cells from damage caused by low temperature. The suspensions were kept in cryovials marked for date and passage number and stored overnight at - 80°C freezer for slow cooling. Over the next three days, the cryovials were transferred into a cryogenic freezer containing liquid nitrogen at a temperature of <150°C.

2.6.2 Thawing of Jurkat T cells

Thawing of Jurkat cells involved retrieving the cells that were previously stored in liquid nitrogen at low temperature. Prior to thawing, cryovials containing cells were moved from liquid nitrogen into a water bath heated to 37°C. In a cell culture hood, cells were then transferred from the cryovials into an appropriate volume of pre-warmed (37°C) growth medium to allow dilution

of the cryoprotector DMSO. Cells were then transferred into a 175 cm^2 cell culture flask and an appropriate volume of growth medium (250mL) was added to allow cell growth.

2.6.3 Growth of Jurkat T cells

The cells were grown in a 175 cm^2 cell culture flask. Cell passage and splitting was performed every two days. Cell confluency was assessed by a light optical microscope. Cells were then counted using a bright-line hemocytometer. The average of four different counts was used to calculate cell numbers in a 1 ml suspension. After cell counting, cell suspensions were either split in a ratio of 1 to 4 into a new 175 cm^2 cell culture flask or seeded into multi-well cell culture plates to be used for subsequent experiments. Cell incubation was always performed at 37°C and 5% CO_2 in humidified air.

2.6.4 Inhibitors and antioxidants

Jurkat T cells were treated with inhibitors and antioxidants in RPMI 1640 supplemented with 10% (v/v) FBS (PAN Biotech), 100U/mL penicillin (Biochrom AG) and 100 μg/mL streptomycin at 37°C and 5% CO_2. The specific duration and concentrations of the treatments of inhibitors are described in the corresponding experimental design.

2.7 Transfection by electroporation

Electroporation-mediated transfection was conducted using the Gene Pulser II System (BIORAD, Hercules, CA, USA). Cells were passaged one day prior to transfection. The day of transfection, cells were transferred to a 50 mL sterile centrifuge tube and pelleted by centrifugation at 400 x g for 5–7 min at room temperature. $20x10^6$ cell pellets were resuspended in 390μL RPMI 1640 (without penicillin/streptomycin) and transfected together with 5-30μg plasmid DNA into a 4mm electroporation cuvette (VWR). The pulse conditions were set at 230V and 950μF. Immediately after the pulse, cells were transferred into 50mL pre-warmed RPMI 1640 medium with 10%FBS (without

penicillin/streptomycin). The growth medium is composed of 50% of freshly prepared medium and 50% of “conditioned” culture medium (media harvested from previously cultured cells). The cells were cultured overnight and the transient gene expression were assayed next day (15 hrs. following electroporation).

2.8 Cell stimulation with soluble Antibodies (sAbs)

Jurkat T-cell lines were stimulated in solution with the anti-TCR and anti-CD3 antibodies C305 or UCHT1, respectively. $1x10^6$ cells were resuspended in 100μL RPMI 1640. Next, 100μL of C305 supernatant or alternatively 1μL of UCHT1 (0.2 mg/ml) were added. Subsequently, the samples were gently mixed and incubated in a thermomixer at 37^{o}C for the selected time points. 1 mL of ice-cold PBS was added in each sample to terminate the stimulation and cells were incubated on ice prior to further analysis.

2.9 Western Blotting

2.9.1 Cell lysis

Jurkat T-cells were collected by centrifugation (16,000g, 10sec, 4^{o}C). Next, the supernatant was removed and cells were lysed in **Lysis Buffer 1** (30 μL per 10^6 cells) and cells were incubated on ice for 20 min (for some experiments these procedures were performed at room temperature/ 25^{o}C). Subsequently, lysates were centrifuged for 10min at 16,000g (4^{o}C) to remove cellular debris. 5x times reducing agent was added to each sample in microcentrifuge tubes and samples were boiled in a thermomixer at 99^{o}C for 5min.

2.9.2 SDS-PAGE and Immunoblotting analysis

Proteins were separated by gel electrophoresis on 10% (or 12%) SDS-polyacrilamid gels (Bio-Rad). Proteins were transferred onto nitrocellulose membranes (Amersham Biosciences) using a semi-dry apparatus (Bio-Rad) and **Transfer Buffer**. Membranes were blocked for 30 minutes at room

temperature with 5% non-fat milk (or BSA, Bovine serum albumin) in Tris-buffered saline (TBS) (**Antibody Buffer**). Incubation with primary antibodies (diluted in blocking buffer) was performed for 2 h at room temperature or overnight at 4°C under rotation (the time of incubation with primary antibodies varies between antibodies with different specificities). After washing with TBS-Tween for 3 times and TBS the membranes were incubated with secondary antibodies at room temperature for 1 hour followed by extensive washing with TBS-Tween and TBS.

For detection with enhanced chemiluminescence (ECL), membranes were incubated with a suitable secondary antibody which is labeled with horseradish peroxidase (Dianova). X-ray film (Amersham GE Healthcare) and enhanced chemiluminescence system was used for the detection of the signals. The process was performed in a dark room. Films were scanned and band intensities were quantified. Intensities were normalized by multiplication of the density of the target protein in each lane by the ratio of loading control (β-actin) density from the control sample (lane 1) to the loading control density of other lanes, or as indicated at the respective experiment.

For the detection by fluorescence, membranes were incubated with a suitable fluorophore-labeled secondary antibody (IRDye 680LT or 800CW, diluted in blocking buffer). The protein bands were visualized by densitometry scanning using the Odyssey Classic Infrared Imager System (LI-COR Biosciences). Images were quantified using the LI-COR Image Studio 2.1.15 software.

Intensities were normalized against the loading control (β-actin) or as indicated at the respective experiment.

2.10 Immunoprecipitation

Immediately after cell lysis, supernatants were transferred in fresh microcentrifuge tubes. 30μl of each sample were kept as an input control in a different microcentrifuge tube and prepared for Western blotting (5x times sample buffer, boiling in a thermomixer at 99^{o}C for 5min). For the immunoprecipitation, 2μg of each antibody was added and antibody-antigen

reaction took place for 2h on a rotator (4°C) incubated. Subsequently, Protein G beads (30µl per sample) were added to the sample. Beads were pelleted by centrifugation at 7500g for 2min. The complexes (beads/antibody/protein) were subsequently washed 5 times with 1mL **IP Wash Buffer**. The beads were mixed with 1x reducing sample buffer followed by incubation at 99°C for 5 min for protein denaturation. The samples were stored at -20°C or used directly for immunoblotting.

2.11 Flow cytometry analysis

Flow cytometry is a technique of single-cell-based analysis used to detect and measure physical and chemical characteristics of a population of cells or particles. In a flow cytometer, a cell population suspension is funneled through a nozzle that creates a single-cell stream. The population then flows through a set of laser light sources, one cell at a time, and the light scattered is characteristic to the cells and their components. For the analysis and quantification of LCK protein expression (either YFP-tagged WT or mutants) in J.LCK cells a FACS (fluorescence-activated cell sorting) Calibur was used. Initially, living Jurkat T cells were selected according to FSC/SSC parameters (forward scatter/ side scatter). Next, LCK expression was determined according to fluorescence of the YFP-tag (green laser) and the MFI (mean florescence intensity) was determined.

2.12 Immunofluorescence microscopy analysis

The immunofluorescence analysis of LCK was based on a recently published protocol from our group (Philipsen et al., 2017). After transfection and subsequent treatment, cells were transferred to adhesion slides (Marienfeld) and allowed to settle down for 10 min before the next steps. Fixation was performed on ice by 1% PFA (Paraformaldehyde) and 0.02% glutaraldehyde (GA) in PBS for 15 min. Cells were permeabilized for 10 min with 0.2% Triton X-100 (Sigma) in PBS and then blocked with 1% BSA / 0.1% Tween 20 (Sigma) in PBS. Primary and secondary antibody stainings and washing steps were performed at room temperature in **Blocking Buffer**. Rabbit anti-pSRC Y416

(which recognizes pY394 of LCK), rabbit anti-LCK Y505 (both polyclonal, Cell Signaling), mouse anti-LCK (clone 3A5, Santa Cruz Biotechnology), and anti-CD3/ζ-chains (Santa Cruz Biotechnology) were used as primary antibodies. Alexa Fluor 555-labeled goat anti-rabbit IgG (Cell signaling), Alexa Fluor 488-labeled goat anti-mouse IgG and goat anti-rabbit IgG (Cell signaling) and Atto 550-labeled goat anti-mouse IgG2b (Antibodies-Online) were used as secondary antibodies. Imaging was performed with Leica TCS SP2 confocal laser scanning microscope (Leica) with Leica IRE2 stand equipment with a 63x 1.40 HCX APO CS objective (Leica), an argon laser (488nm), and a HeNe laser (543nm). To avoid spectral overlap, the samples were sequentially scanned with a beam splitter HTF 488/543/633. Green and red fluorescence emissions were red out at 500 to 551 nm and 571 to 626nm, respectively. Image data were acquired, stored, and analyzed with a pixel depth of 8 bits. The LCK pools were marked and segmented manually in the Image J software. From these data, the five segments analyzed, which included plasma membrane, inner compartment without the intracellular pool of LCK, intracellular pool of LCK, inner compartment together with intracellular pool of LCK, and total cells, were derived.

For quantitative analysis, the data extracted from the segmented images were normalized to the mean value of the untreated controls of each respective experiment in a single cell-based manner. Fluorescent ratios (plasma membrane to total cell, inner compartment with intracellular pool to total cell, inner compartment without intracellular pool to total cell, plasma membrane to inner compartment with or/and without intracellular pool) were determined for each cell. The resulting tables of fluorescent ratios and total cell fluorescent values were analyzed with Prism Software (version 7, GraphPad).

2.13 FLIM/FRET measurements

For the FLIM/FRET (Fluorescence lifetime imaging microscopy/Förster resonance energy transfer analysis) transfected cells (with the biosensor constructs, either TqLck-V2 or TqLck-V5) were first preselected on the basis of their shape (rounded) and having a low surface spreading when analyzed by

transmitted light. Additionally, upon analysis of epifluorescence, cells were preselected for exhibiting intermediate fluorescence and having the biosensor localized both at the membrane and in the intracellular pool.

For the wide-field nonscanning FLIM, TSCSP Counting (Time- and Space Correlated Single Photon) was used. Using an 8 MHz-pulsed frequency-doubled laser (Spectra Physics), selected cells were excited at 420nm. Subsequently, the fluorescent signal was collected, after passing a 460nm long-pass emission filter, from an IX81 inverted microscope (Olympus). In order to detect donor and acceptor fluorophore, a 505nm beam splitter and 460 to 500nm and 520 to 560nm bandpass filters were used respectively. In the analysis of the time domain FLIM data, the instrument response function (IRF) was performed using a reference dye (Auramine, Sigma-Aldrich, saturated solution in H_2O). (For a detailed description of the FLIM/FRET analysis see the published work of our group and others, (Nair et al., 2006, Stirnweiss et al., 2013, Hartig et al., 2014, Philipsen et al., 2017).

To visualize the spatio-temporal distribution of the different excited states of the fluorophores inside the cells (high or low FRET), the mean lifetimes were plotted and the resulting pseudo color-coded lifetime maps show the distribution of mean lifetimes and thus of the distance of the two fluorophores acting as donor and acceptor. All photons collected were included in the determination of mean lifetimes, for final quantitative analysis.

2.14 *In vitro* non-radioactive kinase assay

To measure the enzymatic activity of LCK, a modified approach of a non-radioactive *in vitro* kinase assay (*Promega*) was used. The kinase Assay measures ADP formed from a kinase reaction. The ATP is converted into ADP, which is used to generate light in a luciferase reaction. The luminescence generated correlates with kinase activity.

J.LCK cells were first transfected and 24 hours after transfection $1x10^7$cells were lysed in 1 mL of **Lysis Buffer 2**. Next, LCK was immuno-precipitated from transfected cells using Protein G beads. The beads were washed five times with 1mL **Washing Buffer 2**, one time with PBS and one

time with **Tyrosine Kinase Buffer**. Subsequently, 90% of the protein was used to measure the enzymatic activity via the non-radioactive kinase assay. The rest 10% of the immune-precipitated protein was used to test the efficiency of immune-precipitation by immunoblotting analysis**.**

The kinase assay begins with the kinase reaction. LCK is incubated with ATP (**ATP Mix**), **substrate** (PolyE4Y1) and **Tyrosine Kinase Buffer,** in a ratio 1:1:2 (100μL:100μL:200μL), respectively. 40μL per sample was added in the mixture and incubated for 60 min at room temperature. In order to terminate the kinase reaction and deplete the remaining ATP, 40μL of **ADP-Glo** (Luciferase) per sample was added in the reaction, and incubated for 40 min in room temperature. As a second step, 80μL of the **Kinase Detection Reagent,** per sample, is added to the reaction. The samples were transferred to multi-well plate and incubated for 30 min at room temperature. This step facilitates the measurement of the newly synthesized ADP using a luciferase/luciferin reaction in a Luminometer. The luminescent signal positively correlates with ADP amount and kinase activity.

To evaluate the efficiency of the assay to detect the enzymatic activity of LCK, purified LCK was used as control (**Fig. 2.1)**. All the experiments were performed at 37ºC.

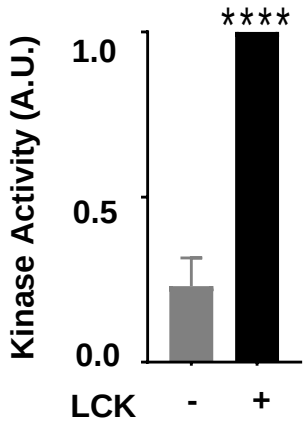

Figure 2.1: *In vitro* non-radioactive kinase assay and analysis of LCK enzymatic activity
Values were normalized to the purified LCK sample which was set to 1. Then values were expressed in Arbitrary Units (A.U.). Bar graphs show mean ± SEM of 3 independent experiments. Statistical analysis was performed using one sample *t*-Test ***p<0.001.

2.15 DCP-Bio1 labelling (Detection of Sulfenylation)

Stable and specific labelling of sulfenylated thiols has been reported to be achieved with the use of dimedone-based probes conjugated with biotin (Charles et al., 2007). To study sulfenylation of cysteine residues, a dimedone-based probe, DCP-Bio1, was used (Poole et al., 2007). DCP-Bio1 labelling is a trapping approach, which takes advantage of the high reactivity of DCP-Bio1 with sulfenylated proteins which generates a stable, alkylated form of the protein (**Fig. 2.2**). In DCP-Bio 1, DCP is linked to biotin, which allows pulling-down of labeled proteins and their detection by immunoblotting analysis.

24 hours after transfection, J.LCK cells ($1.5x10^7$) were separated in three groups. To exclude false positive signals, $5x10^6$ were treated, prior to cell lysis, for 1h at 37ºC and 5% CO_2 with N-Acetyl Cysteine (NAC), which has a well-established antioxidant and reducing activity (Aldini et al., 2018). Subsequently, after washing (spin down 10s, 1ml PBS) $5x10^6$ cells from all groups were lysed in 500μL for 30min at room temperature. During lysis, $5x10^6$ were treated with 0,1mM DCP-Bio1 and $5x10^6$ were lysed without treatment with DCP-Bio1. In order to prevent further biotinylation of proteins and free DCP-Bio1 from competing with biotinylated protein for binding to the streptavidin binding sites, proteins in the cell lysate are separated from small molecules immediately via size exclusion chromatography using Spin Desalting Columns (ThermoFisher). Columns were equilibrated for 3 times with 1 mL 20mM Tris buffer pH 7.2 followed by centrifugation at 1000g. Cell lysates were applied to the top of each column, centrifuged (2 min, 1000g), and collected in labeled microcentrifuge tubes.

Lysates were pulled-down using streptavidin-coated beads. Prior to pull-down assays, 30μL of each lysate were taken to analyze protein “input” by immunoblotting analysis. Subsequently 70μL of High-Capacity Streptavidin Agarose (Pierce) was added in each sample and microcentrifuge tubes were incubated for 12-16 hours in an end-over-end rotator at 4ºC. Beads were pelleted by centrifugation at 600rpm for 1 min and 4ºC and washed for 30 min in 500μL lysis buffer supplemented with: (1) 1% SDS, (2) 2M Urea, (3) 1M NaCl, (4) 10mM DTT, and finally (5) only lysis buffer. The samples were boiled for 10

min in the presence of 8% SDS. Lysates were forwarded to SDS-PAGE and immunoblotting analysis.

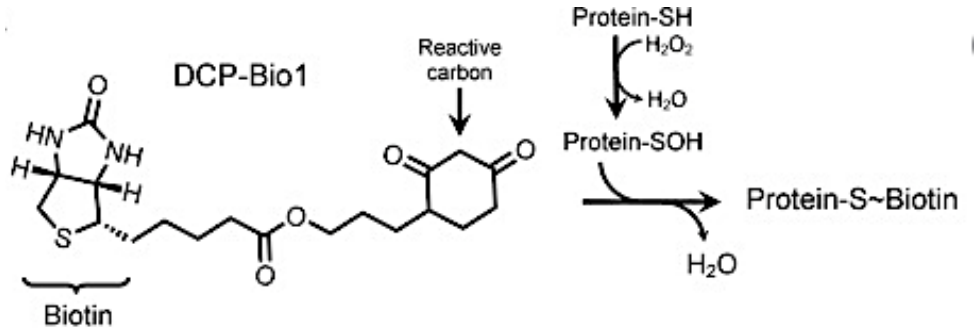

Figure 2.2: Trapping of protein sulfenylation on cysteine residues using DCP-Bio1 (modified from Keyes J. D. et al., 2017)

2.16 Statistical Analysis

Statistical analyses of the data were performed using the GraphPad Prism 7 software. All data are presented as mean ± SEM (standard error of the mean). Normality and variance equality assumptions were checked using Shapiro-Wilk and Levene tests, respectively. Potential population mean differences were explored, using one sample and independent two-samples *t*-Tests, when appropriate. In cases where group comparisons were performed exhibiting dependence, we used the appropriate Bonferroni adjusted p-values. For mean comparisons among more than two samples, one-way ANOVA was performed and post-hoc Tukey HSD or Dunnett tests were performed for multiple comparison purposes. Unless otherwise stated, the significance level is set to a=5%.

3.RESULTS

3.1 Functional characterization of the highly conserved cysteine residue C476 in LCK

During the last years, cysteine residues have been in the center of attention because of their unique biochemical characteristics. The chemical reactivity of the thiol group allows a number of both reversible and non-reversible post-translational modifications. This makes cysteines powerful molecular regulators of the features of proteins including the structure, the stability, and the activity. Protein tyrosine phosphatases (PTPs) represent the best-known example in this regard. As mentioned in the introduction (chapter 1.8), the conserved cysteine residue in the catalytic center of PTPs, which is essential for catalyzing the removal of the phosphate group from phosphorylated tyrosine residues, can be sulfenylated by hydrogen peroxide and thus the enzyme becomes inactivated (Klomsiri et al., 2011). This oxidized cysteine rapidly rearranges to form a sulfenylamide or a disulfide bond with a nearby cysteine. These states contribute to protect the catalytic cysteine from further irreversible hyper-oxidation (Wu et al., 2017). Recently, it has been proposed that oxidative modifications of the thiol group of cysteine residues located both in catalytic and non-catalytic domains of PTKs may regulate their enzymatic activity, half-life, and function (Dustin et al., 2020). As mentioned in the introduction, protein tyrosine kinases of the SFKs, such as c-SRC, have been shown to be regulated by oxidative modifications (Rahman et al., 2010).

Regarding LCK, little is known about a possible regulation of its activity in a redox-dependent manner and previous studies have proposed that post-translational modifications of LCK´s cysteines may be involved in the regulation of its activity (Nakamura et al., 1993). As shown in **Figure 3.1A,** LCK possess five highly conserved cysteine residues: C217 and C224 within the SH2 domain and C378, C465, and C476 within the kinase domain. More than two decades ago, an initial study by the group of Andre´ Veillette showed that cysteine residues C378, C465, and C476 of LCK are crucial for its enzymatic activity, as cysteine to alanine mutants of these residues exhibited an impaired autophosphorylation and *in vitro* kinase activity (Veillette et al., 1993).

Furthermore, it was observed that alteration of cysteine 476 resulted in a dramatic reduction of the half-life of LCK. A different study has shown that C378, C465, and C476 react with isothiazolones and that this results in the inhibition of LCK´s enzymatic activity (Trevillyan et al., 1999). Previously, my working group performed a preliminary screening of the function of cysteine to alanine LCK mutants (C217A, C224A, C378A, C465A, and C476A). Cysteine to alanine LCK mutants were expressed in LCK-deficient Jurkat T cells (JCaM1.6) and their ability to reconstitute TCR signaling (i.e. ERK1/2 activation) was evaluated by intracellular flow cytometry, using a phospho-specific ERK1/2 antibody (Straus and Weiss, 1992). C224A, C217A, and C378A LCK mutants partially reconstitute ERK1/2 activation (**Fig. 3.1B**). In the case of C465A LCK, reconstitution of pERK1/2 was reduced to 65% of WT LCK. Interestingly, the LCK mutant carrying the C476A mutation was unable to reconstitute TCR-mediated ERK1/2 activation (only 25% of WT LCK as shown in **Fig. 3.1B**).

A

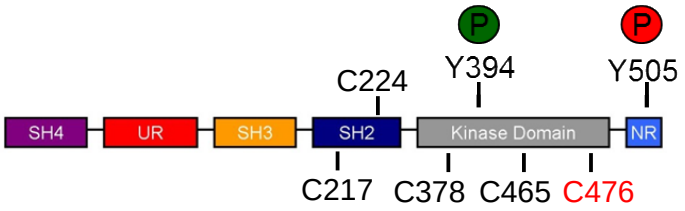

B

LCK	Impact on pERK1/2	% reconstitution of pERK1/2
WT	↑	100%
C217A	↓	75%
C224A	↓	70%
C378A	↓	75%
C465A	↓	65%
C476A	↓↓↓	25%
K273R	↓↓↓	5%

Figure 3.1: Functional screening of the cysteine to alanine LCK mutants
(A) LCK possesses five highly conserved cysteine residues: C217 and C224 within the SH2 domain and C378, C465 and C476 within the kinase domain. (B) Summary of the functional screening of LCK cysteine to alanine mutants. Arrows indicate the impact of the mutation on the reconstitution of pERK1/2 activation that was evaluated by intracellular flow cytometry, using a phospho-specific ERK1/2 antibody. The respective percentages of pERK1/2 reconstitution are listed on the right column. The ability of WT LCK to reconstitute ERK1/2 activation was set to 100%. The K273R kinase dead LCK mutant on the bottom of the list was used as a negative control.

C476 is located at the kinase domain of LCK, in an α helix within the C-lobe (**Fig. 3.2A**). As shown in **Fig. 3.2B,** this cysteine residue is conserved among many other kinases. Previously published data from our group have shown that this cysteine residue is located within a conserved Mx_2CWx_6R amino acid motif (where x indicates any amino acid) (Thurm et al., 2017a). In addition, our study has shown that the corresponding residue C575 in the protein tyrosine kinase ZAP-70 regulates the stability and the function of the protein (Thurm et al., 2017a). Moreover, a number of previous publications revealed that this conserved cysteine residue is crucial for the kinase activity of many other kinases such as c-SRC (C498), c-RET (C376) and PDGFR-beta (C940) (Kato et al., 2000, Lee et al., 2004, Rahman et al., 2010). Thus, I hypothesized that C476 may also play an important role in the regulation of LCK function. Therefore, I have investigated the role of LCK C476 in the regulation of LCK activity and function in more details.

A

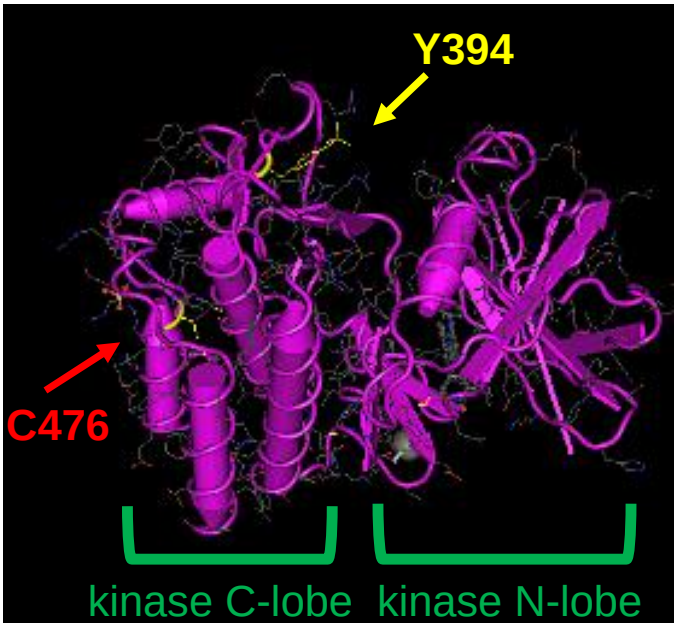

B

ZAP-70	A	L	M	S	D	C	W	I	Y	K	W	E	D	R	P	D	F	**C575**
SRC	D	L	M	C	Q	C	W	R	K	E	P	E	E	R	P	T	F	**C498**
c-YES	E	L	M	N	L	C	W	K	K	D	P	D	E	R	P	T	F	**C506**
LYN	D	I	M	K	M	C	W	K	E	K	A	E	E	R	P	T	F	**C479**
LCK	Q	L	M	R	L	C	W	K	E	R	P	E	D	R	P	T	F	**C476**
FAK	S	L	M	T	K	C	W	A	Y	D	P	S	R	R	P	R	F	**C658**
PDGFRβ	E	I	M	Q	K	C	W	E	E	K	F	E	I	R	P	P	F	**C940**
RET	R	L	M	L	Q	C	W	K	Q	E	P	D	K	R	P	V	F	**C376**

Figure 3.2: The cysteine residue C476 in the kinase domain of LCK is highly conserved among tyrosine kinases

(A) Ribbon diagram illustrating the structure of the kinase domain of LCK. The tyrosine kinase domain, colored in magenta, is divided in two lobes (the N-lobe and the C-lobe). The yellow arrow indicates the autophosphorylation (activatory) tyrosine residue Y394 within the activation loop of the kinase domain. The red arrow indicates the position of cysteine residue 476 within C-lobe of the kinase domain. (B) C476 is conserved among many kinases and is located within a conserved Mx_2CWx_6R amino acid motif.

To study the function of C476, I generated a C476A (cysteine to alanine) LCK mutant. To date, substitution of a cysteine with an alanine is the conventional way to replace the side chain (-SH) of a cysteine residue and examine its involvement in post-translational modifications (e.g. oxidation) and side chain interactions (e.g. disulfide bond formation). Alternatively, it is also possible to substitute a cysteine with a serine. Although serine and cysteine have similar chemical properties (they differ only in the swap of a sulfur atom with an oxygen), serine is less hydrophobic than cysteine and it is possible to

occasionally allow for unexpected post-translational modifications such as phosphorylation or glycosylation (Proba et al., 1997). Therefore, the replacement of cysteine with an alanine it is considered the preferable choice. To investigate the function of LCK C476A, two different LCK constructs were generated. As shown in **Fig. 3.3,** the first construct (Construct 1) allows the simultaneous expression of a non-tagged human LCK and EGFP protein under two separate EF1A promoters. The second construct (Construct 2, **Fig. 3.3**) allows the expression of an YFP-tagged human LCK. The expression of the fluorophores (EGFP or YFP) allows the monitoring of transfected cells. For the functional characterization of LCK C476A, I expressed LCK WT or LCK C476A in J.LCK cells, an LCK-deficient Jurkat T-cell variant displaying impaired TCR-mediated signaling, which has been recently generated by CRISPR/Cas (Courtney et al., 2017). Subsequently, I analyzed the expression/stability of LCK C476A, its cellular localization as well as its ability to reconstitute TCR-mediated signaling.

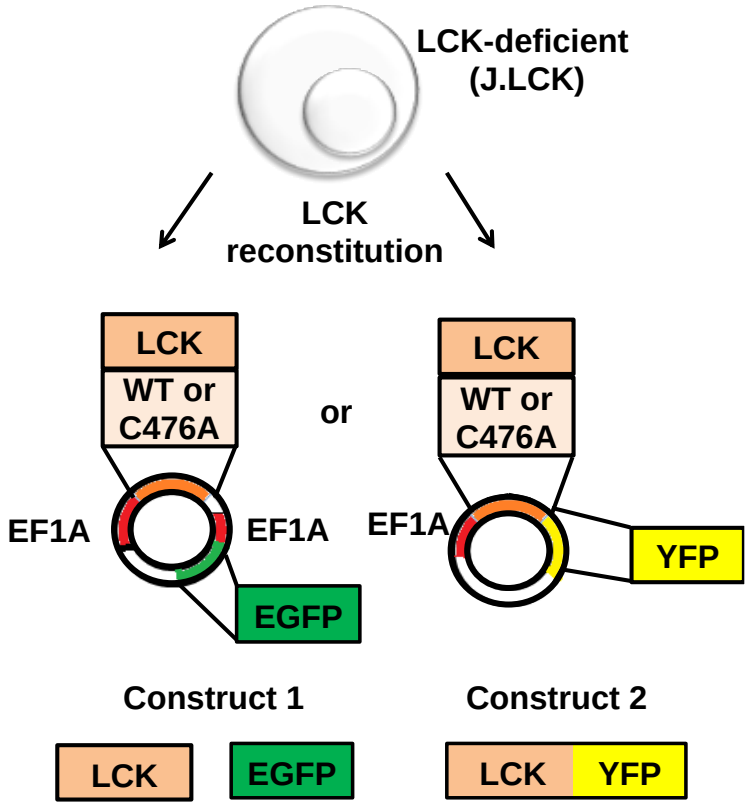

Figure 3.3: Experimental setup used for the functional characterization of LCK C476A
An LCK C476A mutant was generated using standard mutagenesis**.** J.LCK cells (an LCK-deficient Jurkat T-cell variant) were transiently transfected with constructs coding for either LCK WT or LCK C476A.Two different LCK constructs were generated: **Construct 1** allows the simultaneous expression of a non-tagged human LCK and EGFP protein under two separate EF1A promoters. **Construct 2** allows the expression of an YFP-tagged human LCK.

3.2 C476 regulates the stability of LCK

Initially, I assessed the expression of LCK C476A in J.LCK cells by Immunoblotting analysis (**Fig. 3.4A and 3.4B**). The expression of both LCK WT and LCK C476A was detected at the expected molecular weight (56-59kDa). Conversely to LCK WT that was detected with both the characteristic 56kDa and 59kDa LCK bands, LCK C476A was detected only by the appearance of one band migrating at 56kDa. Moreover, **Fig. 3.4A and 3.4B** clearly show that the protein level of LCK C476A was significantly reduced (about 30-40%) compared to LCK WT. It must be pointed out that this observation is different from previously published data showing that substitution of the corresponding cysteine with an alanine in murine LCK (C475), resulted in an almost complete loss of protein expression in NIH 3T3 fibroblast (Veillette et al., 1993).

In addition to immunoblotting analysis, I took advantage of the YFP-tagged construct (construct 2, **Fig. 3.4C and 3.4D**) and I evaluated the expression of LCK C476A by assessing the mean fluorescence intensity of the YFP fluorophore by flow cytometry. As shown in **Fig. 3.4C,** J.LCK cells were equally transfected with YFP-expressing LCK WT and/or LCK C476A constructs as indicated by comparable proportion of cells expressing YFP (approx. 27%). In line with the immunoblotting analysis data, the protein level of LCK C476A was strongly reduced (about 30%) compared to LCK WT as indicated by the lower mean fluorescent intensity (MFI) (**Fig. 3.4C and 3.4D**). Taken together, the Immunoblotting analysis and flow cytometry data show that LCK C476A is expressed at about 60-70% of the level of LCK WT.

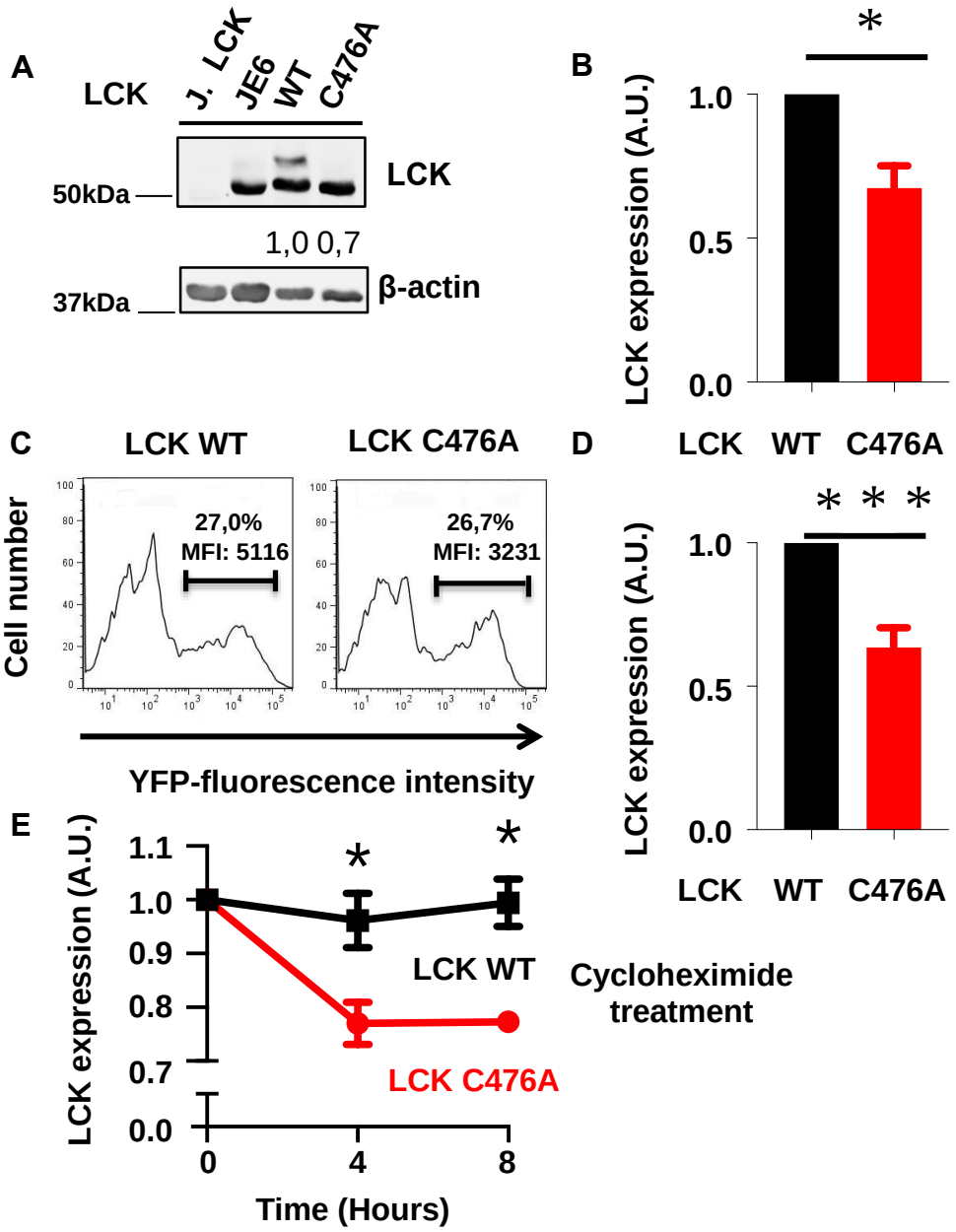

Figure 3.4: C476 regulates the expression and stability of LCK
(A) J.LCK cells were transfected with construct 1 expressing either LCK WT or LCK C476A. LCK expression was evaluated by Immunoblotting analysis. JE6 Jurkat cells, endogenously expressing LCK, were used as a positive control. Due to its general expression across all eukaryotic cell types and due to the fact that its expression levels do not vary drastically upon cellular treatment, β-actin was used as loading control. One representative of 5 independent experiments is shown. (B) Bar graphs show the quantification (mean ± SEM) of the data shown in (A) (n=5). (C-E) J.LCK cells were transfected with YFP-tagged constructs expressing either LCK WT or LCK C476A: (C) LCK expression was evaluated by flow cytometry. The transfection efficiency is indicated by percentages, whereas the expression levels by the mean fluorescence intensity (MFI). One representative histogram is shown. (D) Quantification of the data shown in (C) represented as mean ± SEM of MFI from 12 independent experiments. 12 hours after transfection, cells were treated with 20 µg/ml Cycloheximide to block protein synthesis. Subsequently, LCK expression was evaluated by flow cytometry up to 8 hours. MFI of LCK-YFP constructs was measured and the graph shows mean ± SEM of 3 independent experiments. (A-D) LCK expression was always quantified and normalized to LCK WT which was set to 1 and expressed in Arbitrary Units (A.U.). (E) LCK expression was quantified and normalized to the values at time 0, for both WT and C476A, which was set to 1 and expressed in Arbitrary Units (A.U.). Statistical analysis was performed using unpaired two-samples Student´s *t*-Test (for E) and one sample *t*-Test (for B and D). *p<0.05, ***p<0.001. Standard error of the mean (SEM).

To shed light on how the C476A mutation affects LCK expression, I assessed LCK stability using cycloheximide, an inhibitor of *de novo* protein synthesis (Baliga et al., 1969). Upon treatment with cycloheximide, the expression of LCK would gradually decrease because of the block in the synthesis of new protein. I assumed that if the stability of LCK WT and LCK C476A is similar, no major differences should be detected in the expression upon cycloheximide treatment. The data presented in **Fig. 3.4E** indicate that LCK WT remains stable up to 8 hours upon treatment with cycloheximide. Conversely to LCK WT, the expression of LCK C476A drops significantly (20%) upon 4 hrs incubation with cycloheximide, thus indicating that LCK C476A is less stable than LCK WT. Collectively these data show that the introduction of a C476A mutation affects LCK stability.

3.3 LCK C476A has an altered cellular localization

Having observed that the C476A mutation affects LCK stability, I then examined whether the mutation also affects the subcellular localization of LCK. It has been previously described that LCK localizes at the plasma membrane and in a characteristic intracellular vesicular pool (Ley et al., 1994, Antón et al., 2008, Philipsen et al., 2017). To study the localization of LCK C476A, I took advantage of a standard operating procedure (SOP) protocol, which has been established in our group. This protocol enables a quantitative, single cell–based confocal analysis of total LCK and its phosphorylated forms (Philipsen et al., 2017). I applied this SOP protocol to J.LCK cells transiently transfected with either LCK C476A or WT. In line with my previous findings (shown in **Fig. 3.4)**, confocal microscopy analysis showed that the overall expression of LCK C476A is reduced in comparison to LCK WT (**Fig. 3.5A)**. Indeed, quantification of the LCK fluorescence signal revealed a 40% reduction in the expression of the LCK C476A (**Fig. 3.5B**). As expected, J.LCK cells transfected with an **empty vector** showed no specific signal for LCK expression either at the plasma membrane or in the intracellular compartment (**Fig. 3.5A**).

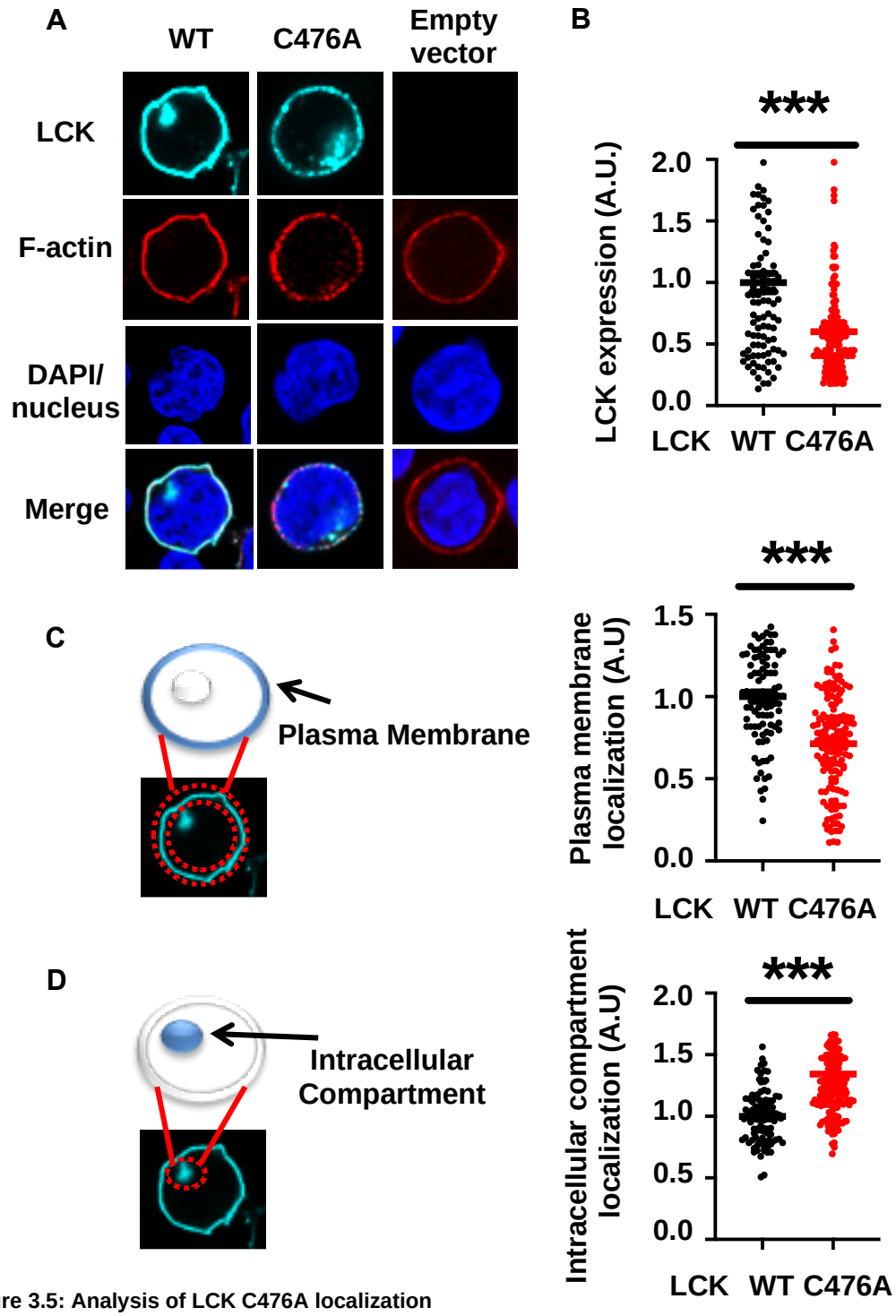

Figure 3.5: Analysis of LCK C476A localization
J.LCK cells were transfected with construct 1 expressing either LCK WT or LCK C476A or with an empty vector: (A) Analysis of LCK localization and expression using immunofluorescence imaging and confocal microscopy. Cells were stained with a specific LCK antibody (clone 3A5) and in parallel with phalloidin for F-actin detection and DAPI for nuclear staining. Images are representative of four independent experiments. (B) LCK expression, was measured from the entire cell. Each dot represents a cell. (C) Gating strategy applied to analyze LCK expression at the plasma membrane (left) and corresponding quantifications (right). (D) Gating strategy applied to analyze LCK expression in the intracellular compartment (left) and corresponding quantifications (right). Fluorescence intensity from different subcellular compartments was quantified and always normalized to whole cell LCK expression. Next, the values were normalized to LCK WT values which were set to 1. Values were then expressed in Arbitrary Units (A.U.). Dot plots contain data pooled from 4 independent experiments. Each dot represents an individual J.LCK T cell. Statistical analysis was performed using unpaired two-sample Student´s *t*-Test, ***p<0.001.

Filamentous actin (F-actin) is known to be localized just beneath the plasma membrane of resting Jurkat T cells (Bunnell et al., 2001) and hence it is widely used as a marker for the identification of the plasma membrane. To prove that LCK is indeed localized at the plasma membrane, I stained my J.LCK transfected cells in parallel with phalloidin for F-actin detection. (**Fig. 3.5A**). I observed that LCK WT co-localizes with the F-actin signal at the plasma membrane (**Fig. 3.5A**), thus confirming the characteristic distribution of LCK at the plasma membrane. Simultaneously, LCK WT is also present in an intracellular vesicular pool (**Fig. 3.5A**) as previously reported (Ley et al., 1994, Antón et al., 2008, Philipsen et al., 2017). LCK C476A is also present at the plasma membrane as well as in the characteristic intracellular vesicular pool. However, it appears that the plasma membrane fraction of LCK C476A is decreased, compared to LCK WT, and conversely LCK C476A appears to be more distributed in the entire cytoplasm and more specifically in the intracellular vesicular pool (**Fig. 3.5A**).

Next, I investigated the expression of LCK in the different subcellular compartments (i.e. plasma membrane and intracellular compartment) (**Fig. 3.5C-D**). I took advantage of the Image J program for image analysis and I quantified the localization of LCK constructs in the different subcellular compartments. As shown in **Fig. 3.5C,** the fraction of LCK C476A localized specifically at the plasma membrane is reduced (about 30%) compared to LCK WT. On the contrary, the expression of LCK C476A in the intracellular compartment is significantly increased (about 20%) (**Fig. 3.5D).** As previously mentioned, a careful observation of **Fig. 3.5A** reveals that LCK C476A was also found increased in area of the cytoplasm outside of the distinct intracellular vesicular pool.

Collectively, it appears that LCK C476A has an altered distribution within T cells as this mutant shows a decreased localization at the plasma membrane and an increased expression in the cytoplasm as well as in the intracellular vesicular compartment. Furthermore, immunofluorescence imaging confirmed the reduction of LCK C476A protein expression levels that I observed by immunoblotting analysis and flow cytometry.

3.4 Analysis of LCK C476A activation and function

3.4.1 LCK C476A is less phosphorylated on both Y394 and Y505 under both resting conditions and upon TCR stimulation

The data presented above indicate that LCK C476A is less stable than LCK WT and that it also has an altered distribution within the cells. Next, I examined whether LCK activation and function is affected by the introduction of the C476A mutation. As mentioned before, LCK is crucial for the initiation of proximal TCR signaling and its activation is tightly regulated by phosphorylation/dephosphorylation on regulatory Y394 (activatory) and Y505 (inhibitory) residues. As the two phosphorylation sites are crucial indicators of LCK activity and conformation, I initially investigated the phosphorylation of Y394 and Y505 in cells expressing either LCK C476A or LCK WT by immunoblotting analysis. Data shown in **Fig. 3.6** suggest that LCK C476A is significantly less phosphorylated on both regulatory Y394 (**Fig. 3.6A**) and Y505 (**Fig. 3.6B**) than LCK WT under both resting conditions and upon TCR stimulation.

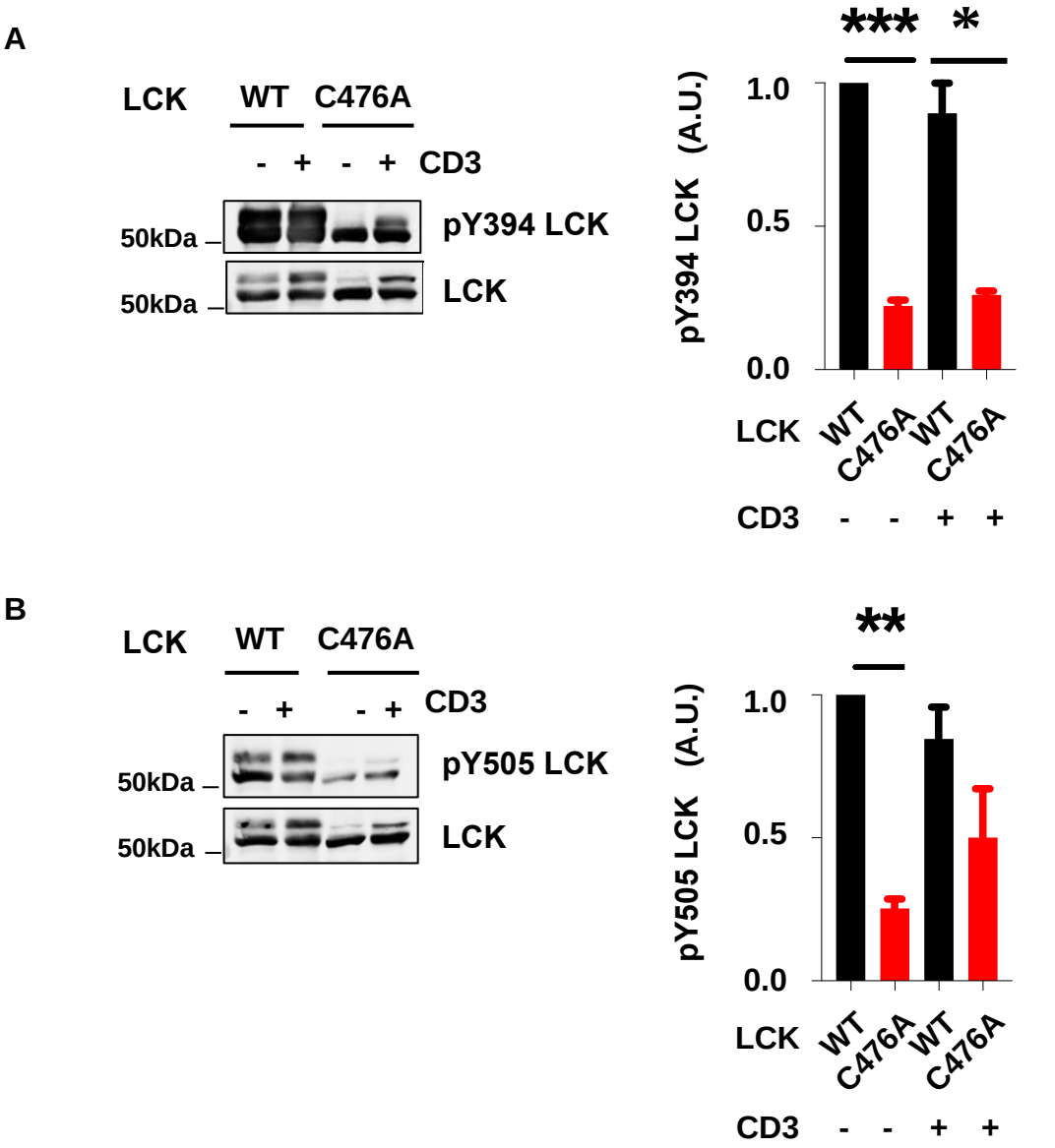

Figure 3.6: LCK C476A is less phosphorylated than LCK WT on both regulatory Y394 and Y505 under resting conditions and upon TCR stimulation
J.LCK cells were transfected with construct 1 expressing either LCK WT or LCK C476A. The phosphorylation levels of Y394 (A) and Y505 (B) under both resting condition and upon CD3 stimulation were analyzed using phospho-specific antibodies by Immunoblotting analysis. One representative of 3 independent experiments is shown. It must be noted here that for the immunoblotting analyses equal protein amounts of WT and C476A LCK have been loaded. LCK phosphorylation was quantified and normalized first to the respective LCK expression. Subsequently, all the obtained values were normalized to the value of LCK WT in resting cells, which was set to 1. Then values were expressed as Arbitrary Units (A.U.). Bar graphs show mean ± SEM of 3 independent experiments. Statistical analysis was performed using one sample *t*-Test for unstimulated samples. For CD3-stimulated samples an unpaired two-sample Student's *t*-Test was used. We did not observe statistical significance between CD3-stimulated samples in panel B. *p<0.05, **p<0.005, ***p<0.001

Next, to determine whether the reduced phosphorylation of LCK is due to an impaired enzymatic activity, I used the SFKs inhibitor PP2 (Hanke et al., 1996). PP2 is a small molecule which binds to a deep hydrophobic pocket near

the ATP-binding cleft of the enzyme and it likely disrupts the ability of the enzyme to bind ATP (Zhu et al., 1999).

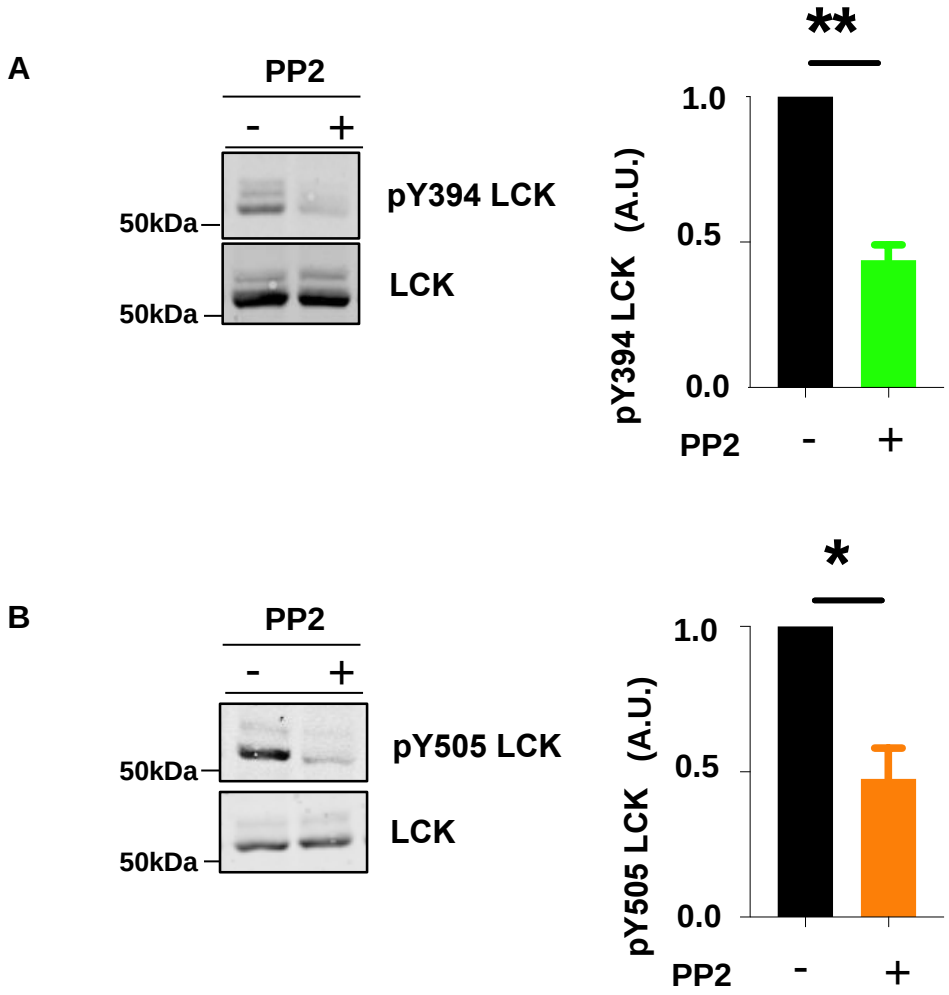

Figure 3.7: Phosphorylation of both regulatory Y394 and Y505 of LCK is decreased upon treatment with the SFK inhibitor PP2
Jurkat T cells endogenously expressing LCK (J.E6) were either left untreated or treated for 1 hour, at 37ºC, with the SRC-family kinase inhibitor PP2. Subsequently, the phosphorylation levels of Y394 (A) and Y505 (B) were analyzed using phospho-specific antibodies by Immunoblotting analysis. One representative of 3 independent experiments is shown. Graphs in A) and B) represent quantifications of LCK phosphorylation. The levels of phosphorylated LCK were normalized to the levels of total LCK. Subsequently, normalized values from all samples were further divided by the normalized value of the untreated samples which were set to 1. Then, values were expressed as Arbitrary Units (A.U.). Bar graphs show mean ± SEM of 3 independent experiments. Statistical analyses were performed using one sample *t*-Test. *p<0.05, **p<0.005

I treated Jurkat T cells (J.E6), which endogenously express LCK, for 1 hour at 37ºC with the PP2 inhibitor and, subsequently, I analyzed the phosphorylation levels on both Y394 and Y505 by immunoblotting analyses. In **Fig. 3.7,** it is clearly shown that treatment with the PP2 inhibitor strongly decreases the phosphorylation levels of both Y394 (**Fig. 3.7A**) and Y505 (**Fig.**

3.7B). Therefore, this result suggests that the reduction of the phosphorylation of Y394 and Y505 can be due to a reduced kinase activity of LCK C476A**.**

3.4.2. LCK C476A shows a decreased kinase activity

To test the hypothesis that LCK C476A has a decreased kinase activity, I directly measured the enzymatic activity of LCK by using a non-radioactive *in vitro* kinase assay. In this *in vitro* kinase assay, the analysis of the enzymatic activity of LCK is based on the measurement of the luminescent signal produced after the conversion of ATP to ADP during a kinase reaction where LCK phosphorylates a specific substrate (please, for a detailed description of the assay see Materials and Methods). J.LCK cells were first transfected with LCK constructs expressing LCK WT, LCK C476A, LCK Y394F, or an empty vector. The Y394F mutation results in an inactivation of LCK and hence this construct was used as a negative control. Next, LCK was immunoprecipitated and 90% of the immunoprecipitates were used to measure the enzymatic activity via the non-radioactive kinase assay (**Fig. 3.8A**). The rest 10% of the immunoprecipitated protein was used to test the efficiency of LCK immunoprecipitation. Immunoblotting analysis of the 10% fraction of immunoprecipitated LCK shown in **Fig. 3.8B** illustrates that the immunoprecipitation of LCK was efficient for all the LCK-expressing constructs. To evaluate the efficiency of the immunoprecipitation of WT, C476A, and Y394F, three control samples were used: (1) an antibody control (**Ab CTRL**), (2) lysates from J.LCK cells transfected with an empty vector (**J.LCK**), and (3) Lysis buffer control (**LB CTRL**) (**Fig. 3.8B**).

To evaluate the function of the *in vitro* kinase assay, three control samples were used (these control samples are different from the ones used for the evaluation of the immunoprecipitation efficiency, as they aim to evaluate a different experimental technique). First, a sample including only the kinase assay buffer, without any immunoprecipitated protein (**Fig. 3.8A, CTRL, grey bar**). As expected, there was no kinase activity detected from the buffer sample. Second, as additional negative control, I used LCK immunoprecipitates from J.LCK cells transfected with an empty vector (**Fig. 3.8A, white bar**). As shown in **Fig. 3.8B,** these cells don't express LCK and therefore the kinase activity

detected was minimal and without statistically significant difference from the CTRL sample. The third negative control consists of LCK immunoprecipitates from J.LCK cells transfected with LCK Y394F, which as mentioned above is kinase dead **(Fig. 3.8A green bar**). LCK Y394F exhibits very low kinase activity, which is not significantly different form CTRL sample and sample from the empty-vector transfected J.LCK cells. Subsequently, I tested the kinase activity of LCK WT. As shown in **Fig. 3.8A (black bar),** the values of kinase activity of LCK WT were significantly higher than the control samples. Next, I tested the kinase activity of LCK C476A. In line with my hypothesis, the non-radioactive *in vitro* kinase assay revealed that LCK C476A shows a strongly reduced kinase activity in comparison to LCK WT (**Fig. 3.8A, red bar**). The kinase activity of LCK C476A is at the same levels than the kinase activity exhibited by the negative control samples. This observation suggests that LCK C476A is enzymatically inactive.

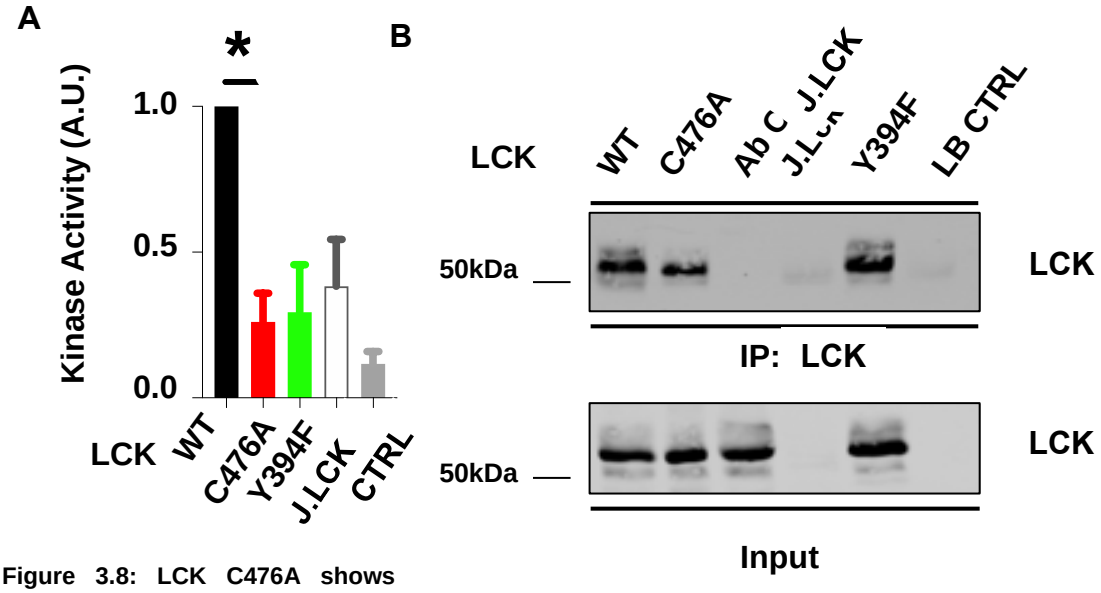

Figure 3.8: LCK C476A shows impaired kinase activity

(A) Analysis of the enzymatic activity of LCK immunoprecipitated from J.LCK cells transfected with construct 1 expressing either LCK WT or LCK C476A. J.LCK cells transfected with an empty vector (J.LCK) or LCK Y394F and kinase assay buffer (CTRL) were used as negative controls. The values of the LCK kinase activity were first normalized to the respective protein level of immunoprecipitated LCK (shown in B). Subsequently, normalized values from all samples were divided by the normalized value of LCK WT which was set to 1. Values were expressed in Arbitrary Units (A.U.). Bar graphs show mean ± SEM of 3 independent experiments. (B) Immunoblotting analysis of the immunoprecipitated LCK. An antibody control sample (Ab CTRL) was used to prove the specific interaction of the protein stained with the anti-LCK antibody. J.LCK cells transfected with an empty vector (J.LCK) sample and Lysis Buffer Control sample (LB CTRL) were used to test the specificity of the immunoprecipitation. One representative of 3 independent experiments is shown. All the experiments were performed at 37°C. For the comparison between WT and C476A samples, one sample *t*-Test was performed (*p<0.05) Additionally, solely for comparison purposes between C476A and controls (Y394F, J.LCK, CTRL), one-way ANOVA test was used (p=0.4820, F=0.9129,). No statistically significant differences were found between C476A and controls. The p-values of the post-hoc Dunnett test were: p=0.9955 for C476A vs Y394F, p=0.8032 for C476A vs J.LCK and p=0.7257 for C476A vs CTRL.

3.4.3 LCK C476A adopts a "primed" conformation

As previously described, the conformational state of LCK depends on the phosphorylation levels of the two regulatory sites Y394 and Y505. Phosphorylation of Y394 is believed to open and to activate LCK (Philipsen et al., 2017), whereas Y505 phosphorylation is thought to generate a closed, inactive form of LCK. The absence of phosphorylation on both Y394 and Y505 generates an inactive but "***open***" LCK which is also known as "***primed***" LCK (Nika et al., 2010, Stirnweiss et al., 2013, Philipsen et al., 2017). On the basis of my data showing that LCK C476A is hypo-phosphorylated on both regulatory Y394 and Y505 and that LCK C476A is enzymatically inactive, I hypothesized that LCK C476A adopts the so called "***primed***" conformation.

To test this hypothesis, I took advantage of a previously developed LCK-biosensor (**Fig. 3.9A**), which allows the analysis of the conformational states of LCK directly in living cells by using dynamic fluorescence lifetime imaging microscopy/Förster resonance energy transfer (FLIM/FRET) measurements (Stirnweiss et al., 2013, Philipsen et al., 2017).

As represented in **Fig. 3.9A**, the LCK-biosensor possesses a donor fluorophore (mTurquoise) and an acceptor fluorophore (mVenus). Before the FLIM/FRET measurement, the donor fluorophore (mTurquoise) is excited to a high energy state. Subsequently energy is transferred to the acceptor fluorophore (mVenus) through nonradiative dipole–dipole coupling. The efficiency of the energy transfer is inversely proportional to the distance between donor and acceptor. In our experiments, we measured the mean fluorescence lifetime of the donor fluorophore. Energy transfer from the donor fluorophore to the acceptor fluorophore decreases the lifetime of the donor fluorophore. Thus, measuring of fluorescence lifetime during FRET measurements allowed us to discriminate between the energy states of the fluorophores. When LCK adopts the "***closed*** "conformation, there is a high energy transfer (FRET) between the donor and acceptor fluorophores and thus lower fluorescence lifetimes. On the contrary, when LCK adopts an "***open***" conformation, there is low energy transfer (FRET) between the donor and acceptor fluorophores and therefore the fluorescence lifetime is higher. In resting J.LCK cells, LCK WT exhibited a mean lifetime of 3.55 ns, whereas LCK

C476A showed a more "***open"*** conformation with a mean fluorescence lifetime of the donor fluorophore of 3.75 ns, (**Fig. 3.9B**).

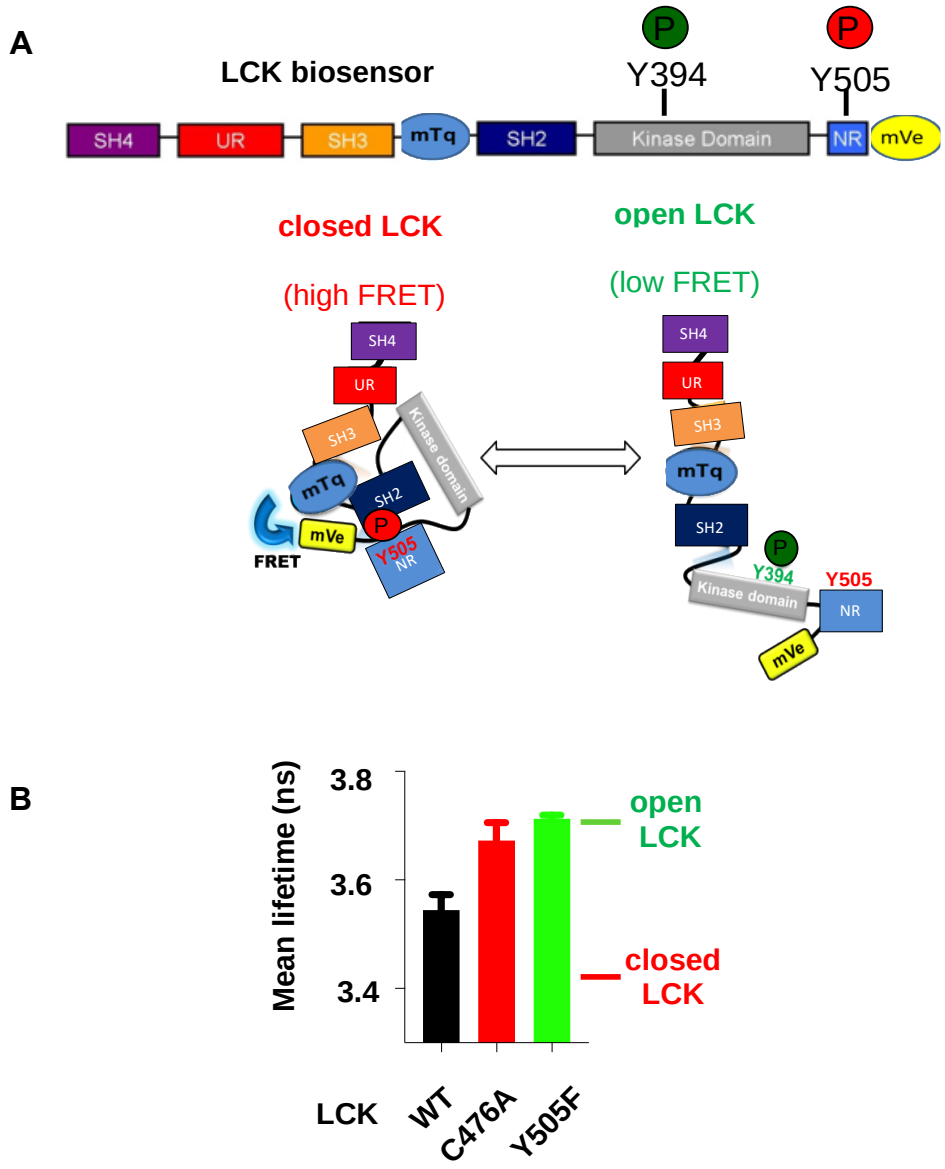

Figure 3.9: Analysis of LCK C476A conformation
(A) Graphical representation of the LCK-biosensor. The LCK-biosensor possesses a donor fluorophore (mTurquoise) between the SH3 and SH2 domains and an acceptor fluorophore (mVenus) at the C-terminal tail. When LCK adopts the "*closed* "conformation, there is high energy transfer (FRET) between the donor and acceptor fluorophores. On the contrary, when LCK adopts an "*open*" conformation there is low energy transfer (FRET) between the donor and acceptor fluorophores. (B) J.LCK cells were transfected with either LCK WT or LCK C476A or LCK Y505F biosensors. LCK Y505F has lost its ability to become phosphorylated on tyrosine Y505 and hence is constitutively in an "open" conformation. FRET intensities (and hence the conformation of LCK) were analyzed by measuring the Mean Lifetimes using FLIM. To be noted that the bar indicated for "closed LCK" is based on previous FLIM/FRET measurements using a constitutively closed LCK Y394F mutant. Bar graphs show mean ± SEM of 3 independent experiments. To statistically compare WT, C476A, and Y505F samples one-way ANOVA was performed. Results showed statistically significant differences (p=0,000038, F=11.77,). Post-hoc Tukey HSD multiple comparison test showed significantly higher mean lifetime of C476A compared to WT (p=0.001) and significantly higher mean lifetime of Y505F compared to WT (p=0,00018). Nano-seconds (ns), fluorescence lifetime imaging microscopy/Förster resonance energy transfer (FLIM/FRET).

I also investigated the conformational state of another LCK mutant, LCK Y505F, in which the tyrosine (Y) residue has been replaced with a phenylalanine (F). Substitution of a tyrosine residue to phenylalanine abolishes its ability to become phosphorylated.

As mentioned before absence of phosphorylation on regulatory Y505 keeps LCK in an "***open***" conformation. Thus, the LCK Y505F mutant is believed to mimic a constitutively "***open***" form of LCK. The mean fluorescence lifetime of LCK C476A appears to have no significant difference from the constitutively ***open*** LCK Y505F.

Thus, my data illustrate that LCK C476A has an "***open"*** conformation, is hypo-phosphorylated on both regulatory Y394 and Y505 residues and is enzymatically inactive. Collectively, these data support my hypothesis that LCK C476A adopts a "***primed***" conformation.

3.5. Impaired signaling in T cells expressing LCK C476A

I have so far shown that LCK C476A likely adopts the "***primed***" conformation. To further examine the function of LCK C476A, I assessed the global tyrosine phosphorylation by immunoblotting analyses in resting J.LCK cells as readout of ongoing tonic/basal TCR signaling. There is evidence that even in the absence of robust and activating antigen triggers, T cells exhibit low-level constitutive signaling in the resting state that is known as "tonic/basal signaling". Tonic TCR signaling takes place in the presence of low affinity interactions (e.g. transient contacts with self-pMHC) and appears to affect the sensitivity of the TCR toward foreign antigens and to be important for the threshold required for T-cell activation (Myers et al., 2017). As it has been previously explained, LCK is crucial for the initiation of TCR signaling and also tonic/basal TCR signaling is dependent on LCK. This explains why LCK-deficient J.LCK cells transfected only with an empty vector (pBOS) do not exhibit any global tyrosine phosphorylation under resting conditions (**Fig. 3.10A, pBOS sample, first line**). Conversely, when J.LCK were reconstituted with LCK WT, I observed clear ongoing tonic/basal TCR signaling (**Fig. 3.10A, WT sample, second line**). The evaluation of global tyrosine phosphorylation

in J.LCK cells expressing LCK C476A, under resting conditions, revealed that this mutant exhibits a strongly reduced tonic/basal signaling compared to LCK WT (**Fig. 3.10A, C476A sample, third line**). To further evaluate the function of the LCK C476A mutant, I investigated CD69 expression, which is the earliest activation marker of T cells (Ziegler et al., 1993), using flow cytometry. **Fig. 3.10B** (**upper panel**) clearly shows that J.LCK cells transfected only with an empty vector (pBOS) do not exhibit any CD69 expression. Therefore, the expression of this early activation marker appears to be dependent on tonic signals and on the expression of LCK in Jurkat T cells. Indeed, reconstitution of J.LCK with LCK WT leads to a 20% upregulation of CD69 (**Fig. 3.10B, middle panel**). Conversely, J.LCK cells reconstituted with LCK C476A exhibit an almost absent (only 1,5%) expression of CD69 (**Fig. 3.10B, lower panel**). Collectively, these data demonstrate that LCK C476A is not able to reconstitute tonic/basal TCR signaling and CD69 expression.

Next, I assessed also global tyrosine phosphorylation upon agonistic TCR stimulation using CD3 antibodies (**Fig. 3.10C**). As TCR signaling strongly depends on LCK, J.LCK cells transfected only with an empty vector (pBOS) do not show any induction of global tyrosine phosphorylation upon TCR stimulation. On the contrary, J.LCK cells reconstituted with LCK WT show a strong induction of global tyrosine phosphorylation upon TCR stimulation using CD3 antibodies (**Fig. 3.10C, WT sample**). On the other hand, LCK C476A exhibits only a weak induction of TCR signaling in J.LCK cells, upon agonistic TCR stimulation (**Fig. 3.10C, C476A sample**). As an additional readout for TCR signaling, I investigated the induction of phosphorylation levels of ERK1/2, upon TCR stimulation. In line with the global tyrosine phosphorylation, T cells expressing LCK C476A show a weak induction of TCR-mediated phosphorylation of ERK1/2 in comparison to cells expressing LCK WT (**Fig. 3.10D-E**).

Collectively, my data suggest that the C476A mutation strongly affects LCK function.

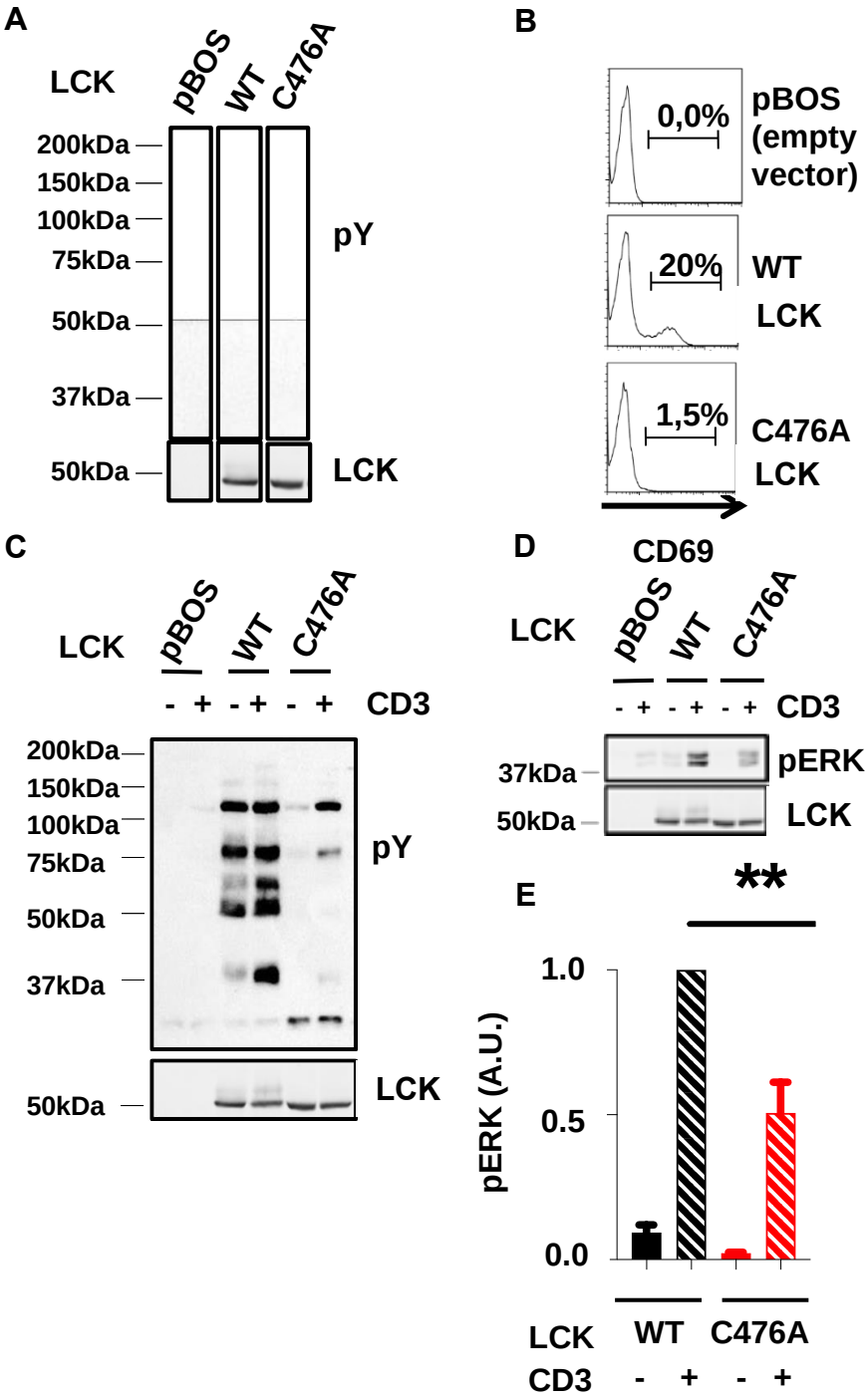

Figure 3.10: Impaired signaling in Jurkat T cells expressing LCK C476A
J.LCK cells were transfected with construct 1 expressing either LCK WT or LCK C476A or an empty vector (pBOS): (A) the levels of global tyrosine phosphorylation resulting from basal/tonic signaling (steady-state condition) were analyzed by immunoblotting. (B) CD69 expression in steady-state conditions was analyzed by flow cytometry. One representative of 3 independent experiments is shown. (C) The levels of global tyrosine phosphorylation upon TCR stimulation (CD3) were analyzed by Immunoblotting analysis. One representative of 3 independent experiments is shown. (D) The levels of ERK1/2 phosphorylation upon TCR stimulation (CD3) were analyzed by Immunoblotting. One representative experiment is shown (n=3) (E) Bar graphs show mean ± SEM of ERK1/2 phosphorylation from 3 independent experiments. The phosphorylation signals were quantified and normalized first to the respective levels of total LCK. Subsequently, all normalized values were divided by the normalized value of LCK WT and expressed as Arbitrary Units (A.U.). To show statically significant differences in the CD3-mediated ERK activation between WT and C476A, we performed one-sample *t*-Test. **p<0.005

3.6. CDC37 regulates the stability of LCK C476A

It has been previously shown that the chaperone/co-chaperone complex HSP90-CDC37 plays a crucial role in the expression and stability of kinases (Verba et al., 2016). In our group, it has been shown that overexpression of the co-chaperone CDC37 is able to partially stabilize a ZAP-70 C575A mutant (Thurm et al., 2017a). To test the hypothesis of a possible involvement of the co-chaperone CDC37 also in the regulation of LCK C476A stability, I have overexpressed CDC37 with either LCK WT or LCK C476A in J.LCK cells and assessed LCK expression by immunoblotting analysis. As shown in **Fig. 3.11A and 3.11B**, overexpression of CDC37 is able to rescue the expression of LCK C476A (expression increased from 0,73 to 0,99). Conversely, the effect of CDC37 overexpression on the protein levels of LCK WT was not significant. These data suggest that, similarly to ZAP-70 C575A, the co-chaperone CDC37 is also important for the stability of LCK C476A (Thurm et al., 2017a).

I wanted to further investigate whether protein stabilization of LCK C476A by CDC37 impacts also its function. To test this hypothesis, I have over-expressed CDC37 with either LCK WT or LCK C476A and assessed global tyrosine phosphorylation in resting J.LCK cells by Immunoblotting analysis. As shown in **Fig. 3.11C** and **Fig. 3.11D**, overexpression of CDC37 increases the levels of tonic/basal signaling in resting J.LCK cells expressing LCK C476A. However, overexpression of CDC37 had no effect on ongoing tonic/basal signaling in J.LCK cells expressing LCK WT. These data are in line with published data from my group showing that CDC37 is dispensable for the regulation of LCK WT activity/stability (Kowallik et al., 2020) These findings indicate that CDC37 is important for the regulation of the expression/stability of LCK C476A. It is likely that the CDC37-mediated stabilization of LCK C476A, partially rescued its activity and hence its function.

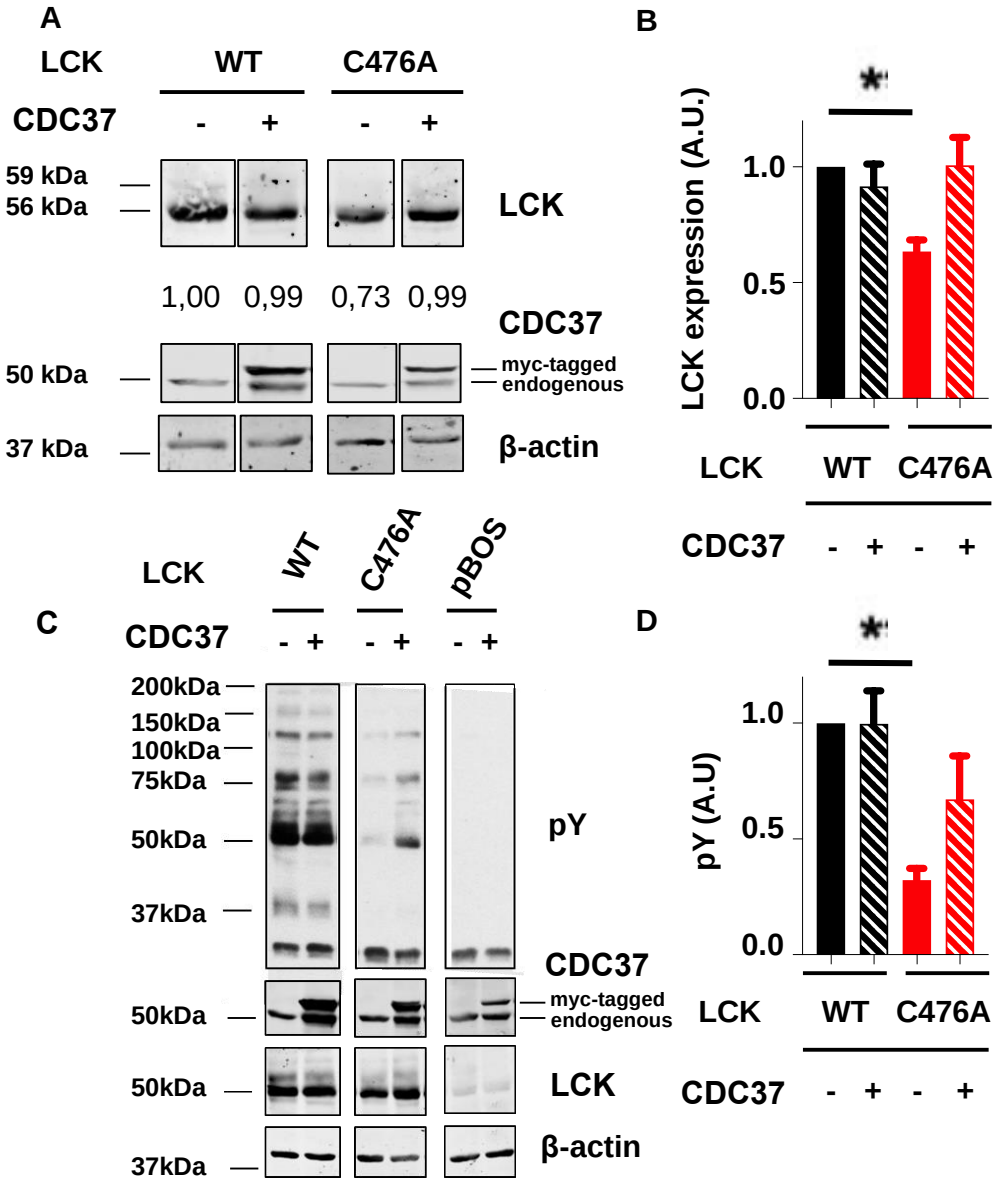

Figure 3.11: CDC37 is important for the stability and the activity of LCK C476A
J.LCK cells were co-transfected with CDC37 and constructs expressing either LCK WT or LCK C476A. (A) LCK expression was evaluated by immunoblotting analyses. One representative experiment is shown. LCK expression was first quantified and divided to LCK WT, in the absence of CDC37. Then the values were expressed in Arbitrary Units (A.U.). Numbers indicate the relative expression of LCK normalized to LCK WT. The two bands appearing on the CDC37 blot belong to the endogenously expressed CDC37 and to the Myc-tagged transfected CDC37, respectively. (B) Bar graphs show mean ± SEM of 3 independent experiments of (A). (C) The levels of global tyrosine phosphorylation were analyzed by immunoblotting analyses. One representative experiment is shown. (D) Bar graphs show mean ± SEM of 3 independent experiments of (C). β-actin was used as loading control. Phosphorylation was quantified and normalized first to LCK expression. Subsequently, all normalized values were divided by the normalized value of LCK WT untreated sample which was set to 1. Values were finally expressed in Arbitrary Units (A.U.). Statistical analyses were performed as follow: for comparisons between WT and C476A samples without CDC37, we used one-sample *t*-Test. For omparisons between WT and C476A samples upon CDC37 expression, we used an unpaired two-sample Student's *t*-Test. No statistically significant differences were found between samples upon CDC37 expression. *p<0.05

3.7 LCK C476A is temperature-sensitive

During my work in the lab, I made a surprising observation. Upon incubation of LCK C476A transfected J.LCK T cells at 25ºC, I have found that basal/tonic signaling was strongly increased. These results indicate that the temperature influences the function of LCK C476A. Therefore, I decided to further examine this phenomenon and to evaluate whether LCK C476A is temperature-sensitive.

As a measure of the enzymatic activity of the kinase, I assessed global tyrosine phosphorylation (tonic signaling) upon incubation of transfected J.LCK cells at different temperatures (25ºC, 33ºC, 37ºC and 39ºC) (**Fig. 3.12A**). Initially, I observed that global tyrosine phosphorylation in J.LCK cells expressing LCK C476A is significantly higher at lower temperatures (i.e. 25ºC and 33ºC) than at higher temperatures (i.e. 37ºC and 39ºC) (**Fig. 3.12A, lines 5 and 6 in comparison to 7 and 8, respectively).** Moreover, data shown in **Fig. 3.12A (lines 3 and 4 in comparison to 7 and 8, respectively)** and their respective quantification in **Fig. 3.12B,** show that at higher temperatures (i.e. 37ºC and 39ºC) LCK C476A expressing J.LCK cells exhibit a strongly reduced basal/tonic signaling in comparison to LCK WT. On the contrary, at lower temperatures (25ºC) it appears that the LCK C476A expressing J.LCK cells exhibit a higher basal/tonic signaling in comparison to LCK WT (**Fig. 3.12A, line 5 in comparison to 1).** As expected, there was no detectable tyrosine phosphorylation in J.LCK cells transfected with an empty vector (pBOS) (**Fig. 3.12A, lines 9 to 12**).

The protein expression of LCK constructs is also affected at the different temperatures. It is important to note that the transfection of J.LCK with DNA constructs expressing either LCK WT or LCK C476A was adjusted in this experimental setup in order to achieve an equal expression between LCK WT and C476A. It is clear in **Fig. 3.12A (middle blot)** and **Fig. 3.12C** that protein expression of both LCK WT and LCK C476A gradually decreases while temperature increases, thus indicating that LCK becomes less stable at higher temperatures (**Fig. 3.12A, middle blot and Fig. 3.12C)**.

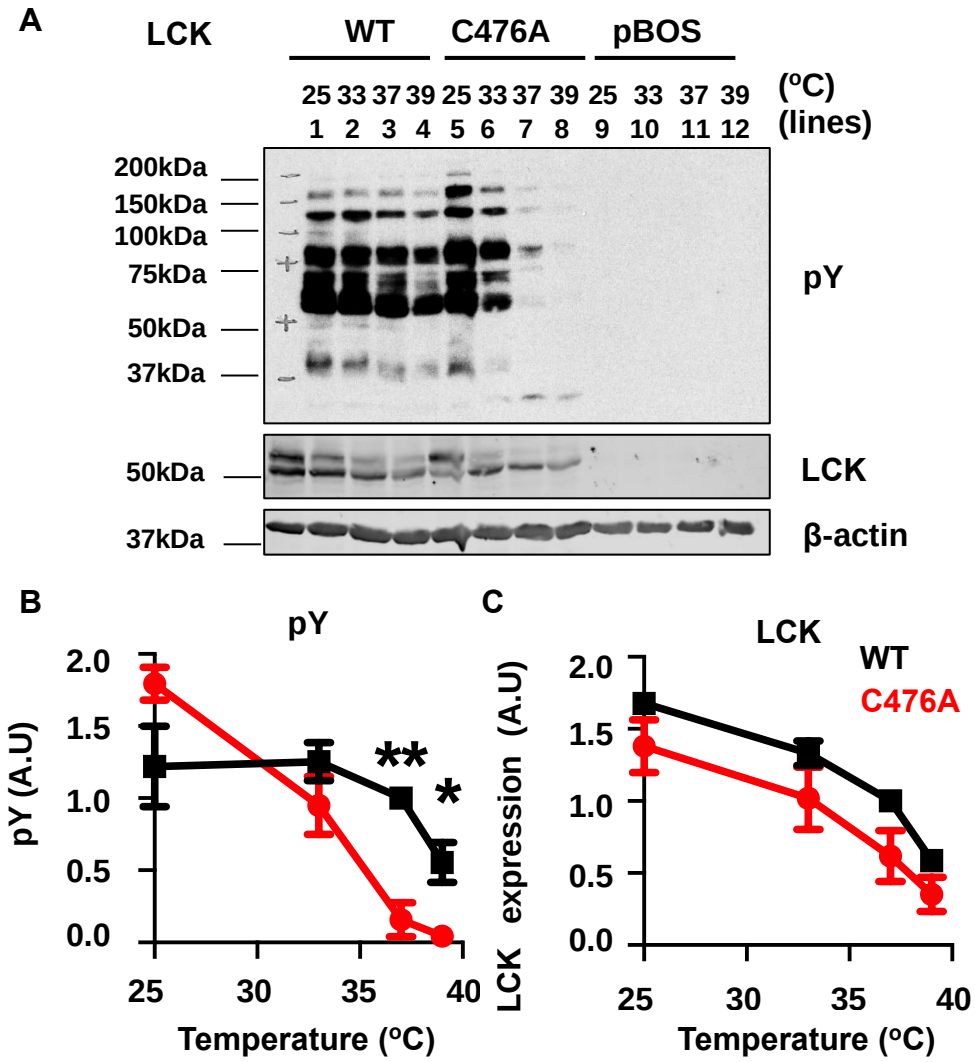

Figure 3.12: LCK C476A is temperature-sensitive
J.LCK expressing LCK WT, LCK C476A, or an empty vector (pBOS) were incubated for 1 hr at different temperatures as indicated. First, (A) the levels of global tyrosine phosphorylation and LCK expression were analyzed by immunoblotting analyses. One representative of 3 independent experiments is shown. (B) Bar graphs show mean ± SEM of the levels of global tyrosine phosphorylation. Global tyrosine phosphorylation and LCK expression were quantified. The values of global tyrosine phosphorylation were first normalized to the respective LCK expression. Subsequently, the normalized values were divided with the value from LCK WT at 37ºC which was set to 1 and values were expressed in Arbitrary Units (A.U.). (C) LCK expression, from 3 independent experiments, was divided with the value of LCK WT expression at 37ºC which was set to 1. Values were then expressed in Arbitrary Units (A.U.). Statistical analysis was performed using unpaired two sample Student´s, *t*-Test. *p<0.05, **p<0.005.

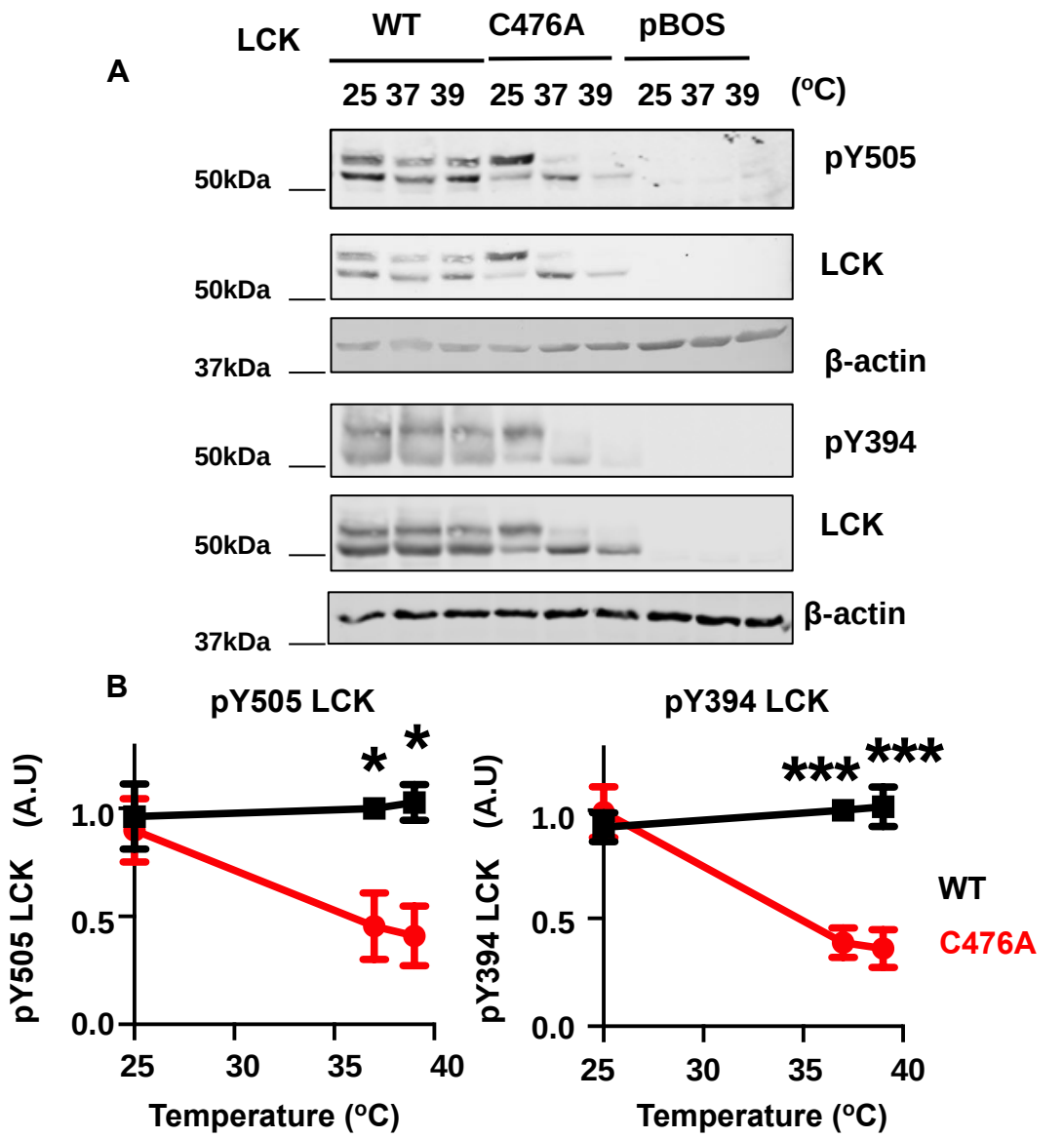

Figure 3.13: Phosphorylation of the regulatory Y394 and Y505 increases at lower temperature in T cells expressing LCK C476A

J.LCK cells expressing LCK WT, LCK C476A or an empty vector (pBos) were incubated for 1 hr at different temperatures as indicated. (A) The phosphorylation levels of Y394 and Y505 under resting conditions were analyzed using phospho-specific antibodies by Immunoblotting. One representative of 3 independent experiments is shown (B) Bar graphs show mean ± SEM of the phosphorylation levels of Y394 and Y505 from 3 independent experiments. Phosphorylation and LCK expression were quantified. The values of Y394 and Y505 phosphorylation were first normalized to the respective LCK expression. Subsequently, the normalized values were divided by the value from LCK WT at 37ºC which was set to 1. Values were then expressed in Arbitrary Units (A.U.). Statistical analysis was performed using unpaired two-sample Student´s, *t*-Test. *p<0.05, ***p<0.001

In order to assess whether the temperature has an effect on the phosphorylation of regulatory Y505 and Y394, I performed immunoblot analyses. Data in **Fig. 3.13A-B** clearly illustrate that at 25ºC the phosphorylation of both Y505 and Y394 (**Fig. 3.13B**), is similar for LCK WT and LCK C476A. On the contrary at higher temperatures (37ºC and 39ºC) the

phosphorylation of Y394 and Y505 (**Fig. 3.13B**) severely decrease for J.LCK T cells expressing LCK C476A.

Taken together, these data suggest that LCK C476A is temperature-sensitive and hence its function/activity is strongly influenced by temperature changes.

3.8 Analysis of the activity/function of LCK C476A at 25ºC

I showed previously that LCK C476A is highly active at 25°C. I hypothesize that, at this temperature, LCK C476A is thermodynamically more stable and thus more active enzymatically. Moreover, it seems that in resting cells LCK C476A exhibits an even stronger global tyrosine phosphorylation than LCK WT indicating that tonic signaling is enhanced. To shed light onto this phenomenon, I initially assessed the expression of LCK C476A in J.LCK cells by Immunoblotting analysis.

The expression of LCK C476A was also significantly reduced at 25°C (about 30%) in comparison to LCK WT (**Fig. 3.14**), an observation that is in line with the data reported above obtained at 37ºC (**Fig. 3.4**). Thus, the enhanced tonic signaling observed at 25°C is not due to an increase in the expression of the LCK mutant.

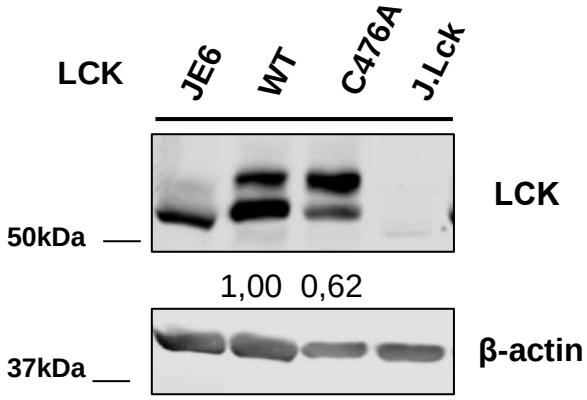

Figure 3.14: LCK C476A is less expressed than LCK WT also at 25ºC
J.LCK cells were transfected with construct 1 expressing either LCK WT or LCK C476A: LCK expression was evaluated by Immunoblotting analysis. JE6 Jurkat cells, expressing endogenously LCK, were used as a positive control. β-actin was used as loading control. One representative of 5 independent experiments is shown. The values were divided with LCK WT value which were set to 1. Values were then expressed in Arbitrary Units (A.U.).

I previously evaluated whether the activation of LCK C476A is increased at 25°C by assessing the phosphorylation of the regulatory Y394 and of Y505

in resting J.LCK cells by immunoblotting analysis. Data in **Fig. 3.13A-B** clearly illustrate that at 25ºC the phosphorylation of both Y505 and Y394 (**Fig. 3.13B**), is similar for LCK WT and LCK C476A. On the basis of these data, it can be concluded that there are no significant differences in the overall activity between LCK C476A and WT. However, tonic signaling is emanated from the TCR at the plasma membrane. Therefore, I wanted to investigate more in detail the phosphorylation of the fraction of LCK C476A localized specifically at the plasma membrane. To this aim, I took again advantage of the immunofluorescence SOP protocol for the confocal analysis of total LCK and its phosphorylated forms (Philipsen et al., 2017) (**Fig. 3.15A**).

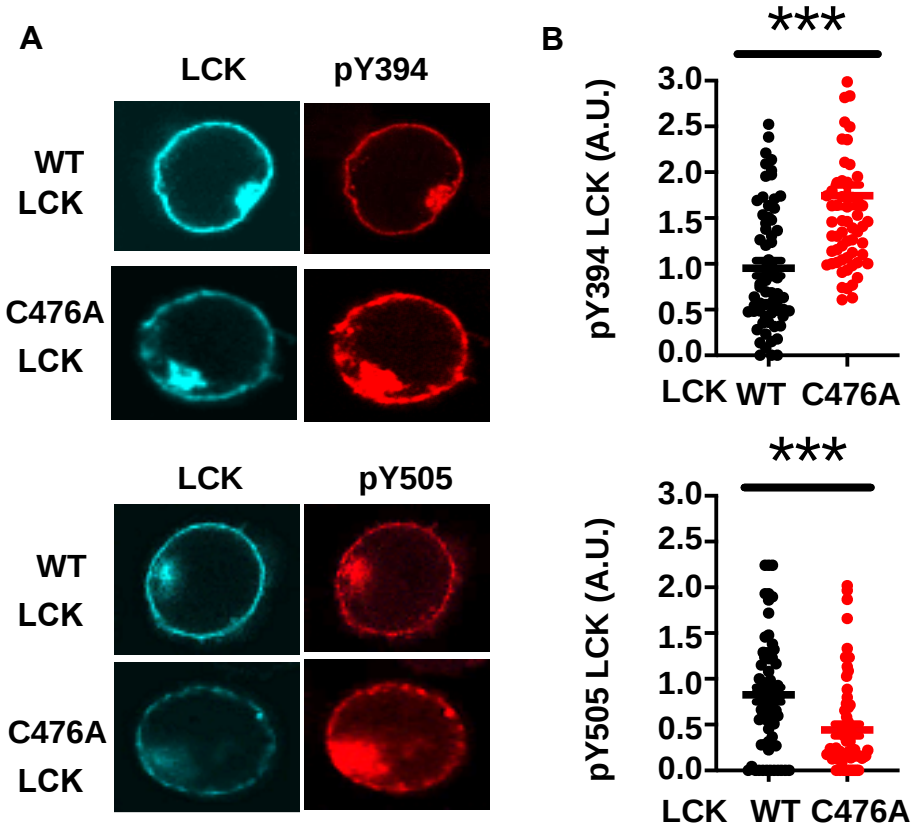

Figure 3.15: LCK C476A is more phosphorylated on Y394 and less phosphorylated on Y505 than LCK WT at the plasma membrane of Jurkat T cells
J.LCK cells were transfected with construct 1 expressing either LCK WT or LCK C476A: (A) Phosphorylation levels of regulatory Y394 and Y505, at the plasma membrane of J.LCK cells, were analyzed using confocal microscopy, with the same methodology as shown in **Figure 5**. One representative of 3 independent experiments is shown. (B) Fluorescence intensity from LCK phosphorylation from different subcellular compartments was quantified and normalized to the respective LCK expression level. Next, the values were divided with LCK WT values which were set to 1. Values were then expressed in Arbitrary Units (A.U.). Dot plots contain data pooled from 3 independent experiments. Each dot represents an individual J.LCK T cell. Statistical analysis was performed using unpaired two-sample Student´s *t*-Test, ***p<0.001.

I quantified the fluorescence signal of phospho-specific antibodies that detect Y394 or Y505 from the plasma membrane area (**Fig. 3.15B**). Data shown

in **Fig. 3.15B** suggest that at the plasma membrane, LCK C476A is significantly more phosphorylated on Y394 (**Fig. 3.15B**, **upper graph**) and less phosphorylated on Y505 (**Fig. 3.15B**, **lower graph**) than LCK WT. The higher phosphorylation on Y394 of LCK C476A at the plasma membrane suggests that at 25ºC LCK C476A is likely more active than LCK WT.

3.8.1 LCK C476A has an enhanced kinase activity at 25ºC

Since LCK C476A appears to be more active at 25ºC, I decided to further assess its kinase activity. To this aim, I have set up an "in cell" kinase activity assay (**Fig. 3.16A**). I evaluated the ability of either LCK WT or LCK C476A to phosphorylate on Y394 a YFP-tagged kinase dead mutant of LCK (LCK K273R), which functions as a substrate, as readout for LCK's enzymatic activity. As shown in **Fig. 3.16B (upper panel)**, LCK K273R doesn't exhibit any phosphorylation of Y394 as it is neither able to auto-phosphorylate nor to trans-phosphorylate other LCK molecules. Evaluation of the kinase activity of LCK WT and LCK C476A in "*in cell*" kinase activity assay and subsequent quantification of the immunoblotting analysis revealed that LCK C476A is able to phosphorylate its substrate LCK K273R better (40-50%) than LCK WT (**Fig. 3.16B, upper panel and Fig. 3.16C**), thus indicating that LCK C476A display an enhanced enzymatic activity at 25ºC in resting J.LCK T cells.

Collectively, the data reported above indicate that LCK C476A has an enhanced activity at 25ºC.

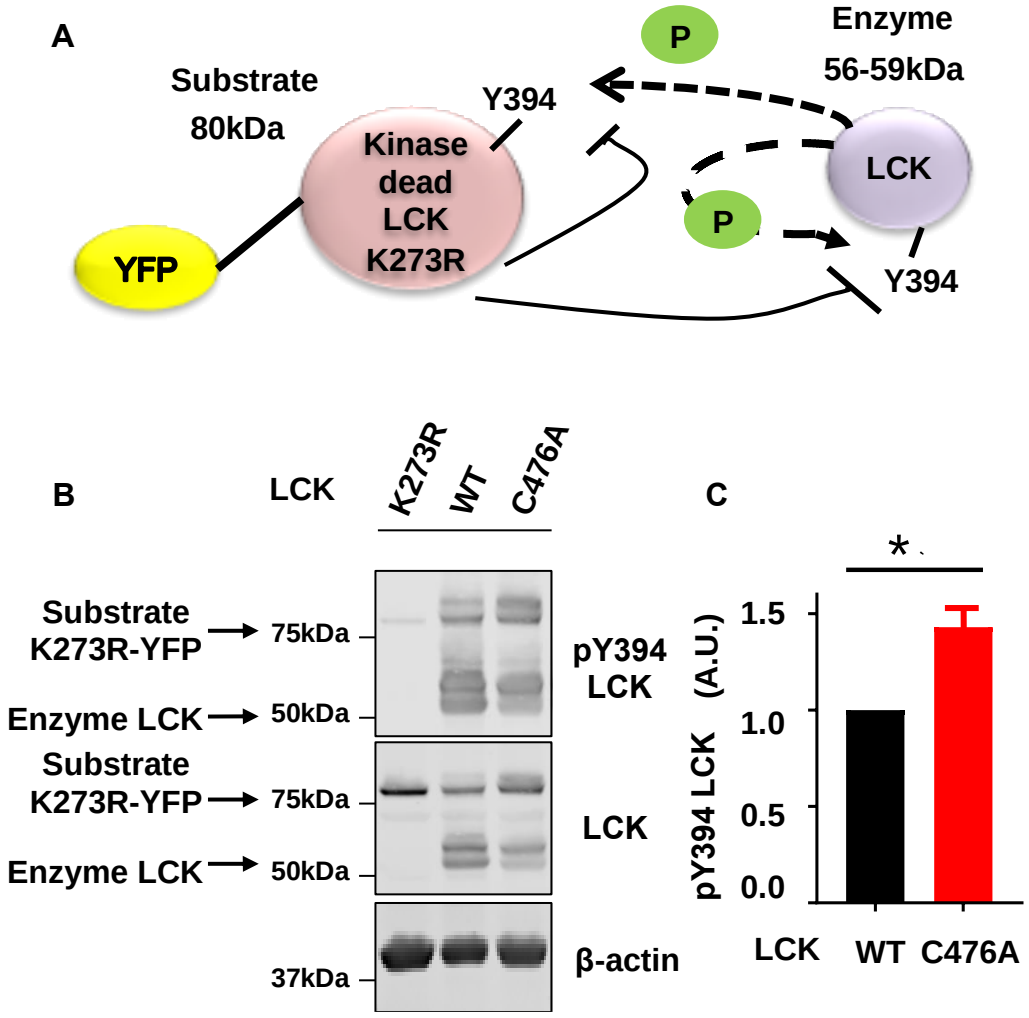

Figure 3.16: Analysis of LCK C476A enzymatic activity at 25ºC
(A) Graphical representation of the "*in cell*" kinase activity assay. LCK is able to trans- phosphorylate and auto-phosphorylate on Y394. The phosphorylation on Y394 of a kinase dead LCK K273R mutant was used to detect the kinase activity of either LCK WT or LCK C476A. LCK K273R is a suitable substrate as it can be phosphorylated on Y394 but is not able to auto- trans-phosphorylate because of the lack of kinase activity. In order to distinguish, during the Immunoblotting analysis, the two different LCK molecules, a LCK K273R-YFP tagged construct was used that can be detected at ~80kDa, whereas LCK WT and LCK C476A can be detected at 56-59kDa. (B) LCK WT or LCK C476A were expressed in J.LCK cells, and the phosphorylation on Y394 of LCK and the protein expression of LCK K273R and LCK WT or C476A were assessed by immunoblotting analysis using phospho-LCK (Y394) and anti-LCK antibodies, respectively. One representative of 3 independent experiments is shown. (C) Bar graphs show mean ± SEM of Y394 phosphorylation from 3 independent experiments. Here it is important to be noted that, after quantification of the immunoblotting analysis, the data from Y394 phosphorylation of LCK K273R were normalized twice: first to the respective protein expression of the K273R mutant and subsequently to the expression of either LCK WT or LCK C476A. (non-tagged constructs, 56-59kDa). Then all values were divided with the normalized value of LCK WT sample which was set to 1. Values were then expressed in Arbitrary Units (A.U.). Statistical analysis was performed using one sample *t*-Test (for C) *p<0.05.

3.8.2 Spontaneous clustering of activated LCK C476A and increased co-localization with the TCR/CD3-complex at the plasma membrane at 25ºC

During the analyses of the Y394 phosphorylation using the immunofluorescence microscopy SOP protocol, I observed that LCK C476A, but not LCK WT, spontaneously forms clusters at the plasma membrane (**Fig. 3.17A, quantification in Fig. 3.17B**). These clusters appear to contain an active form of LCK. As previously described, the phosphorylation of conserved tyrosine residues (ITAMs) in the CD3ζ chain by LCK is a crucial step in the initiation of TCR signaling. I hypothesized that the LCK C476A clusters may also contain activated TCR/CD3 complex. This hypothesis can explain why tonic signaling is enhanced in J.LCK T cells expressing LCK C476A at 25°C. Therefore, I analyzed the co-localization of CD3ζ chain with LCK WT and LCK C476A in transfected J.LCK cells using confocal microscopy. As shown in **Fig. 3.17A (lower panel)** and **Fig. 3.17C** the co-localization between LCK C476A and the CD3ζ chain is significantly higher in comparison to LCK WT. To further assess whether the CD3ζ chain is also more phosphorylated, I investigated the phosphorylation of the CD3ζ chain by immunoprecipitation followed by immunoblotting. As clearly shown in **Fig. 3.17D,** J.LCK cells reconstituted with LCK C476A display a higher phosphorylation of the CD3ζ chain compared to J.LCK cells reconstituted with LCK WT.

In conclusion, I have shown that at 25ºC LCK C476A clusters spontaneously, thus enhancing LCK transphosphorylation and activation. Additionally, LCK C476A co-localizes with and phosphorylates the TCR/CD3 complex, thus enhancing basal/tonic signaling.

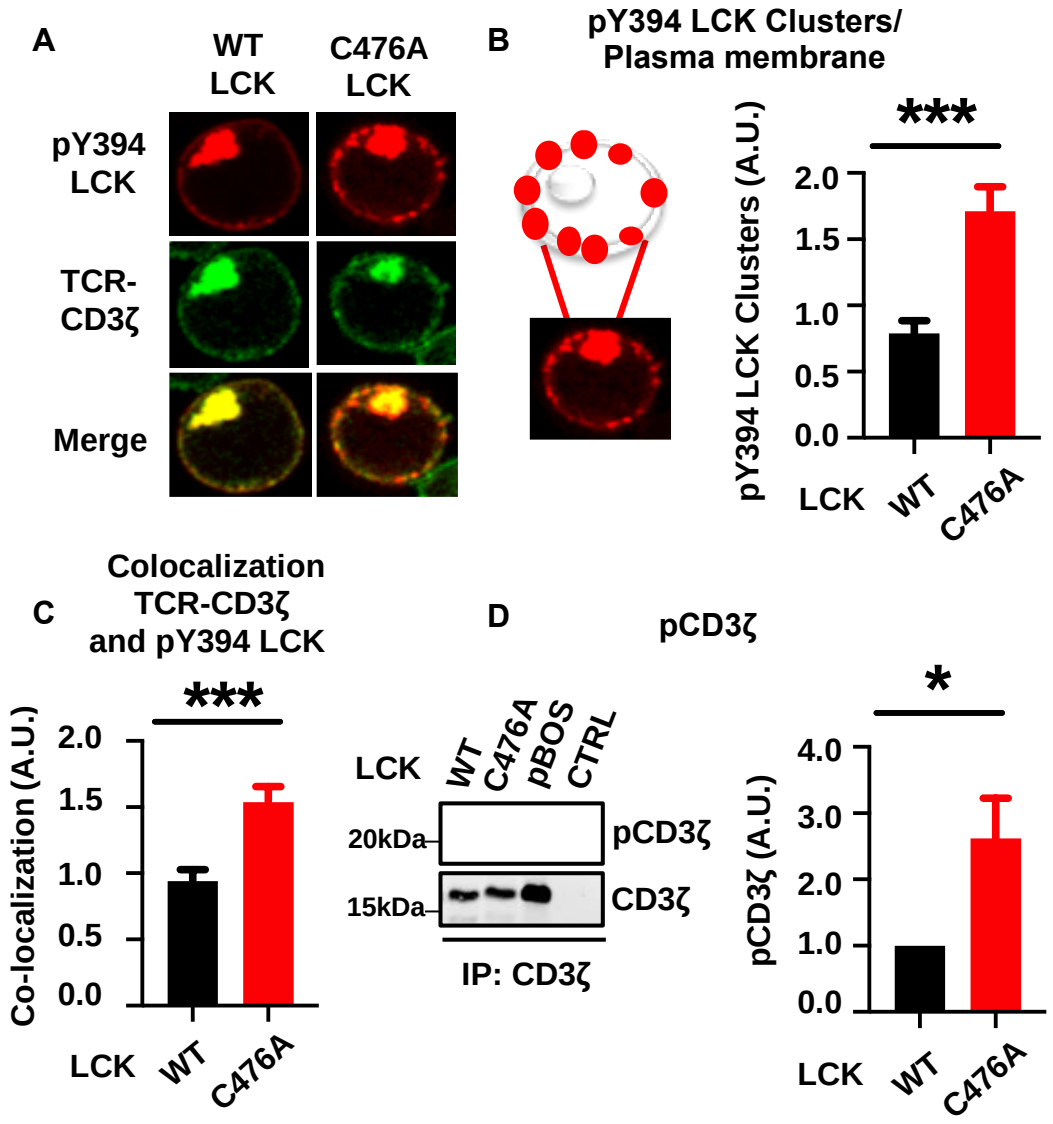

Figure 3.17: Spontaneous clustering of LCK C476A and increased co-localization with the TCR/CD3 -complex at the plasma membrane at 25ºC

J.LCK cells were transfected with constructs expressing either LCK WT or LCK C476A: (A) the phosphorylation levels of Y394 and the expression levels of TCR/CD3ζ were analyzed using confocal microscopy. Cells were stained with specific phospho-LCK (Y394) and anti-CD3ζ chain antibodies. (B) Analysis of LCK clustering at the plasma membrane using confocal microscopy. Using a predefined same-size field of view, transfected cells with either LCK WT or LCK C476A, were distributed into two groups: cells exhibiting a clustering pattern at the plasma membrane (scheme) and cells that do not exhibit this pattern. Bar graphs show mean ± SEM of clustering pattern from 3 independent experiments and 5 different fields of view per experiment. Values were normalized to LCK WT value. Values were then expressed as Arbitrary Units (A.U.). (C) Co-localization analysis between LCK-phosphorylated on Y394 and the CD3ζ chain, using confocal microscopy imaging. Measurements of co-localization were performed with the image processing program ImageJ, using Pearson's correlation coefficient. Bar graphs show mean ± SEM of co-localization analysis between LCK WT or LCK C476A and the CD3ζ chain, from 3 independent experiments and from (at least) 50 different cells. Values were normalized to LCK WT sample. Values were then expressed as Arbitrary Units (A.U.). (D) J.LCK cells were transfected with constructs expressing either LCK WT or LCK C476A or an empty vector (pBOS). The CD3ζ chain was immunoprecipitated and the levels of CD3ζ phosphorylation were analyzed by immunoblotting analysis using a phospho-CD3ζ (Y142) antibody. One representative of 3 independent experiments is shown. Bar graphs show mean ± SEM of CD3ζ phosphorylation from 3 independent experiments. CD3ζ phosphorylation was normalized to the protein levels of immunoprecipitated-CD3ζ chain. Then, the values were divided with the normalized values from LCK WT value which was set to 1. Values were then expressed in Arbitrary Units (A.U.). All experiments were performed at 25ºC. Statistical analyses were performed using an unpaired two-sample Student´s, *t*-Test (B and C), and one sample *t*-Test (D). *p<0.05, ***p<0.001

3.9 Analysis of LCK C476A oxidation

The data presented above indicate that C476 has a crucial role in the regulation of LCK activity. Recently, it has been proposed that reactive oxygen species (ROS) may directly influence the activity of PTKs (Belikov et al., 2015, Simeoni and Bogeski, 2015, Simeoni et al., 2016). Cysteine residues have become the center of attention because of their important role in the regulation of the activity on many enzymes and specifically PTKs. The thiol group of cysteines has particular chemical properties allowing reactions with reactive oxygen species, coordination of transition metal ions, or reactions with electrophiles. As mentioned above, our group has recently shown that cysteine at position 575 in the tyrosine kinase ZAP-70 regulates the stability and the function of the protein and it is also a target of sulfenylation (Thurm et al., 2017a). This cysteine is highly conserved among tyrosine kinases (**Fig. 3.2B)** and previous studies showed that this residue is sulfenylated and that it is crucial for the kinase activity of many other kinases such as c-SRC (C498), c-RET (C376) and PDGFR-beta (C940) (Kato et al., 2000, Rahman et al., 2010). In LCK, the conserved cysteine residue is located at position 476. Therefore, I decided to investigate whether C476 is also sulfenylated.

3.9.1 C476 does not appear to be sulfenylated

The sulfenic acid modification (or sulfenylation) describes the R-SOH group that is generated from the oxidation of a thiolate by hydrogen peroxide (H_2O_2). Stable and specific labelling of sulfenylated thiols has been reported to be achieved with the use of dimedone-based probes conjugated with biotin (Charles et al., 2007). Therefore, to study whether C476 is a possible target of sulfenylation, I took advantage of the dimedone-based probe DCP-Bio1. J.LCK cells were transfected with constructs expressing either LCK WT or LCK C476A. Subsequently, cells were treated with 1mM DCP-Bio1 or vehicle (DMSO) for 1 hour at 37^{o}C, which was followed by cells lysis and pull-down of biotinylated proteins with streptavidin coated beads. Afterwards, sulfenylation

of LCK was analyzed by immunoblotting analysis using an anti-LCK antibody. As shown in **Fig. 3.18A** (**upper panel, lines 5 and 6**), I detected sulfenylation of both LCK WT or LCK C476A under these conditions. Quantification of four experiments revealed no statistically significant difference in the sulfenylation levels between LCK WT and LCK C476A (**Fig. 3.18B, bars 1 and 2**). As negative control, part of the transfected cells were treated, prior to cell lysis, with N-Acetyl Cysteine (NAC), which has a well-established antioxidant and reducing activity (Aldini et al., 2018). As it can be clearly seen in **Fig. 3.18A** (**upper panel, lines 7 and 8**) the sulfenylation detected on both LCK WT or LCK C476A transfected cells, is strongly decreased upon treatment with NAC, thus indicating that the observed sulfenylation signals was highly specific. Quantification of several experiments validated the statistically significant reduction of sulfenylation upon treatment with NAC (**Fig. 3.18B, bars 3 and 4**). As a positive control, membranes from the pull-down experiments were reprobed with a SHP1 antibody. SHP1 is an already known target of cysteine sulfenylation and hence was used as positive control (Weibrecht et al., 2007). As shown in **Figure 3.18A** (**lower panel**) SHP1 was found to be sulfenylated under these conditions (**Fig. 3.18A, lower panel, lines 5 and 6**) and also that NAC treatment reduces its sulfenic acid levels (**Fig. 3.18A, lower panel, lines 7 and 8).** It is important to mention that the input protein levels from both LCK WT and LCK C476A were comparable (**Fig. 3.18A, upper panel, lines 1 and 2**).

On the basis of these results, I conclude that LCK is sulfenylated in J.LCK cells under resting conditions. As the substitution of the cysteine at position 476 does not reduce the total sulfenylation level of LCK, it can be concluded that LCK C476 is likely not sulfenylated.

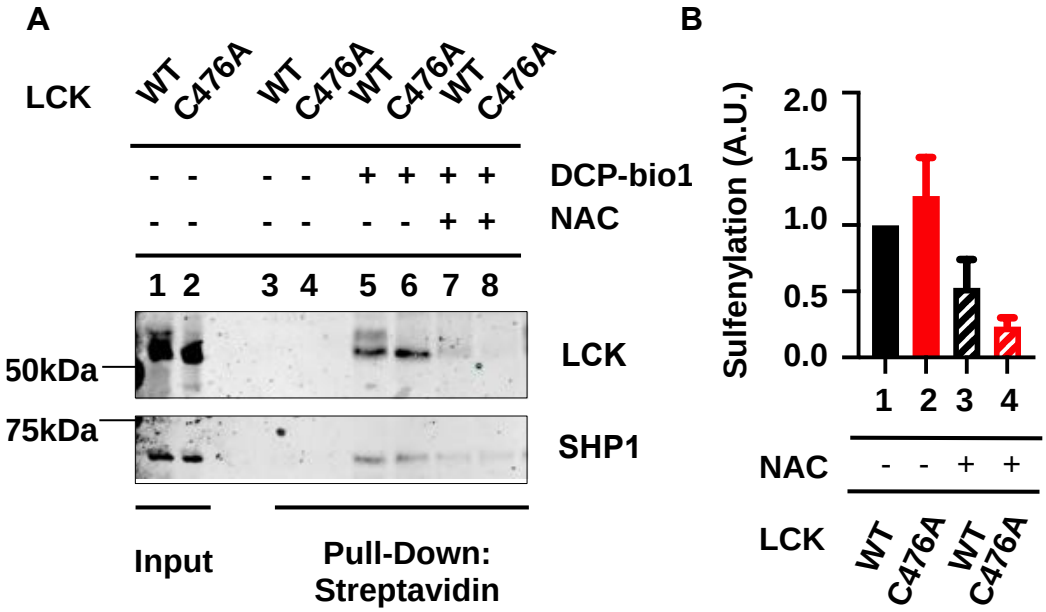

Figure 3.18: C476 does not appear to be a major sulfenylation target
(A) J.LCK cells were transfected with constructs expressing either LCK WT or LCK C476A. As a negative control, part of the cells was treated with 20mM of N-Acetyl Cysteine (NAC) (lines 7 and 8**)**, a well-established antioxidant agent. Subsequently, cells were treated with 1mM DCP-Bio1 (lines 5-8**)** or vehicle (DMSO) (lines 4 and 5**)** for 1 hour at 37ºC. Next, cells were lysed and biotinylated proteins were pulled-down using Streptavidin coated beads. LCK levels were analyzed by immunoblotting analysis using an anti-LCK antibody (upper panel). As a positive control, SHP1 sulfenylation was analyzed by immunoblotting analysis using an SHP1 antibody (lower panel). A small fraction of total cell lysates was analyzed by immunoblotting analysis to determine the amount of LCK and SHP1 "input" (lines 1 and 2**)**. One representative of 3 independent experiments is shown. (B) Bar graphs show mean ± SEM of 3 independent experiments. Values were divided with the values from the untreated, with NAC, LCK WT sample which were set to 1. Values were then expressed in Arbitrary Units (A.U.). In order to examine mean sulfenylation differences between untreated samples WT and C476A a one-sample *t*-Test was used. No statistically significant differences were revealed (p=1.0000). In order to examine mean sulfenylation differences between samples WT and WT treated with NAC a one-sample *t*-Test was used. No statistically significant differences were revealed (p=0.4737). In order to examine mean sulfenylation differences between samples C476A and C476A treated with NAC an unpaired two-sample Student's *t*-Test was used. No statistically significant differences were revealed (p=0.2124). In order to examine mean sulfenylation differences between samples WT and C476A, both treated with NAC, an unpaired two-sample Student's *t*-Test was used. No statistically significant differences were revealed (p=0.967755). The above four p-values have been adjusted using the Bonferroni correction, as the comparisons cannot be assumed to be independent of one another.

4. DISCUSSION

4.1 Conclusions

The data presented in this PhD thesis led to the following conclusions:

i. The highly conserved C476 regulates different aspects of LCK including its subcellular localization, its stability, its enzymatic activity and conformation.
ii. Overexpression of the co-chaperone CDC37 rescues the stability and partially the activity of the LCK C476A mutant.
iii. The C476A substitution converts LCK into a temperature sensitive mutant.
iv. C476 doesn't appear to be targeted for sulfenylation.

4.2 How does C476 regulate LCK activity/function?

As previously described, the kinase activity of LCK is tightly regulated upon phosphorylation of the regulatory Y394 and Y505, which in turn determines the conformational status of the kinase. Interestingly, despite the fact that LCK C476A is enzymatically inactive, conformational analyses showed that LCK C476A does not adopt a "*closed*" conformation. Indeed, experiments using an LCK-biosensor revealed that LCK C476A adopts an "*open*" conformation instead. Moreover, LCK C476A appears to be hypo-phosphorylated on both regulatory sites, Y505 and Y394. Collectively, I propose that the non-phosphorylated, inactive but conformationally "*open*" LCK resembles the so called "*primed*" LCK (Nika et al., 2010, Stirnweiss et al., 2013, Philipsen et al., 2017). However, it cannot be ruled out that C476A substitution may drive LCK to a completely new conformational status that is not the same as "*primed*" LCK.

The "altered" conformation of LCK C467A may affects the interaction with binding partners of the kinase. It is possible that, among others, the association between PTPs and LCK C476A is changed. As already described, the regulatory tyrosine residues Y394 and Y505 are targeted from several PTPs

for dephosphorylation. CD45 acts predominately positively on LCK activity by dephosphorylating Y505 (D'Oro and Ashwell, 1999, Wong et al., 2008). However, it has also been reported that CD45 can also dephosphorylate Y394 (McNeill et al., 2007, Wong et al., 2008), although it is well described that SHP1 is the main PTP dephosphorylating Y394 (Chiang and Sefton, 2001). Therefore, it can be postulated that LCK C476A adopts a conformation that exposes the kinase to the action of phosphatases such as CD45 and SHP1 and hence LCK C476A becomes dephosphorylated on both Y394 and Y505. Our group and others have recently showed an analogue mechanism of LCK regulation, which involves the residue Y192 (Courtney et al., 2017, Kästle et al., 2020). These data propose that phosphorylation of Y192 impairs the interaction between CD45 and LCK (Courtney et al., 2017, Kästle et al., 2020). Consequently, CD45 cannot longer dephosphorylate LCK, which in turn becomes hyperphosphorylated on Y505 and hence inactivated (Courtney et al., 2017). In line with the hypothesis that LCK C476A is more sensitive to the action of phosphatases is the observation that the function and activity of LCK C476A are restored at 25^{o}C. Indeed, it is known that PTPs show decreased activity at lower temperatures (below 30^{o}C) (Yun et al., 2018). This can indirectly indicate that, while at 37^{o}C LCK C476A is exposed to PTPs and therefore becomes dephosphorylated and inactive, at 25^{o}C the phosphatase activity of PTPs is minimal and therefore PTPs are no longer capable of dephosphorylating LCK C476A and hence this mutant remains phosphorylated on the regulatory tyrosines and active.

Alternatively, it can also be hypothesized that also the association with other partners, such as the C-terminal Src kinase (CSK), which phosphorylates Y505, can be altered (Bergman et al., 1992). In this particular case, I propose that the phosphorylation of Y505 is possible to become attenuated (Bougeret et al., 1996). Therefore, the analysis of the association between LCK C476A and PTPs or other interaction partners is an important goal for future experiments.

4.3 How does C476 regulate LCK stability?

The analysis of the expression level of LCK C476A revealed a 30-40% reduction compared to that of LCK WT. I have shown that the decreased expression of the LCK mutant is due to decreased protein stability. However, previously published data showed a more dramatic effect of the C476A substitution on the stability of murine LCK. A murine LCK C475A mutant (C475 corresponds to C476 in the mouse protein sequence) expressed in the NIH 3T3 fibroblast cell line results in an almost complete loss of protein expression (Veillette et al., 1993). In my experiments, I have used the human J.LCK Jurkat T-cell line as well as human LCK C476A cDNA. Therefore, the discrepancy may be due to the different cell lines used in the studies (T cells vs. fibroblasts) or due to differences in the used cDNA (human vs. mouse). In the same report, LCK C475A was also shown to be enzymatically inactive and not functional (Veillette et al., 1993). The latter data are in line with the data provided in this thesis regarding LCK C476A protein activity and function.

However, no data regarding the intracellular localization of LCK C475A were provided in the study of Veillette and coworkers (Veillette et al., 1993). The analysis of the subcellular localization of LCK C476A that I performed in my studies showed that LCK C476A remains mainly localized at the plasma membrane. However, it was revealed that LCK C476A shows a decreased localization at the plasma membrane and an increased expression in the cytoplasm as well as in the intracellular vesicular compartment. It is well established that anchoring of LCK at the plasma membrane is crucial for its function (Yasuda et al., 2000), (Kabouridis et al., 1997). Therefore, it needs to be further investigated whether the altered subcellular distribution of LCK C476A can also contribute for both reduced protein stability and activity.

Previous work has already proposed that the regulation of the stability and kinase activity of LCK mutants require the association with the HSP90-CDC37 chaperone complex (Nika et al., 2010, Hartson et al., 1996). Conversely to these studies, published data from our group show that CDC37 is dispensable for the regulation of LCK WT activity/stability (Kowallik et al., 2020). The results generated for this Ph.D. thesis confirm that CDC37 is

dispensable for the regulation of the stability of LCK WT. However, they clearly show that overexpression of CDC37 can completely rescue the protein expression and partially the activity of the LCK C476A mutant**.** In line with these results, unpublished data from our group indicate that suppression of CDC37 expression further destabilizes LCK C476A. Taken together, these data indicate that conversely to LCK WT, LCK C476A is more dependent on the activity of CDC37. The reason why the mutant becomes dependent on CDC37 is not yet clear. It is possible that the different conformation of the LCK C476A mutant allows the interaction with CDC37. In this regard, it has been shown that the different conformational forms of LCK are differentially regulated by CDC37 (Giannini and Bijlmakers, 2004b, Prince and Matts, 2004, Nika et al., 2010).

Similar to the results discussed above, published data from our group showed that overexpression of CDC37 rescues (partially) the stability and kinase activity of a ZAP-70 C575A mutant (please keep in mind that C575 in the amino acid sequence of ZAP-70 corresponds to C476 in LCK) (Thurm et al., 2017). In this published study, we proposed that the highly conserved cysteine residue within the conserved $Mx_{(2)}CWx_{(6)}R$ motif could be an important additional interacting sequence between ZAP-70 and CDC37 and that this interaction might be prevented by the oxidation of C575 (Thurm, 2018). Whether the conserved motif mediates the interaction between CDC37 and LCK C476A and whether this interaction is redox-dependent, through oxidation of the core C476 cysteine, needs to be further investigated.

4.4 LCK C476A is temperature sensitive

During my experiments, I observed an interesting behavior of LCK C476A. The data presented in the results part of this thesis clearly show that the C476A substitution converts LCK into a temperature-sensitive mutant. More precisely, at 37^{o}C and higher temperatures (39^{o}C) LCK C476A exhibits an impaired activity, whereas at lower temperature (25 °C) LCK C476A is active. Mutations in the kinase domain of other SFKs (e.g., v-SRC, HCK) have been previously reported to convert protein kinases into temperature-sensitive mutants (Garber E. A. et al., 1987, Scholz G. et al., 2000). More specifically, a

single C to A mutation in C498 in v-SRC (corresponding to C476 in LCK) resulted in the suppression of its activity and converted v-SRC in a temperature-sensitive mutant (Senga et al., 2000)(Oo et al., 2003). Moreover, mutations within the kinase domain of HCK (I433M and P475S substitutions) converted HCK to a temperature sensitive mutant (Scholz et al., 2000). The catalytic activity, function and protein expression of the HCK temperature sensitive mutant were, similarly to LCK C476A, severely decreased at higher temperatures (37^{o}C and 39^{o}C). In line with these reports, a different study reported that an M572L substitution of ZAP-70 kinase in T cells from a CD8 deficiency patient (M572 is part of highly conserved $Mx_{(2)}CWx_{(6)}R$ motif among PTKs) drives the kinase to a temperature-sensitive behavior, affecting both the protein stability and the kinase activity of ZAP-70 (Matsuda et al., 1999). Additionally, it has been shown that temperature-sensitive mutants of SFKs show higher levels of interaction with the co-chaperone CDC37 (Brugge, 1986). Therefore, it has been postulated that proteins of the chaperone's machinery (e.g., HSP-90) and co-chaperones (e.g., CDC37) are able to contribute to the stability and the kinase activity of these temperature-sensitive mutants (Scholz et al., 2000).

Conversely to its function at higher temperatures, at lower temperatures (e.g., 25^{o}C) it appears that LCK C476A shifts to a status of increased kinase activity and function. It is important to be noted that the difference in protein expression that is observed between LCK C476A and LCK WT at higher temperatures is not restored at lower temperatures**.** Therefore, it is proposed that increased function of LCK C476A observed at lower temperatures is likely not due to the normalization of protein expression. As previously mentioned, it is possible that, at lower temperatures, PTPs are less active and hence do not dephosphorylate LCK C476A. Therefore, LCK C476A maintains its protein activity.

4.5 Is LCK C476 a potential redox-active residue?

LCK has been suggested to be a target of oxidative post-translational modification but little is known about the specific type of oxidation that can affect LCK. LCK C476 represents the core cysteine within a $Mx_{(2)}CWx_{(6)}R$ motif, which is highly conserved among all human PTKs. This motif and its core redox-active cysteine residue has been proposed to be essential for the regulation of protein stability and kinase activity in all human PTKs (Thurm et al., 2017b)(Nakashima et al., 2005). Previous studies showed that this residue is oxidized in many PTKs including ZAP-70 (C575) (Thurm et al., 2017b), c-SRC (C498) (Rahman et al., 2010), and PDGFR-beta (C940) (Kato et al., 2000). An important question that I examined within this PhD thesis was whether C476 directly undergoes a specific type of oxidation. The data presented in this thesis clearly show that LCK undergoes oxidation and more precisely LCK is sulfenylated in J.Lck T cells under resting conditions. However, my data suggest that LCK C476 is likely not sulfenylated, as the global level of sulfenylation is comparable between LCK WT and the mutant.

This finding doesn't exclude the possibility that LCK C476 undergoes other types of post-translational modifications. In line with this hypothesis, theoretical studies of electrostatic, steric, and hydrophobic properties of SFKs proposed that the position in the protein, of C476 residue, increases the possibility that C476 undergoes *S*-nitrosylation. In fact, C498 (the respective conserved residue of c-SRC) was found to be a target of *S*-nitrosylation (Rahman et al., 2010). Unfortunately, due to technical limitations, I was not able to show in the context of my thesis that LCK C476 undergoes *S*-nitrosylation.

Moreover, it has been recently shown that another important PTK, ZAP-70, undergoes a different type of post-translational modification which is called S-acylation (Tewari et al., 2020). ZAP-70 is S-acylated at C564 which is also conserved in LCK (C465). The authors showed that this modification is essential for the interaction with its protein substrates. Therefore, it cannot be ruled out that LCK C476 also undergoes S-acylation. Further investigations need to be performed in order to reveal whether and how LCK C476 is oxidized or post-translationally modified.

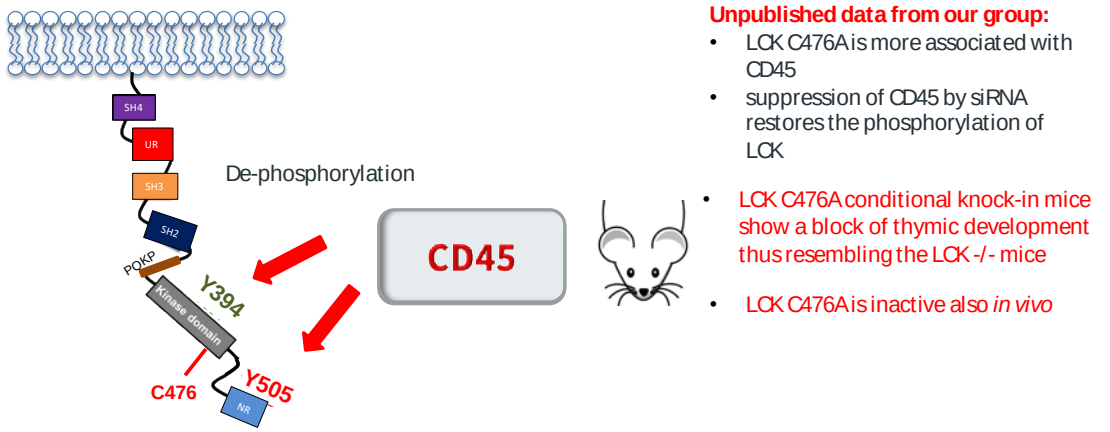

Figure 4.1: Working model for the function of LCK C476
Unpublished data from our group indicate that LCK C476A is more associated with the PTP CD45. Suppression of CD45 by siRNA restores the phosphorylation of LCK. Therefore, it is likely that LCK C476A adopts a conformation that exposes the kinase to the action of phosphatases such as CD45 and hence LCK C476A becomes dephosphorylated on both Y394 and Y505 and deactivated. Additionally, LCK C476A conditional *knock-in* mice shows a block of thymic development thus resembling the LCK -/- mice. The latter indicates that LCK C476A is inactive as well *in vivo*.

4.6 Cysteine residues of PTKs as targets for the development of drugs modulating kinase activity

Deregulation of protein kinase function through environmental and genetic alterations is a hallmark of many pathological conditions. To date, approximately 40 kinases are actively tested as potential therapeutic targets, especially in oncology (Barf and Kaptein, 2012). Recently, the interest for the development of irreversible inhibitors that form covalent bonds with cysteine residues, or other nucleophilic residues, has been renewed.

Notably, three irreversible inhibitors, the EGFR inhibitor Afatinib, the BTK inhibitor Ibrutinib and Osimertinib, have obtained recently the approval of FDA for human use (Zhao et al., 2017). More in detail, Afatinib and Osimertinib are tyrosine-kinase inhibitors that covalently bind to C797 of the EGFR and they are used to treat cases of non-small cell lung carcinoma (NSCLC) that harbor mutations in the EGFR gene (Bowles et al., 2013, Santarpia et al., 2017). Ibrutinib is a small molecule that forms a covalent bond with C481 in the ATP-binding domain of BTK and inhibits Bruton's tyrosine kinase, that is critical for B-cell survival and proliferation. Ibrutinib has shown profound anti-tumor activity in a variety of hematologic malignancies such as chronic lymphocytic leukemia (CLL) and mantle cell lymphoma (MCL) (Davids and Brown, 2014). Recently, it

was also published that a potent inhibitor (RDN009) of the tyrosine kinase ZAP-70, that targets C346, was discovered (Rao et al., 2021).

As previously described in detail, there is accumulating evidence for the major role of LCK in several inflammatory mediated pathological conditions as well as cancer and cancer immunotherapy (Bommhardt et al., 2019). Therefore, LCK and the regulation of its protein kinase activity, function and expression, emerge as novel potential objectives for the development of targeted therapeutic approaches or inhibitors. The data presented in this thesis, clearly show that C476 residue, within the kinase domain of LCK, is crucial for the regulation of both its protein kinase activity/function and its stability. More research has to be performed in two directions: first to better understand the role of LCK C476 in physiology and as a next step to explore the possibilities for the development of new therapeutic approaches such as specific irreversible LCK tyrosine-kinase inhibitors that target for example C476.

5. BIBLIOGRAPHY

Abdal Dayem, A., Hossain, M. K., Lee, S. B., Kim, K., Saha, S. K., Yang, G.-M., Choi, H. Y., & Cho, S.-G. (2017). The Role of Reactive Oxygen Species (ROS) in the Biological Activities of Metallic Nanoparticles. *International Journal of Molecular Sciences*, *18*(1). https://doi.org/10.3390/ijms18010120

Abraham, R. T., & Weiss, A. (2004). Jurkat T cells and development of the T-cell receptor signalling paradigm. *Nature Reviews. Immunology*, *4*(4), 301–308. https://doi.org/10.1038/nri1330

Acuto, O., Di Bartolo, V., & Michel, F. (2008). Tailoring T-cell receptor signals by proximal negative feedback mechanisms. *Nature Reviews. Immunology*, *8*(9), 699–712. https://doi.org/10.1038/nri2397

Aivazian, D., & Stern, L. J. (2000). Phosphorylation of T cell receptor zeta is regulated by a lipid dependent folding transition. *Nature Structural Biology*, *7*(11), 1023–1026. https://doi.org/10.1038/80930

Alarcón, B., Mestre, D., & Martínez-Martín, N. (2011). The immunological synapse: A cause or consequence of T-cell receptor triggering? *Immunology*, *133*(4), 420–425. https://doi.org/10.1111/j.1365-2567.2011.03458.x

Alcock, L. J., Perkins, M. V., & Chalker, J. M. (2018). Chemical methods for mapping cysteine oxidation. *Chemical Society Reviews*, *47*(1), 231–268. https://doi.org/10.1039/C7CS00607A

Alderton, W. K., Cooper, C. E., & Knowles, R. G. (2001). Nitric oxide synthases: Structure, function and inhibition. *The Biochemical Journal*, *357*(Pt 3), 593–615. https://doi.org/10.1042/0264-6021:3570593

Aldini, G., Altomare, A., Baron, G., Vistoli, G., Carini, M., Borsani, L., & Sergio, F. (2018). N-Acetylcysteine as an antioxidant and disulphide breaking agent: The reasons why. *Free Radical Research*, *52*(7), 751–762. https://doi.org/10.1080/10715762.2018.1468564

Alonso, M., & Milan, J. (2001). The role of lipid rafts in signalling and membrane trafficking inT lymphocytes. *Journal of Cell Science*, *114*.

Andre, F. R., dos Santos, P. F., & Rando, D. G. (2016). Theoretical studies of the role of C-terminal cysteines in the process of S-nitrosylation of human Src kinases. *Journal of Molecular Modeling*, *22*(1), 23. https://doi.org/10.1007/s00894-015-2892-x

Andrés-Delgado, L., Antón, O. M., Madrid, R., Byrne, J. A., & Alonso, M. A. (2010). Formin INF2 regulates MAL-mediated transport of Lck to the plasma membrane of human T lymphocytes. *Blood*, *116*(26), 5919–5929. https://doi.org/10.1182/blood-2010-08-300665

BIBLIOGRAPHY

Anselmo, A. N., & Cobb, M. H. (2004). Protein kinase function and glutathionylation. *The Biochemical Journal*, *381*(Pt 3), e1-2. https://doi.org/10.1042/BJ20040873

Antón, O., Batista, A., Millán, J., Andrés-Delgado, L., Puertollano, R., Correas, I., & Alonso, M. A. (2008). An essential role for the MAL protein in targeting Lck to the plasma membrane of human T lymphocytes. *The Journal of Experimental Medicine*, *205*(13), 3201–3213. https://doi.org/10.1084/jem.20080552

Baliga, B. S., Pronczuk, A. W., & Munro, H. N. (1969). Mechanism of Cycloheximide Inhibition of Protein Synthesis in a Cell-free System Prepared from Rat Liver. *Journal of Biological Chemistry*, *244*(16), 4480–4489.

Barf, T., & Kaptein, A. (2012). Irreversible protein kinase inhibitors: Balancing the benefits and risks. *Journal of Medicinal Chemistry*, *55*(14), 6243–6262. https://doi.org/10.1021/jm3003203

Beedle, A. E. M., Lynham, S., & Garcia-Manyes, S. (2016). Protein S-sulfenylation is a fleeting molecular switch that regulates non-enzymatic oxidative folding. *Nature Communications*, *7*(1), 12490. https://doi.org/10.1038/ncomms12490

Belikov, A. V., Schraven, B., & Simeoni, L. (2014). TCR-triggered extracellular superoxide production is not required for T-cell activation. *Cell Communication and Signaling : CCS*, *12*, 50. https://doi.org/10.1186/s12964-014-0050-1

Belikov, A. V., Schraven, B., & Simeoni, L. (2015). T cells and reactive oxygen species. *Journal of Biomedical Science*, *22*. https://doi.org/10.1186/s12929-015-0194-3

Bergman, M., Mustelin, T., Oetken, C., Partanen, J., Flint, N. A., Amrein, K. E., Autero, M., Burn, P., & Alitalo, K. (1992). The human p50csk tyrosine kinase phosphorylates p56lck at Tyr-505 and down regulates its catalytic activity. *The EMBO Journal*, *11*(8), 2919–2924.

Bijlmakers, M.-J. J. E., & Marsh, M. (2000). Hsp90 Is Essential for the Synthesis and Subsequent Membrane Association, But Not the Maintenance, of the Src-Kinase p56lck. *Molecular Biology of the Cell*, *11*(5), 1585–1595.

Boggon, T. J., & Eck, M. J. (2004). Structure and regulation of Src family kinases. *Oncogene*, *23*(48), 7918–7927. https://doi.org/10.1038/sj.onc.1208081

Bommhardt, U., Schraven, B., & Simeoni, L. (2019). Beyond TCR Signaling: Emerging Functions of Lck in Cancer and Immunotherapy. *International Journal of Molecular Sciences*, *20*(14). https://doi.org/10.3390/ijms20143500

BIBLIOGRAPHY

Bougeret, C., Delaunay, T., Romero, F., Jullien, P., Sabe, H., Hanafusa, H., Benarous, R., & Fischer, S. (1996). Detection of a Physical and Functional Interaction between Csk and Lck Which Involves the SH2 Domain of Csk and Is Mediated by Autophosphorylation of Lck on Tyrosine 394 (∗). *Journal of Biological Chemistry*, *271*(13), 7465–7472. https://doi.org/10.1074/jbc.271.13.7465

Bowles, D. W., Weickhardt, A., & Jimeno, A. (2013). Afatinib for the treatment of patients with EGFR-positive non-small cell lung cancer. *Drugs of Today (Barcelona, Spain: 1998)*, *49*(9), 523–535. https://doi.org/10.1358/dot.2013.49.9.2016610

Bradshaw, J. M. (2010). The Src, Syk, and Tec family kinases: Distinct types of molecular switches. *Cellular Signalling*, *22*(8), 1175–1184. https://doi.org/10.1016/j.cellsig.2010.03.001

Brownlie, R. J., & Zamoyska, R. (2013). T cell receptor signalling networks: Branched, diversified and bounded. *Nature Reviews. Immunology*, *13*(4), 257–269. https://doi.org/10.1038/nri3403

Brugge, J. S. (1986). Interaction of the Rous sarcoma virus protein pp60src with the cellular proteins pp50 and pp90. *Current Topics in Microbiology and Immunology*, *123*, 1–22. https://doi.org/10.1007/978-3-642-70810-7_1

Bunnell, S. C., Kapoor, V., Trible, R. P., Zhang, W., & Samelson, L. E. (2001). Dynamic actin polymerization drives T cell receptor-induced spreading: A role for the signal transduction adaptor LAT. *Immunity*, *14*(3), 315–329. https://doi.org/10.1016/s1074-7613(01)00112-1

Cantrell, D. (2015). Signaling in Lymphocyte Activation. *Cold Spring Harbor Perspectives in Biology*, *7*(6). https://doi.org/10.1101/cshperspect.a018788

Capasso, M., Bhamrah, M. K., Henley, T., Boyd, R. S., Langlais, C., Cain, K., Dinsdale, D., Pulford, K., Khan, M., Musset, B., Cherny, V. V., Morgan, D., Gascoyne, R. D., Vigorito, E., DeCoursey, T. E., MacLennan, I. C. M., & Dyer, M. J. S. (2010). HVCN1 modulates BCR signal strength via regulation of BCR-dependent generation of reactive oxygen species. *Nature Immunology*, *11*(3), 265–272. https://doi.org/10.1038/ni.1843

Casas, J., Brzostek, J., Zarnitsyna, V. I., Hong, J., Wei, Q., Hoerter, J. A. H., Fu, G., Ampudia, J., Zamoyska, R., Zhu, C., & Gascoigne, N. R. J. (2014). Ligand engaged TCR is triggered by Lck not associated with CD8 coreceptor. *Nature Communications*, *5*, 5624. https://doi.org/10.1038/ncomms6624

Charles, R. L., Schröder, E., May, G., Free, P., Gaffney, P. R. J., Wait, R., Begum, S., Heads, R. J., & Eaton, P. (2007). Protein sulfenation as a redox sensor: Proteomics studies using a novel biotinylated dimedone analogue. *Molecular & Cellular Proteomics: MCP*, *6*(9), 1473–1484. https://doi.org/10.1074/mcp.M700065-MCP200

BIBLIOGRAPHY

Chiang, G. G., & Sefton, B. M. (2001). Specific Dephosphorylation of the Lck Tyrosine Protein Kinase at Tyr-394 by the SHP-1 Protein-tyrosine Phosphatase *. *Journal of Biological Chemistry*, *276*(25), 23173–23178. https://doi.org/10.1074/jbc.M101219200

Chung, H. S., Wang, S.-B., Venkatraman, V., Murray, C. I., & Van Eyk, J. E. (2013). Cysteine oxidative posttranslational modifications: Emerging regulation in the cardiovascular system. *Circulation Research*, *112*(2), 382–392. https://doi.org/10.1161/CIRCRESAHA.112.268680

Conzelmann, A., Pink, R., Acuto, O., Mach, J. P., Dolivo, S., & Nabholz, M. (1980). Presence of T 145 on cytolytic T cell lines and their lectin-resistant mutants. *European Journal of Immunology*, *10*(11), 860–868. https://doi.org/10.1002/eji.1830101111

Corcoran, A., & Cotter, T. G. (2013). Redox regulation of protein kinases. *The FEBS Journal*, *280*(9), 1944–1965. https://doi.org/10.1111/febs.12224

Courtney, A. H., Amacher, J. F., Kadlecek, T. A., Mollenauer, M. N., Au-Yeung, B. B., Kuriyan, J., & Weiss, A. (2017). A PHOSPHOSITE WITHIN THE SH2 DOMAIN OF LCK REGULATES ITS ACTIVATION BY CD45. *Molecular Cell*, *67*(3), 498-511.e6. https://doi.org/10.1016/j.molcel.2017.06.024

Courtney, A. H., Lo, W.-L., & Weiss, A. (2018). TCR Signaling: Mechanisms of Initiation and Propagation. *Trends in Biochemical Sciences*, *43*(2), 108–123. https://doi.org/10.1016/j.tibs.2017.11.008

Couture, C., Songyang, Z., Jascur, T., Williams, S., Tailor, P., Cantley, L. C., & Mustelin, T. (1996). Regulation of the Lck SH2 domain by tyrosine phosphorylation. *The Journal of Biological Chemistry*, *271*(40), 24880–24884. https://doi.org/10.1074/jbc.271.40.24880

Cunnick, J. M., Dorsey, J. F., Mei, L., & Wu, J. (1998). Reversible regulation of SHP-1 tyrosine phosphatase activity by oxidation. *Biochemistry and Molecular Biology International*, *45*(5), 887–894. https://doi.org/10.1002/iub.7510450506

Davids, M. S., & Brown, J. R. (2014). Ibrutinib: A first in class covalent inhibitor of Bruton's tyrosine kinase. *Future Oncology (London, England)*, *10*(6), 957–967. https://doi.org/10.2217/fon.14.51

Davis, D. M., & Dustin, M. L. (2004). What is the importance of the immunological synapse? *Trends in Immunology*, *25*(6), 323–327. https://doi.org/10.1016/j.it.2004.03.007

Di Meo, S., Reed, T. T., Venditti, P., & Victor, V. M. (2016). Role of ROS and RNS Sources in Physiological and Pathological Conditions. *Oxidative Medicine and Cellular Longevity*, *2016*, 1245049. https://doi.org/10.1155/2016/1245049

D'Oro, U., & Ashwell, J. D. (1999). Cutting edge: The CD45 tyrosine phosphatase is an inhibitor of Lck activity in thymocytes. *Journal of Immunology (Baltimore, Md.: 1950)*, *162*(4), 1879–1883.

BIBLIOGRAPHY

Dustin, C. M., Heppner, D. E., Lin, M.-C. J., & van der Vliet, A. (2020). Redox regulation of tyrosine kinase signalling: More than meets the eye. *Journal of Biochemistry*, *167*(2), 151–163. https://doi.org/10.1093/jb/mvz085

Dutta, D., Barr, V. A., Akpan, I., Mittelstadt, P. R., Singha, L. I., Samelson, L. E., & Ashwell, J. D. (2017). Recruitment of calcineurin to the TCR positively regulates T cell activation. *Nature Immunology*, *18*(2), 196–204. https://doi.org/10.1038/ni.3640

Esensten, J. H., Helou, Y. A., Chopra, G., Weiss, A., & Bluestone, J. A. (2016). CD28 costimulation: From mechanism to therapy. *Immunity*, *44*(5), 973–988. https://doi.org/10.1016/j.immuni.2016.04.020

Feske, S., Gwack, Y., Prakriya, M., Srikanth, S., Puppel, S.-H., Tanasa, B., Hogan, P. G., Lewis, R. S., Daly, M., & Rao, A. (2006). A mutation in Orai1 causes immune deficiency by abrogating CRAC channel function. *Nature*, *441*(7090), 179–185. https://doi.org/10.1038/nature04702

Forman, H. J., Zhang, H., & Rinna, A. (2009). Glutathione: Overview of its protective roles, measurement, and biosynthesis. *Molecular Aspects of Medicine*, *30*(1–2), 1–12. https://doi.org/10.1016/j.mam.2008.08.006

Fra, A., Yoboue, E. D., & Sitia, R. (2017). Cysteines as Redox Molecular Switches and Targets of Disease. *Frontiers in Molecular Neuroscience*, *10*. https://doi.org/10.3389/fnmol.2017.00167

García-Ortiz, A., & Serrador, J. M. (2018). Nitric Oxide Signaling in T Cell-Mediated Immunity. *Trends in Molecular Medicine*, *24*(4), 412–427. https://doi.org/10.1016/j.molmed.2018.02.002

Gaud, G., Lesourne, R., & Love, P. E. (2018). Regulatory mechanisms in T cell receptor signalling. *Nature Reviews Immunology*, *18*(8), 485–497. https://doi.org/10.1038/s41577-018-0020-8

Giannini, A., & Bijlmakers, M.-J. (2004a). Regulation of the Src Family Kinase Lck by Hsp90 and Ubiquitination. *Molecular and Cellular Biology*, *24*(13), 5667–5676. https://doi.org/10.1128/MCB.24.13.5667-5676.2004

Giannini, A., & Bijlmakers, M.-J. (2004b). Regulation of the Src Family Kinase Lck by Hsp90 and Ubiquitination. *Molecular and Cellular Biology*, *24*(13), 5667–5676. https://doi.org/10.1128/MCB.24.13.5667-5676.2004

Giannoni, E., Buricchi, F., Raugei, G., Ramponi, G., & Chiarugi, P. (2005). Intracellular reactive oxygen species activate Src tyrosine kinase during cell adhesion and anchorage-dependent cell growth. *Molecular and Cellular Biology*, *25*(15), 6391–6403. https://doi.org/10.1128/MCB.25.15.6391-6403.2005

BIBLIOGRAPHY

Giannoni, E., Taddei, M., & Chiarugi, P. (2010). Src redox regulation: Again in the front line. *Free Radical Biology & Medicine*, *49*, 516–527. https://doi.org/10.1016/j.freeradbiomed.2010.04.025

Gillis, S., & Watson, J. (1980). Biochemical and biological characterization of lymphocyte regulatory molecules. V. Identification of an interleukin 2-producing human leukemia T cell line. *The Journal of Experimental Medicine*, *152*(6), 1709–1719. https://doi.org/10.1084/jem.152.6.1709

Gjörloff-Wingren, A., Saxena, M., Williams, S., Hammi, D., & Mustelin, T. (1999). Characterization of TCR-induced receptor-proximal signaling events negatively regulated by the protein tyrosine phosphatase PEP. *European Journal of Immunology*, *29*(12), 3845–3854. https://doi.org/10.1002/(SICI)1521-4141(199912)29:12<3845::AID-IMMU3845>3.0.CO;2-U

Goodfellow, H. S., Frushicheva, M. P., Ji, Q., Cheng, D. A., Kadlecek, T. A., Cantor, A. J., Kuriyan, J., Chakraborty, A. K., Salomon, A., & Weiss, A. (2015). The catalytic activity of the kinase ZAP-70 mediates basal signaling and negative feedback of the T cell receptor pathway. *Science Signaling*, *8*(377), ra49. https://doi.org/10.1126/scisignal.2005596

Gorska, M. M., Liang, Q., Karim, Z., & Alam, R. (2009). Uncoordinated 119 Protein Controls Trafficking of Lck via the Rab11 Endosome and Is Critical for Immunological Synapse Formation. *The Journal of Immunology*. https://doi.org/10.4049/jimmunol.0900792

Granum, S., Sundvold-Gjerstad, V., Gopalakrishnan, R. P., Berge, T., Koll, L., Abrahamsen, G., Sørlie, M., & Spurkland, A. (2014). The kinase Itk and the adaptor TSAd change the specificity of the kinase Lck in T cells by promoting the phosphorylation of Tyr192. *Science Signaling*, *7*(355), ra118. https://doi.org/10.1126/scisignal.2005384

Hanke, J. H., Gardner, J. P., Dow, R. L., Changelian, P. S., Brissette, W. H., Weringer, E. J., Pollok, B. A., & Connelly, P. A. (1996). Discovery of a Novel, Potent, and Src Family-selective Tyrosine Kinase Inhibitor STUDY OF Lck- AND FynT-DEPENDENT T CELL ACTIVATION. *Journal of Biological Chemistry*, *271*(2), 695–701. https://doi.org/10.1074/jbc.271.2.695

Hao, L., Wei, X., Guo, P., Zhang, G., & Qi, S. (2016). Neuroprotective Effects of Inhibiting Fyn S-Nitrosylation on Cerebral Ischemia/Reperfusion-Induced Damage to CA1 Hippocampal Neurons. *International Journal of Molecular Sciences*, *17*(7). https://doi.org/10.3390/ijms17071100

Hartig, R., Prokazov, Y., Turbin, E., & Zuschratter, W. (2014). Wide-field fluorescence lifetime imaging with multi-anode detectors. *Methods in Molecular Biology (Clifton, N.J.)*, *1076*, 457–480. https://doi.org/10.1007/978-1-62703-649-8_20

BIBLIOGRAPHY

Hartl, F. A., Beck-Garcìa, E., Woessner, N. M., Flachsmann, L. J., Cárdenas, R. M.-H. V., Brandl, S. M., Taromi, S., Fiala, G. J., Morath, A., Mishra, P., Yousefi, O. S., Zimmermann, J., Hoefflin, N., Köhn, M., Wöhrl, B. M., Zeiser, R., Schweimer, K., Günther, S., Schamel, W. W., & Minguet, S. (2020). Noncanonical binding of Lck to CD3ε promotes TCR signaling and CAR function. *Nature Immunology*, *21*(8), 902–913. https://doi.org/10.1038/s41590-020-0732-3

Hartl, F. U., Bracher, A., & Hayer-Hartl, M. (2011). Molecular chaperones in protein folding and proteostasis. *Nature*, *475*(7356), 324–332. https://doi.org/10.1038/nature10317

Hartson, S. D., Barrett, D. J., Burn, P., & Matts, R. L. (1996). Hsp90-mediated folding of the lymphoid cell kinase p56lck. *Biochemistry*, *35*(41), 13451–13459. https://doi.org/10.1021/bi961332c

Hartson, S. D., & Matts, R. L. (1994). Association of Hsp90 with cellular Src-family kinases in a cell-free system correlates with altered kinase structure and function. *Biochemistry*, *33*(30), 8912–8920. https://doi.org/10.1021/bi00196a008

Heppner, D. E., Dustin, C. M., Liao, C., Hristova, M., Veith, C., Little, A. C., Ahlers, B. A., White, S. L., Deng, B., Lam, Y.-W., Li, J., & van der Vliet, A. (2018). Direct cysteine sulfenylation drives activation of the Src kinase. *Nature Communications*, *9*. https://doi.org/10.1038/s41467-018-06790-1

Holdorf, A. D., Green, J. M., Levin, S. D., Denny, M. F., Straus, D. B., Link, V., Changelian, P. S., Allen, P. M., & Shaw, A. S. (1999). Proline residues in CD28 and the Src homology (SH)3 domain of Lck are required for T cell costimulation. *The Journal of Experimental Medicine*, *190*(3), 375–384. https://doi.org/10.1084/jem.190.3.375

Holtmeier, W., & Kabelitz, D. (2005). Gammadelta T cells link innate and adaptive immune responses. *Chemical Immunology and Allergy*, *86*, 151–183. https://doi.org/10.1159/000086659

Huang, R., Fang, P., Hao, Z., & Kay, B. K. (2016). Directed Evolution of a Highly Specific FN3 Monobody to the SH3 Domain of Human Lyn Tyrosine Kinase. *PloS One*, *11*(1), e0145872. https://doi.org/10.1371/journal.pone.0145872

Hubbard, S. R., & Till, J. H. (2000). Protein tyrosine kinase structure and function. *Annual Review of Biochemistry*, *69*, 373–398. https://doi.org/10.1146/annurev.biochem.69.1.373

Hui, E., & Vale, R. D. (2014). In vitro membrane reconstitution of the T-cell receptor proximal signaling network. *Nature Structural & Molecular Biology*, *21*(2), 133–142. https://doi.org/10.1038/nsmb.2762

Hunter, T. (1997). Oncoprotein networks. *Cell*, *88*(3), 333–346. https://doi.org/10.1016/s0092-8674(00)81872-3

BIBLIOGRAPHY

Hunter, T., & Sefton, B. M. (1980). Transforming gene product of Rous sarcoma virus phosphorylates tyrosine. *Proceedings of the National Academy of Sciences of the United States of America*, *77*(3), 1311–1315.

Huyer, G., Liu, S., Kelly, J., Moffat, J., Payette, P., Kennedy, B., Tsaprailis, G., Gresser, M. J., & Ramachandran, C. (1997). Mechanism of inhibition of protein-tyrosine phosphatases by vanadate and pervanadate. *The Journal of Biological Chemistry*, *272*(2), 843–851. https://doi.org/10.1074/jbc.272.2.843

Jun, J. E., Rubio, I., & Roose, J. P. (2013). Regulation of ras exchange factors and cellular localization of ras activation by lipid messengers in T cells. *Frontiers in Immunology*, *4*, 239. https://doi.org/10.3389/fimmu.2013.00239

Kabouridis, P. S., Magee, A. I., & Ley, S. C. (1997). S-acylation of LCK protein tyrosine kinase is essential for its signalling function in T lymphocytes. *The EMBO Journal*, *16*(16), 4983–4998. https://doi.org/10.1093/emboj/16.16.4983

Kaludercic, N., Deshwal, S., & Di Lisa, F. (2014). Reactive oxygen species and redox compartmentalization. *Frontiers in Physiology*, *5*. https://doi.org/10.3389/fphys.2014.00285

Kang, D. H., Lee, D. J., Lee, K. W., Park, Y. S., Lee, J. Y., Lee, S.-H., Koh, Y. J., Koh, G.-Y., Choi, C., Yu, D.-Y., Kim, J., & Kang, S. W. (2011). Peroxiredoxin II Is an Essential Antioxidant Enzyme that Prevents the Oxidative Inactivation of VEGF Receptor-2 in Vascular Endothelial Cells. *Molecular Cell*, *44*(4), 545–558. https://doi.org/10.1016/j.molcel.2011.08.040

Kästle, M., Merten, C., Hartig, R., Kaehne, T., Liaunardy-Jopeace, A., Woessner, N. M., Schamel, W. W., James, J., Minguet, S., Simeoni, L., & Schraven, B. (2020). Tyrosine 192 within the SH2 domain of the Src-protein tyrosine kinase p56Lck regulates T-cell activation independently of Lck/CD45 interactions. *Cell Communication and Signaling: CCS*, *18*(1), 183. https://doi.org/10.1186/s12964-020-00673-z

Kato, M., Iwashita, T., Akhand, A. A., Liu, W., Takeda, K., Takeuchi, K., Yoshihara, M., Hossain, K., Wu, J., Du, J., Oh, C., Kawamoto, Y., Suzuki, H., Takahashi, M., & Nakashima, I. (2000). Molecular mechanism of activation and superactivation of Ret tyrosine kinases by ultraviolet light irradiation. *Antioxidants & Redox Signaling*, *2*(4), 841–849. https://doi.org/10.1089/ars.2000.2.4-841

Kemble, D. J., & Sun, G. (2009). Direct and specific inactivation of protein tyrosine kinases in the Src and FGFR families by reversible cysteine oxidation. *Proceedings of the National Academy of Sciences of the United States of America*, *106*(13), 5070–5075. https://doi.org/10.1073/pnas.0806117106

Kesarwani, P., Murali, A. K., Al-Khami, A. A., & Mehrotra, S. (2013). Redox regulation of T-cell function: From molecular mechanisms to significance in human health and disease. *Antioxidants & Redox Signaling*, *18*(12), 1497–1534. https://doi.org/10.1089/ars.2011.4073

BIBLIOGRAPHY

Keyes, J. D., Parsonage, D., Yammani, R. D., Rogers, L. C., Kesty, C., Furdui, C. M., Nelson, K. J., & Poole, L. B. (2017). Endogenous, Regulatory Cysteine Sulfenylation of ERK Kinases in Response to Proliferative Signals. Free Radical Biology & Medicine, 112, 534–543. https://doi.org/10.1016/j.freeradbiomed.2017.08.018

Kim, P. W., Sun, Z.-Y. J., Blacklow, S. C., Wagner, G., & Eck, M. J. (2003). A Zinc Clasp Structure Tethers Lck to T Cell Coreceptors CD4 and CD8. *Science*, *301*(5640), 1725–1728. https://doi.org/10.1126/science.1085643

King, P. D., Sadra, A., Teng, J. M., Xiao-Rong, L., Han, A., Selvakumar, A., August, A., & Dupont, B. (1997). Analysis of CD28 cytoplasmic tail tyrosine residues as regulators and substrates for the protein tyrosine kinases, EMT and LCK. *Journal of Immunology (Baltimore, Md.: 1950)*, *158*(2), 580–590.

Klomsiri, C., Karplus, P. A., & Poole, L. B. (2011). Cysteine-Based Redox Switches in Enzymes. *Antioxidants & Redox Signaling*, *14*(6), 1065–1077. https://doi.org/10.1089/ars.2010.3376

Knowles, R. G., & Moncada, S. (1994). Nitric oxide synthases in mammals. *The Biochemical Journal*, *298 (Pt 2)*, 249–258. https://doi.org/10.1042/bj2980249

Koegl, M., Zlatkine, P., Ley, S. C., Courtneidge, S. A., & Magee, A. I. (1994). Palmitoylation of multiple Src-family kinases at a homologous N-terminal motif. *The Biochemical Journal*, *303 (Pt 3)*, 749–753. https://doi.org/10.1042/bj3030749

Kong, K.-F., Yokosuka, T., Canonigo-Balancio, A. J., Isakov, N., Saito, T., & Altman, A. (2011). A motif in the V3 domain of the kinase PKC-θ determines its localization in the immunological synapse and functions in T cells via association with CD28. *Nature Immunology*, *12*(11), 1105–1112. https://doi.org/10.1038/ni.2120

Kosugi, A., Sakakura, J., Yasuda, K., Ogata, M., & Hamaoka, T. (2001). Involvement of SHP-1 tyrosine phosphatase in TCR-mediated signaling pathways in lipid rafts. *Immunity*, *14*(6), 669–680. https://doi.org/10.1016/s1074-7613(01)00146-7

Kowallik, S., Kritikos, A., Kästle, M., Thurm, C., Schraven, B., & Simeoni, L. (2020). The Activity and Stability of p56Lck and TCR Signaling Do Not Depend on the Co-Chaperone Cdc37. *International Journal of Molecular Sciences*, *22*(1). https://doi.org/10.3390/ijms22010126

Krauss, G. (2014). *Biochemistry of Signal Transduction and Regulation—Krauss, ReadingSample*. https://www.semanticscholar.org/paper/Biochemistry-of-Signal-Transduction-and-Regulation-Krauss/0b8113019b86c3dff0b85f643577305a620ae598

BIBLIOGRAPHY

Kumar Singh, P., Kashyap, A., & Silakari, O. (2018). Exploration of the therapeutic aspects of Lck: A kinase target in inflammatory mediated pathological conditions. *Biomedicine & Pharmacotherapy*, *108*, 1565–1571. https://doi.org/10.1016/j.biopha.2018.10.002

Kwong, J., & Lublin, D. M. (1995). Amino-terminal palmitate or polybasic domain can provide required second signal to myristate for membrane binding of p56lck. *Biochemical and Biophysical Research Communications*, *207*(2), 868–876. https://doi.org/10.1006/bbrc.1995.1266

Laham, L. E., Mukhopadhyay, N., & Roberts, T. M. (2000). The activation loop in Lck regulates oncogenic potential by inhibiting basal kinase activity and restricting substrate specificity. *Oncogene*, *19*(35), 3961–3970. https://doi.org/10.1038/sj.onc.1203738

Lambert, A. J., & Brand, M. D. (2009). Reactive oxygen species production by mitochondria. *Methods in Molecular Biology (Clifton, N.J.)*, *554*, 165–181. https://doi.org/10.1007/978-1-59745-521-3_11

Lambeth, J. D. (2004). NOX enzymes and the biology of reactive oxygen. *Nature Reviews Immunology*, *4*(3), 181–189. https://doi.org/10.1038/nri1312

Lee, J.-W., Kim, J.-E., Park, E.-J., Kim, J.-H., Lee, C.-H., Lee, S.-R., & Kwon, J. (2004). Two conserved cysteine residues are critical for the enzymic function of the human platelet-derived growth factor receptor-beta: Evidence for different roles of Cys-822 and Cys-940 in the kinase activity. *The Biochemical Journal*, *382*(Pt 2), 631–639. https://doi.org/10.1042/BJ20040624

Ley, S. C., Marsh, M., Bebbington, C. R., Proudfoot, K., & Jordan, P. (1994). Distinct intracellular localization of Lck and Fyn protein tyrosine kinases in human T lymphocytes. *The Journal of Cell Biology*, *125*(3), 639–649. https://doi.org/10.1083/jcb.125.3.639

Li, L., Guo, X., Shi, X., li, C., Wu, W., Yan, C., Wang, H., Li, H., & xu, C. (2017). Ionic CD3−Lck interaction regulates the initiation of T-cell receptor signaling. *Proceedings of the National Academy of Sciences*, *114*, 201701990. https://doi.org/10.1073/pnas.1701990114

Li, W., & Schlessinger, J. (1991). Platelet-derived growth factor (PDGF)-induced disulfide-linked dimerization of PDGF receptor in living cells. *Molecular and Cellular Biology*, *11*(7), 3756–3761. https://doi.org/10.1128/mcb.11.7.3756

Liaunardy-Jopeace, A., Murton, B. L., Mahesh, M., Chin, J. W., & James, J. R. (2017). Encoding optical control in LCK kinase to quantitatively investigate its activity in live cells. *Nature Structural & Molecular Biology*, *24*(12), 1155–1163. https://doi.org/10.1038/nsmb.3492

Lim, W. A., & Pawson, T. (2010). Phosphotyrosine signaling: Evolving a new cellular communication system. *Cell*, *142*(5), 661–667. https://doi.org/10.1016/j.cell.2010.08.023

BIBLIOGRAPHY

Liu, Q., Zhou, H., Langdon, W. Y., & Zhang, J. (2014). E3 ubiquitin ligase Cbl-b in innate and adaptive immunity. *Cell Cycle (Georgetown, Tex.)*, *13*(12), 1875–1884. https://doi.org/10.4161/cc.29213

Lo, W.-L., Shah, N. H., Ahsan, N., Horkova, V., Stepanek, O., Salomon, A. R., Kuriyan, J., & Weiss, A. (2018). Lck promotes Zap70-dependent LAT phosphorylation by bridging Zap70 to LAT. *Nature Immunology*, *19*(7), 733–741. https://doi.org/10.1038/s41590-018-0131-1

LoGrasso, P. V., Hawkins, J., Frank, L. J., Wisniewski, D., & Marcy, A. (1996). Mechanism of activation for Zap-70 catalytic activity. *Proceedings of the National Academy of Sciences*, *93*(22), 12165–12170. https://doi.org/10.1073/pnas.93.22.12165

Love, P. E., & Hayes, S. M. (2010). ITAM-mediated signaling by the T-cell antigen receptor. *Cold Spring Harbor Perspectives in Biology*, *2*(6), a002485. https://doi.org/10.1101/cshperspect.a002485

Marth, J. D., Peet, R., Krebs, E. G., & Perlmutter, R. M. (1985). A lymphocyte-specific protein-tyrosine kinase gene is rearranged and overexpressed in the murine T cell lymphoma LSTRA. *Cell*, *43*(2 Pt 1), 393–404. https://doi.org/10.1016/0092-8674(85)90169-2

Matsuda, S., Suzuki-Fujimoto, T., Minowa, A., Ueno, H., Katamura, K., & Koyasu, S. (1999). Temperature-sensitive ZAP70 mutants degrading through a proteasome-independent pathway. Restoration of a kinase domain mutant by Cdc37. *The Journal of Biological Chemistry*, *274*(49), 34515–34518. https://doi.org/10.1074/jbc.274.49.34515

McNeill, L., Salmond, R. J., Cooper, J. C., Carret, C. K., Cassady-Cain, R. L., Roche-Molina, M., Tandon, P., Holmes, N., & Alexander, D. R. (2007). The differential regulation of Lck kinase phosphorylation sites by CD45 is critical for T cell receptor signaling responses. *Immunity*, *27*(3), 425–437. https://doi.org/10.1016/j.immuni.2007.07.015

Michalek, R. D., Nelson, K. J., Holbrook, B. C., Yi, J. S., Stridiron, D., Daniel, L. W., Fetrow, J. S., King, S. B., Poole, L. B., & Grayson, J. M. (2007). The requirement of reversible cysteine sulfenic acid formation for T cell activation and function. *Journal of Immunology (Baltimore, Md.: 1950)*, *179*(10), 6456–6467. https://doi.org/10.4049/jimmunol.179.10.6456

Modjtahedi, H., Cho, B. C., Michel, M. C., & Solca, F. (2014). A comprehensive review of the preclinical efficacy profile of the ErbB family blocker afatinib in cancer. *Naunyn-Schmiedeberg's Archives of Pharmacology*, *387*(6), 505–521. https://doi.org/10.1007/s00210-014-0967-3

Molina, T. J., Kishihara, K., Siderovski, D. P., van Ewijk, W., Narendran, A., Timms, E., Wakeham, A., Paige, C. J., Hartmann, K. U., & Veillette, A. (1992). Profound block in thymocyte development in mice lacking p56lck. *Nature*, *357*(6374), 161–164. https://doi.org/10.1038/357161a0

BIBLIOGRAPHY

Mustelin, T., & Altman, A. (1990). Dephosphorylation and activation of the T cell tyrosine kinase pp56lck by the leukocyte common antigen (CD45). *Oncogene*, *5*(6), 809–813.

Mustelin, T., Coggeshall, K. M., & Altman, A. (1989). Rapid activation of the T-cell tyrosine protein kinase pp56lck by the CD45 phosphotyrosine phosphatase. *Proceedings of the National Academy of Sciences of the United States of America*, *86*(16), 6302–6306. https://doi.org/10.1073/pnas.86.16.6302

Myers, D. R., Zikherman, J., & Roose, J. P. (2017). Tonic Signals: Why Do Lymphocytes Bother? *Trends in Immunology*, *38*(11), 844–857. https://doi.org/10.1016/j.it.2017.06.010

Nair, D. K., Jose, M., Kuner, T., Zuschratter, W., & Hartig, R. (2006). FRET-FLIM at nanometer spectral resolution from living cells. *Optics Express*, *14*(25), 12217–12229. https://doi.org/10.1364/oe.14.012217

Nakamura, K., Hori, T., Sato, N., Sugie, K., Kawakami, T., & Yodoi, J. (1993). Redox regulation of a src family protein tyrosine kinase p56lck in T cells. *Oncogene*, *8*(11), 3133–3139.

Nakamura, K., Hori, T., & Yodoi, J. (1996). Alternative binding of p56lck and phosphatidylinositol 3-kinase in T cells by sulfhydryl oxidation: Implication of aberrant signaling due to oxidative stress in T lymphocytes. *Molecular Immunology*, *33*(10), 855–865. https://doi.org/10.1016/0161-5890(96)84611-6

Nakashima, I., Takeda, K., Kawamoto, Y., Okuno, Y., Kato, M., & Suzuki, H. (2005). Redox control of catalytic activities of membrane-associated protein tyrosine kinases. *Archives of Biochemistry and Biophysics*, *434*(1), 3–10. https://doi.org/10.1016/j.abb.2004.06.016

Nathan, C., & Cunningham-Bussel, A. (2013). Beyond oxidative stress: An immunologist's guide to reactive oxygen species. *Nature Reviews. Immunology*, *13*(5), 349–361. https://doi.org/10.1038/nri3423

Nika, K., Soldani, C., Salek, M., Paster, W., Gray, A., Etzensperger, R., Fugger, L., Polzella, P., Cerundolo, V., Dushek, O., Höfer, T., Viola, A., & Acuto, O. (2010). Constitutively active Lck kinase in T cells drives antigen receptor signal transduction. *Immunity*, *32*(6), 766–777. https://doi.org/10.1016/j.immuni.2010.05.011

Okada, M. (2012). Regulation of the SRC family kinases by Csk. *International Journal of Biological Sciences*, *8*(10), 1385–1397. https://doi.org/10.7150/ijbs.5141

Oo, M. L., Senga, T., Thant, A. A., Amin, A. R. M. R., Huang, P., Mon, N. N., & Hamaguchi, M. (2003). Cysteine residues in the C-terminal lobe of Src: Their role in the suppression of the Src kinase. *Oncogene*, *22*(9), 1411–1417. https://doi.org/10.1038/sj.onc.1206286

BIBLIOGRAPHY

Ostman, A., Frijhoff, J., Sandin, A., & Böhmer, F.-D. (2011). Regulation of protein tyrosine phosphatases by reversible oxidation. *Journal of Biochemistry*, *150*(4), 345–356. https://doi.org/10.1093/jb/mvr104

Page, T. H., Smolinska, M., Gillespie, J., Urbaniak, A. M., & Foxwell, B. M. J. (2009). Tyrosine kinases and inflammatory signalling. *Current Molecular Medicine*, *9*(1), 69–85. https://doi.org/10.2174/156652409787314507

Palacios, E. H., & Weiss, A. (2004). Function of the Src-family kinases, Lck and Fyn, in T-cell development and activation. *Oncogene*, *23*(48), 7990–8000. https://doi.org/10.1038/sj.onc.1208074

Park, J., Hill, M. M., Hess, D., Brazil, D. P., Hofsteenge, J., & Hemmings, B. A. (2001). Identification of tyrosine phosphorylation sites on 3-phosphoinositide-dependent protein kinase-1 and their role in regulating kinase activity. *The Journal of Biological Chemistry*, *276*(40), 37459–37471. https://doi.org/10.1074/jbc.M105916200

Parsons, S. J., & Parsons, J. T. (2004). Src family kinases, key regulators of signal transduction. *Oncogene*, *23*(48), 7906–7909. https://doi.org/10.1038/sj.onc.1208160

Patwardhan, P., & Resh, M. D. (2010). Myristoylation and Membrane Binding Regulate c-Src Stability and Kinase Activity. *Molecular and Cellular Biology*, *30*(17), 4094–4107. https://doi.org/10.1128/MCB.00246-10

Paul, M. K., & Mukhopadhyay, A. K. (2004). Tyrosine kinase – Role and significance in Cancer. *International Journal of Medical Sciences*, *1*(2), 101–115.

Paulsen, C. E., Truong, T. H., Garcia, F. J., Homann, A., Gupta, V., Leonard, S. E., & Carroll, K. S. (2011). Peroxide-dependent sulfenylation of the EGFR catalytic site enhances kinase activity. *Nature Chemical Biology*, *8*(1), 57–64. https://doi.org/10.1038/nchembio.736

Perez-Villar, J. J., & Kanner, S. B. (1999). Regulated association between the tyrosine kinase Emt/Itk/Tsk and phospholipase-C gamma 1 in human T lymphocytes. *Journal of Immunology (Baltimore, Md.: 1950)*, *163*(12), 6435–6441.

Peri, K. G., Gervais, F. G., Weil, R., Davidson, D., Gish, G. D., & Veillette, A. (1993). Interactions of the SH2 domain of lymphocyte-specific tyrosine protein kinase p56lck with phosphotyrosine-containing proteins. *Oncogene*, *8*(10), 2765–2772.

BIBLIOGRAPHY

Philipsen, L., Reddycherla, A. V., Hartig, R., Gumz, J., Kästle, M., Kritikos, A., Poltorak, M. P., Prokazov, Y., Turbin, E., Weber, A., Zuschratter, W., Schraven, B., Simeoni, L., & Müller, A. J. (2017). De novo phosphorylation and conformational opening of the tyrosine kinase Lck act in concert to initiate T cell receptor signaling. *Science Signaling*, *10*(462). https://doi.org/10.1126/scisignal.aaf4736

Poltorak, M., Meinert, I., Stone, J. C., Schraven, B., & Simeoni, L. (2014). Sos1 regulates sustained TCR-mediated Erk activation. *European Journal of Immunology*, *44*(5), 1535–1540. https://doi.org/10.1002/eji.201344046

Poole, L. B., Klomsiri, C., Knaggs, S. A., Furdui, C. M., Nelson, K. J., Thomas, M. J., Fetrow, J. S., Daniel, L. W., & King, S. B. (2007). Fluorescent and affinity-based tools to detect cysteine sulfenic acid formation in proteins. *Bioconjugate Chemistry*, *18*(6), 2004–2017. https://doi.org/10.1021/bc700257a

Prince, T., & Matts, R. L. (2004). Definition of protein kinase sequence motifs that trigger high affinity binding of Hsp90 and Cdc37. *The Journal of Biological Chemistry*, *279*(38), 39975–39981. https://doi.org/10.1074/jbc.M406882200

Proba, K., Honegger, A., & Plückthun, A. (1997). A natural antibody missing a cysteine in VH: Consequences for thermodynamic stability and folding11Edited by I. A. Wilson. *Journal of Molecular Biology*, *265*(2), 161–172. https://doi.org/10.1006/jmbi.1996.0726

Rahman, M. A., Senga, T., Ito, S., Hyodo, T., Hasegawa, H., & Hamaguchi, M. (2010). S-Nitrosylation at Cysteine 498 of c-Src Tyrosine Kinase Regulates Nitric Oxide-mediated Cell Invasion. *The Journal of Biological Chemistry*, *285*(6), 3806–3814. https://doi.org/10.1074/jbc.M109.059782

Rao, D., Li, H., Ren, X., Sun, Y., Wen, C., Zheng, M., Huang, H., Tang, W., & Xu, S. (2021). Discovery of a potent, selective, and covalent ZAP-70 kinase inhibitor. *European Journal of Medicinal Chemistry*, *219*, 113393. https://doi.org/10.1016/j.ejmech.2021.113393

Rao, N., Miyake, S., Reddi, A. L., Douillard, P., Ghosh, A. K., Dodge, I. L., Zhou, P., Fernandes, N. D., & Band, H. (2002). Negative regulation of Lck by Cbl ubiquitin ligase. *Proceedings of the National Academy of Sciences of the United States of America*, *99*(6), 3794–3799. https://doi.org/10.1073/pnas.062055999

Ray, P. D., Huang, B.-W., & Tsuji, Y. (2012). Reactive oxygen species (ROS) homeostasis and redox regulation in cellular signaling. *Cellular Signalling*, *24*(5), 981–990. https://doi.org/10.1016/j.cellsig.2012.01.008

Roh, K.-H., Lillemeier, B. F., Wang, F., & Davis, M. M. (2015). The coreceptor CD4 is expressed in distinct nanoclusters and does not colocalize with T-cell receptor and active protein tyrosine kinase p56lck. *Proceedings of the National Academy of Sciences of the United States of America*, *112*(13), E1604-1613. https://doi.org/10.1073/pnas.1503532112

BIBLIOGRAPHY

Salmond, R. J., Filby, A., Qureshi, I., Caserta, S., & Zamoyska, R. (2009). T-cell receptor proximal signaling via the Src-family kinases, Lck and Fyn, influences T-cell activation, differentiation, and tolerance. *Immunological Reviews*, *228*(1), 9–22. https://doi.org/10.1111/j.1600-065X.2008.00745.x

Santarpia, M., Liguori, A., Karachaliou, N., Gonzalez-Cao, M., Daffinà, M. G., D'Aveni, A., Marabello, G., Altavilla, G., & Rosell, R. (2017). Osimertinib in the treatment of non-small-cell lung cancer: Design, development and place in therapy. *Lung Cancer: Targets and Therapy*, *8*, 109–125. https://doi.org/10.2147/LCTT.S119644

Schmitt, T. L., Hotz-Wagenblatt, A., Klein, H., & Dröge, W. (2005). Interdependent regulation of insulin receptor kinase activity by ADP and hydrogen peroxide. *The Journal of Biological Chemistry*, *280*(5), 3795–3801. https://doi.org/10.1074/jbc.M410352200

Scholz, G., Hartson, S. D., Cartledge, K., Hall, N., Shao, J., Dunn, A. R., & Matts, R. L. (2000). P50Cdc37 Can Buffer the Temperature-Sensitive Properties of a Mutant of Hck. *Molecular and Cellular Biology*, *20*(18), 6984–6995.

Secrist, J. P., Burns, L. A., Karnitz, L., Koretzky, G. A., & Abraham, R. T. (1993). Stimulatory effects of the protein tyrosine phosphatase inhibitor, pervanadate, on T-cell activation events. *The Journal of Biological Chemistry*, *268*(8), 5886–5893.

Sena, L. A., Li, S., Jairaman, A., Prakriya, M., Ezponda, T., Hildeman, D. A., Wang, C.-R., Schumacker, P. T., Licht, J. D., Perlman, H., Bryce, P. J., & Chandel, N. S. (2013). Mitochondria are required for antigen-specific T cell activation through reactive oxygen species signaling. *Immunity*, *38*(2), 225–236. https://doi.org/10.1016/j.immuni.2012.10.020

Senga, T., Miyazaki, K., Machida, K., Iwata, H., Matsuda, S., Nakashima, I., & Hamaguchi, M. (2000). Clustered cysteine residues in the kinase domain of v-Src: Critical role for protein stability, cell transformation and sensitivity to herbimycin A. *Oncogene*, *19*(2), 273–279. https://doi.org/10.1038/sj.onc.1203296

Simeoni, L. (2017). Lck activation: Puzzling the pieces together. *Oncotarget*, *8*(61), 102761–102762. https://doi.org/10.18632/oncotarget.22309

Simeoni, L., & Bogeski, I. (2015). Redox regulation of T-cell receptor signaling. *Biological Chemistry*, *396*(5), 555–568. https://doi.org/10.1515/hsz-2014-0312

Simeoni, L., Thurm, C., Kritikos, A., & Linkermann, A. (2016). Redox homeostasis, T cells and kidney diseases: Three faces in the dark. *Clinical Kidney Journal*, *9*(1), 1–10. https://doi.org/10.1093/ckj/sfv135

BIBLIOGRAPHY

Smith-Garvin, J. E., Koretzky, G. A., & Jordan, M. S. (2009). T cell activation. *Annual Review of Immunology*, *27*, 591–619. https://doi.org/10.1146/annurev.immunol.021908.132706

Stefanová, I, Saville, M. W., Peters, C., Cleghorn, F. R., Schwartz, D., Venzon, D. J., Weinhold, K. J., Jack, N., Bartholomew, C., Blattner, W. A., Yarchoan, R., Bolen, J. B., & Horak, I. D. (1996). HIV infection—Induced posttranslational modification of T cell signaling molecules associated with disease progression. *Journal of Clinical Investigation*, *98*(6), 1290–1297. https://doi.org/10.1172/JCI118915

Stefanová, Irena, Hemmer, B., Vergelli, M., Martin, R., Biddison, W. E., & Germain, R. N. (2003). TCR ligand discrimination is enforced by competing ERK positive and SHP-1 negative feedback pathways. *Nature Immunology*, *4*(3), 248–254. https://doi.org/10.1038/ni895

Stirnweiss, A., Hartig, R., Gieseler, S., Lindquist, J., Reichardt, P., Philipsen, L., Simeoni, L., Poltorak, M., Merten, C., Zuschratter, W., Prokazov, Y., Paster, W., Stockinger, H., Harder, T., Gunzer, M., & Schraven, B. (2013). T Cell Activation Results in Conformational Changes in the Src Family Kinase Lck to Induce Its Activation. *Science Signaling*, *6*, ra13. https://doi.org/10.1126/scisignal.2003607

Straus, D. B., Chan, A. C., Patai, B., & Weiss, A. (1996). SH2 domain function is essential for the role of the Lck tyrosine kinase in T cell receptor signal transduction. *The Journal of Biological Chemistry*, *271*(17), 9976–9981. https://doi.org/10.1074/jbc.271.17.9976

Straus, D. B., & Weiss, A. (1992). Genetic evidence for the involvement of the lck tyrosine kinase in signal transduction through the T cell antigen receptor. *Cell*, *70*(4), 585–593. https://doi.org/10.1016/0092-8674(92)90428-f

Swamy, M., Beck-Garcia, K., Beck-Garcia, E., Hartl, F. A., Morath, A., Yousefi, O. S., Dopfer, E. P., Molnár, E., Schulze, A. K., Blanco, R., Borroto, A., Martín-Blanco, N., Alarcon, B., Höfer, T., Minguet, S., & Schamel, W. W. A. (2016). A Cholesterol-Based Allostery Model of T Cell Receptor Phosphorylation. *Immunity*, *44*(5), 1091–1101. https://doi.org/10.1016/j.immuni.2016.04.011

Tewari, R., Shayahati, B., Fan, Y., & Akimzhanov, A. M. (2020). T cell receptor-dependent S-acylation of ZAP-70 controls activation of T cells. *BioRxiv*, 2020.06.30.180885. https://doi.org/10.1101/2020.06.30.180885

Thomas, S. M., & Brugge, J. S. (1997). Cellular functions regulated by Src family kinases. *Annual Review of Cell and Developmental Biology*, *13*, 513–609. https://doi.org/10.1146/annurev.cellbio.13.1.513

Thome, M., Charton, J. E., Pelzer, C., & Hailfinger, S. (2010). Antigen Receptor Signaling to NF-κB via CARMA1, BCL10, and MALT1. *Cold Spring Harbor Perspectives in Biology*, *2*(9). https://doi.org/10.1101/cshperspect.a003004

BIBLIOGRAPHY

Thurm, C., Poltorak, M. P., Reimer, E., Brinkmann, M. M., Leichert, L., Schraven, B., & Simeoni, L. (2017a). A highly conserved redox-active Mx(2)CWx(6)R motif regulates Zap70 stability and activity. *Oncotarget*, *8*(19), 30805–30816. https://doi.org/10.18632/oncotarget.16486

Thurm, C., Poltorak, M. P., Reimer, E., Brinkmann, M. M., Leichert, L., Schraven, B., & Simeoni, L. (2017b). A highly conserved redox-active Mx(2)CWx(6)R motif regulates Zap70 stability and activity. *Oncotarget*, *8*(19), 30805–30816. https://doi.org/10.18632/oncotarget.16486

Trevillyan, J. M., Chiou, X. G., Ballaron, S. J., Tang, Q. M., Buko, A., Sheets, M. P., Smith, M. L., Putman, C. B., Wiedeman, P., Tu, N., Madar, D., Smith, H. T., Gubbins, E. J., Warrior, U. P., Chen, Y. W., Mollison, K. W., Faltynek, C. R., & Djurić, S. W. (1999). Inhibition of p56(lck) tyrosine kinase by isothiazolones. *Archives of Biochemistry and Biophysics*, *364*(1), 19–29. https://doi.org/10.1006/abbi.1999.1099

Veillette, A., Dumont, S., & Fournel, M. (1993). Conserved cysteine residues are critical for the enzymatic function of the lymphocyte-specific tyrosine protein kinase p56lck. *The Journal of Biological Chemistry*, *268*(23), 17547–17553.

Verba, K. A., & Agard, D. A. (2017). Protein Expression and Purification of the Hsp90-Cdc37-Cdk4 Kinase Complex from Saccharomyces cerevisiae. *Bio-Protocol*, *7*(19). https://doi.org/10.21769/BioProtoc.2563

Verba, K. A., Wang, R. Y.-R., Arakawa, A., Liu, Y., Shirouzu, M., Yokoyama, S., & Agard, D. A. (2016). Atomic structure of Hsp90-Cdc37-Cdk4 reveals that Hsp90 traps and stabilizes an unfolded kinase. *Science (New York, N.Y.)*, *352*(6293), 1542–1547. https://doi.org/10.1126/science.aaf5023

Wani, R., Nagata, A., & Murray, B. W. (2014). Protein redox chemistry: Post-translational cysteine modifications that regulate signal transduction and drug pharmacology. *Frontiers in Pharmacology*, *5*. https://doi.org/10.3389/fphar.2014.00224

Watts, J. D., Sanghera, J. S., Pelech, S. L., & Aebersold, R. (1993). Phosphorylation of serine 59 of p56lck in activated T cells. *The Journal of Biological Chemistry*, *268*(31), 23275–23282.

Weibrecht, I., Böhmer, S.-A., Dagnell, M., Kappert, K., Ostman, A., & Böhmer, F.-D. (2007). Oxidation sensitivity of the catalytic cysteine of the protein-tyrosine phosphatases SHP-1 and SHP-2. *Free Radical Biology & Medicine*, *43*(1), 100–110. https://doi.org/10.1016/j.freeradbiomed.2007.03.021

Weiss, A., Wiskocil, R. L., & Stobo, J. D. (1984). The role of T3 surface molecules in the activation of human T cells: A two-stimulus requirement for IL 2 production reflects events occurring at a pre-translational level. *The Journal of Immunology*, *133*(1), 123–128.

BIBLIOGRAPHY

Werlen, G., & Palmer, E. (2002). The T-cell receptor signalosome: A dynamic structure with expanding complexity. *Current Opinion in Immunology*, *14*(3), 299–305. https://doi.org/10.1016/s0952-7915(02)00339-4

Wong, N. K. Y., Lai, J. C. Y., Birkenhead, D., Shaw, A. S., & Johnson, P. (2008). CD45 down-regulates Lck-mediated CD44 signaling and modulates actin rearrangement in T cells. *Journal of Immunology (Baltimore, Md.: 1950)*, *181*(10), 7033–7043. https://doi.org/10.4049/jimmunol.181.10.7033

Wu, W., Hale, A. J., Lemeer, S., & den Hertog, J. (2017). Differential oxidation of protein-tyrosine phosphatases during zebrafish caudal fin regeneration. *Scientific Reports*, *7*(1), 1–9. https://doi.org/10.1038/s41598-017-07109-8\

Xu, W., Harrison, S. C., & Eck, M. J. (1997). Three-dimensional structure of the tyrosine kinase c-Src. *Nature*, *385*(6617), 595–602. https://doi.org/10.1038/385595a0

Yan, Q., Barros, T., Visperas, P. R., Deindl, S., Kadlecek, T. A., Weiss, A., & Kuriyan, J. (2013). Structural basis for activation of ZAP-70 by phosphorylation of the SH2-kinase linker. *Molecular and Cellular Biology*, *33*(11), 2188–2201. https://doi.org/10.1128/MCB.01637-12

Yasuda, K., Kosugi, A., Hayashi, F., Saitoh, S., Nagafuku, M., Mori, Y., Ogata, M., & Hamaoka, T. (2000). Serine 6 of Lck tyrosine kinase: A critical site for Lck myristoylation, membrane localization, and function in T lymphocytes. *Journal of Immunology (Baltimore, Md.: 1950)*, *165*(6), 3226–3231. https://doi.org/10.4049/jimmunol.165.6.3226

Yoo, S. K., Starnes, T. W., Deng, Q., & Huttenlocher, A. (2011). Lyn is a redox sensor that mediates leukocyte wound attraction in vivo. *Nature*, *480*(7375), 109–112. https://doi.org/10.1038/nature10632

Young, J. C., Moarefi, I., & Hartl, F. U. (2001). Hsp90: A specialized but essential protein-folding tool. *The Journal of Cell Biology*, *154*(2), 267–273. https://doi.org/10.1083/jcb.200104079

Yun, H.-Y., Lee, J., Kim, H., Ryu, H., Shin, H.-C., Oh, B.-H., Ku, B., & Kim, S. J. (2018). Structural study reveals the temperature-dependent conformational flexibility of Tk-PTP, a protein tyrosine phosphatase from Thermococcus kodakaraensis KOD1. *PLOS ONE*, *13*(5), e0197635. https://doi.org/10.1371/journal.pone.0197635

Zeeshan, H. M. A., Lee, G. H., Kim, H.-R., & Chae, H.-J. (2016). Endoplasmic Reticulum Stress and Associated ROS. *International Journal of Molecular Sciences*, *17*(3). https://doi.org/10.3390/ijms17030327

Zhao, Z., Liu, Q., Bliven, S., Xie, L., & Bourne, P. E. (2017). Determining cysteines available for covalent inhibition across the human kinome. *Journal of Medicinal Chemistry*, *60*(7), 2879–2889. https://doi.org/10.1021/acs.jmedchem.6b01815

Zhu, X., Kim, J. L., Newcomb, J. R., Rose, P. E., Stover, D. R., Toledo, L. M., Zhao, H., & Morgenstern, K. A. (1999). Structural analysis of the lymphocyte-specific kinase Lck in complex with non-selective and Src family selective kinase inhibitors. *Structure (London, England: 1993)*, *7*(6), 651–661. https://doi.org/10.1016/s0969-2126(99)80086-0

Ziegler, S. F., Ramsdell, F., Hjerrild, K. A., Armitage, R. J., Grabstein, K. H., Hennen, K. B., Farrah, T., Fanslow, W. C., Shevach, E. M., & Alderson, M. R. (1993). Molecular characterization of the early activation antigen CD69: A type II membrane glycoprotein related to a family of natural killer cell activation antigens. *European Journal of Immunology*, *23*(7), 1643–1648. https://doi.org/10.1002/eji.1830230737

Zorov, D. B., Juhaszova, M., & Sollott, S. J. (2014). Mitochondrial Reactive Oxygen Species (ROS) and ROS-Induced ROS Release. *Physiological Reviews*, *94*(3), 909–950. https://doi.org/10.1152/physrev.00026.2013

G. Declaration of Honor

“I hereby declare that I prepared this thesis without the impermissible help of third parties and that none other than the aids indicated have been used; all sources of information are clearly marked, including my own publications.
In particular I have not consciously:
• fabricated data or rejected undesirable results,
• misused statistical methods with the aim of drawing other conclusions than those warranted by the available data,
• plagiarized external data or publications,
• presented the results of other researchers in a distorted way.
I am aware that violations of copyright may lead to injunction and damage claims by the author and also to prosecution by the law enforcement authorities.
I hereby agree that the thesis may be electronically reviewed with the aim of identifying plagiarism.
This work has not yet been submitted as a doctoral thesis in the same or a similar form in Germany, nor in any other country. It has not yet been published as a whole.”

Magdeburg, date

M.Sc. Andreas Kritikos